

CUMULATIVE VOLUME AND MASS PROFILES FOR DOMINANT STEMS AND
WHOLE TREES

by

Neil R. Ver Planck

A THESIS

Submitted
to Michigan State University
in partial fulfillment of the requirements
for the degree of

Forestry – Master of Science

2013

ABSTRACT

CUMULATIVE VOLUME AND MASS PROFILES FOR DOMINANT STEMS AND WHOLE TREES

by

Neil R. Ver Planck

Integrated whole-tree biomass and volume equations are in great demand due to the simultaneous need to improve estimation of forest carbon *stocks* and to quantify the distribution of wood volume within trees for estimating whole-tree utilization potential. While the volume of the dominant stem in a tree has been extensively studied, the relative mass and volume of branches has received much less attention. It is particularly challenging to quantify the branch volume and branch mass in trees with a deliquescent branching architecture (i.e., hardwoods) and it is even difficult to model the dominant stem for such trees because the lack of apical dominance makes definition of the dominant stem more obscure.

New profile models allow for volume and mass estimation of the dominant stem and whole tree from ground to the top of the tree. Cumulative branch volume and mass can be estimated at different relative heights from the whole-tree and dominant stem profiles by simple subtraction. The models were developed from intensive, destructive sampling of 32 trees from a temperate hardwood forest in Michigan, USA. The species in the sample were primarily American beech (*Fagus grandifolia* Ehrh.) and sugar maple (*Acer saccharum* Marsh.). A mixed-effects modeling framework was used throughout model development of volume, density, and mass profiles. Non-linear mixed-effects composite models were used for cumulative volume profiles to account for among tree variation and the ability to correlate multiple measurements within an individual tree. Species-specific linear mixed-effects models were developed for basic density profiles. Species-specific non-linear mixed-effects models were also developed for cumulative mass profiles compared to density-integral and constant density models.

This thesis is dedicated to Liisa.

ACKNOWLEDGEMENTS

I would like to sincerely thank my thesis advisor and mentor Dr. David W. MacFarlane for all of his help and guidance throughout my graduate studies. I would also like to thank my committee members, Dr. Andrew O. Finley and Dr. Bert M. Cregg, for their time and assistance with this thesis.

Many thanks to the MSU Sustainability Seed Grant and USDA Forest Service's Forest Inventory and Analysis program for providing me with funding for my research. A special thanks to the staff at the Kellogg Experimental Forest: Greg Kowalewski, Mickey Trimner, Brett Kuipers, and Cody Johnson for assistance in data collection.

Most importantly, a special thanks to my wife, Liisa, for all of her patience, love, and support. I would also like to thank my entire family for all of their support and encouragement through my graduate study years.

TABLE OF CONTENTS

LIST OF TABLES	vii
LIST OF FIGURES	x
CHAPTER 1 INTRODUCTION	1
CHAPTER 2 METHODS	3
2.1 Dominant Stem Volume	3
2.2 Whole-tree Volume — Random Branch Sampling	4
2.3 Density Sampling	8
2.3.1 Tree Density Sampling	8
2.3.2 Bark Density Sampling	10
2.4 Mass Sampling	10
2.4.1 Dominant Stem Mass Sampling	10
2.4.2 Whole-tree Mass — Random Branch Sampling	11
2.5 Study Site	11
2.6 Tree Selection	16
CHAPTER 3 CUMULATIVE VOLUME PROFILES FOR DOMINANT STEMS AND WHOLE TREES	19
3.1 Related Dominant Stem Taper and Volume Modeling	19
3.1.1 Dominant Stem Taper Modeling	19
3.1.2 Volume Modeling	21
3.2 Models	23
3.2.1 Dominant Stem Cumulative Volume Models	23
3.2.2 Whole-tree Cumulative Volume Models	24
3.2.3 Centroid of Dominant Stem and Whole-tree Volume Models	25
3.3 Results	26
3.3.1 Total Volume Estimates	26
3.3.2 Cumulative Volume Profiles	29
3.3.3 Centroid of Dominant Stem and Whole-tree Volume Profiles	34
3.4 Discussion	41
CHAPTER 4 CUMULATIVE MASS AND DENSITY PROFILES FOR DOMINANT STEMS AND WHOLE TREES	44
4.1 Related Biomass Modeling	44
4.1.1 Diameter at Breast Height Based Biomass Modeling	44
4.1.2 Component Ratio Method	45
4.1.3 Weight-ratio and Density-integral Biomass Modeling	45
4.2 Related Tree Density Modeling	46
4.3 Models	49

4.3.1	Dominant Stem Vertical Density Models	49
4.3.2	Random Branch Path Density Models	51
4.3.3	Bark Density Models	52
4.3.4	Dominant Stem Cumulative Mass Models	53
4.3.5	Whole-tree Cumulative Mass Models	54
4.4	Results	56
4.4.1	Dominant Stem Vertical Density Profiles	56
4.4.2	Random Branch Path Density Profiles	60
4.4.3	Comparative Dominant and Random Branch Path Density Profiles .	61
4.4.4	Bark Vertical Density Profiles	65
4.4.5	Total Mass Estimates	70
4.4.6	Cumulative Mass Profiles	72
4.5	Discussion	82
4.5.1	Density	82
4.5.2	Mass	85
CHAPTER 5 CONCLUSION		88
BIBLIOGRAPHY		91

LIST OF TABLES

Table 2.1	Summary of the mean number of trees per ha by species and 10 cm diameter at breast height (DBH) class for the residual stand.	14
Table 2.2	Summary of the average basal area in $\frac{m^2}{ha}$ by species and 10 cm diameter at breast height (DBH) class for the residual stand.	15
Table 2.3	Species, code, sample size (n), diameter at breast height (DBH), and height (H) summary statistics for the data set.	18
Table 3.1	Species code (spp), number of trees (n), mean dominant stem volume (V_{DOM}), mean total volume (V_{WT}) with standard deviation (SD), minimum (min), and maximum (max) values by species.	26
Table 3.2	Species code (spp), diameter at breast height (DBH), DBH class (Dclass), total dominant stem volume (V_{DOM}), total volume estimate from the first random branch sample (V_{WT_1}), total volume estimate from the second random branch sample (V_{WT_2}), mean total volume (V_{WT}), standard deviation of total volume (SD), and coefficient of variation of total volume (CV) summary statistics for each individual tree.	27
Table 3.3	Parameter estimates of model 3.8 for the cumulative volume of the dominant stem for the all-species (ALL), American beech (FG), and sugar maple (AS) mixed-effects models. For the fixed parameters, the standard error of estimates is given in parantheses.	29
Table 3.4	Parameter estimates of model 3.9 for the cumulative whole-tree volume above relative crown height for the all-species (ALL), American beech (FG), and sugar maple (AS) mixed-effects models. For the fixed parameters, the standard error of estimates is given in parantheses.	31
Table 3.5	Parameter estimates of model 3.10 for the cumulative whole-tree volume above relative crown height for the all-species (ALL), American beech (FG), and sugar maple (AS) mixed-effects models. For the fixed parameters, the standard error of estimates is given in parantheses.	31
Table 3.6	The mean centroid of dominant stem volume by species and 10 cm diameter at breast height (DBH) classes. Standard deviation is given in parentheses.	35
Table 3.7	The mean centroid of dominant stem volume by species and crown ratio class (CRC). Standard deviation is given in parentheses.	36

Table 3.8	The mean centroid of whole-tree volume classified by species and 10 cm diameter at breast height (DBH) classes with the standard deviation given in parentheses.	38
Table 3.9	The mean centroid of whole-tree volume by species and crown ratio class (CRC). Standard deviation is given in parentheses.	39
Table 4.1	Relative crown height of the dominant stem (RCH) summary statistics for all species (ALL), American beech (FG), and sugar maple (AS). . . .	51
Table 4.2	Relative height at which the random path diverges from the dominant stem (RHD) summary statistics for all species (ALL), American beech (FG), and sugar maple (AS).	52
Table 4.3	The bark sample size by species, dominant (DOM), and random branch paths (RBP).	53
Table 4.4	Parameter estimates of models 4.12 - 4.14 for the vertical profile of the basic density of the dominant stem for the all-species (ALL), American beech (FG), and sugar maple (AS) mixed-effects models. For the fixed parameters, the standard error of estimates is given in parantheses.	58
Table 4.5	Parameter estimates of models 4.15 - 4.17 for the basic density profile of the random branch path for the all-species (ALL), American beech (FG), and sugar maple (AS) mixed-effects models. For the fixed parameters, the standard error of estimates is given in parantheses.	61
Table 4.6	Parameter estimates of models 4.18 - 4.20 for the vertical profile of the bark basic density of the combined dominant and random branch path for the all-species (ALL), American beech (FG) and sugar maple (AS) mixed-effects models. For the fixed parameters, the standard error of estimates is given in parantheses.	66
Table 4.7	Species code (spp), number of trees (n), mean dominant stem mass (M_{DOM}), mean total mass (M_{WT}) with standard deviation (SD), minimum (min), and maximum (max) values by species.	70
Table 4.8	Parameter estimates of model 4.21 for the cumulative mass of the dominant stem for the all-species (ALL), American beech (FG), and sugar maple (AS) mixed-effects models. For the fixed parameters, the standard error of estimates is given in parantheses.	72
Table 4.9	Model comparison of the residuals among the cumulative dominant stem mass profiles: (1) non-linear mixed-effects (nlme) model 4.21, (2) density-integral (integ) model 4.22, and (3) the constant density (const) model 4.23 for all (ALL), American beech (FG), and sugar maple (AS) trees. . .	76

Table 4.10	Parameter estimates of model 4.24 for cumulative whole-tree mass above relative crown height for the all-species (ALL), American beech (FG), and sugar maple (AS) mixed-effects models. For the fixed parameters, the standard error of estimates is given in parantheses.	78
Table 4.11	Parameter estimates of model 4.25 for cumulative whole-tree mass above relative crown height for the all-species (ALL), American beech (FG), and sugar maple (AS) mixed-effects models. For the fixed parameters, the standard error of estimates is given in parantheses.	78
Table 4.12	Model comparison of the residuals among the cumulative whole-tree mass profiles above relative crown height: (1) non-linear mixed-effects (nlme) model 4.25, (2) density-integral (integ) model 4.27, and (3) the constant density (const) model 4.28 for all (ALL), American beech (FG), and sugar maple (AS) trees.	82

LIST OF FIGURES

Figure 2.1	A simplified hardwood tree schematic where the dominant stem is indicated by horizontal lines, the first random branch path is indicated by a checkered pattern, the second random branch path is indicated by dots, and non-sampled branches are solid. The first branch junction at crown height (CH) demonstrates the length (z) and circumference measurements taken at each branch junction for the before fork (BF) and the after fork (AF) locations.	5
Figure 2.2	A simplified hardwood tree schematic showing the location of branch volume or mass accumulation along the dominant stem as a function of relative height, ranging from zero at base to one at top of the tree. The first branches encountered are at relative crown height (RCH).	7
Figure 2.3	The drying time for discs sampled from an American beech tree with a diameter at breast height, DBH, of 75.4 cm. (a) The oven-drying time for large discs with diameter outside bark, dob, greater than 50.0 cm. (b) The oven-drying time for medium discs with dob ranging from 20.1 to 50.0 cm. (c) The oven-drying time for small discs with dob ranging from 5.1 to 20.0 cm. (d) The oven-drying time for very small discs with dob ranging from 0.1 to 5.0 cm. Each line and symbol represents a different sampled disc in the respective dob size class.	9
Figure 2.4	(A) Shows the location of the 20.8-hectare research area in the 36-hectare second-growth maple-beech stand, fixed-area plots, and sampled trees within the Fred Russ Experimental Forest. (B) The star represents the location of the entrance to the Fred Russ Experimental Forest in Cass County, Michigan.	13
Figure 2.5	Histogram of the relative frequency of the residual stand, represented by diagonal line filled bars, and the sampled trees, represented by gray filled bars, divided into 10 cm diameter at breast height (DBH) classes.	17
Figure 3.1	The total volume, in m^3 , of sampled trees for the dominant stem (DOM) and whole tree (WT) versus diameter at breast height (DBH), in cm, for all trees (ALL), American beech (FG), and sugar maple (AS).	28

Figure 3.2	Cumulative volume, m^3 , profiles for the dominant stem (model 3.8), represented by a dashed line above relative crown height, and whole tree (model 3.11), represented as the solid line, as a function of relative height along the dominant stem for the (a) minimum, (b) median, and (c) maximum diameter at breast height (DBH) American beech (FG) trees. The vertical dashed line represents relative crown height.	32
Figure 3.3	Cumulative volume, m^3 , profiles for the dominant stem (model 3.8), represented by a dashed line above relative crown height, and whole tree (model 3.11), represented as the solid line, as a function of relative height along the dominant stem for the (a) minimum, (b) median, and (c) maximum diameter at breast height (DBH) sugar maple (AS) trees. The vertical dashed line represents relative crown height.	33
Figure 3.4	Dominant stem (model 3.8), represented by a dashed line, and whole-tree (model 3.11), represented as the solid line, relative volume profiles as a function of relative height along the dominant stem for the (a) minimum, (b) median, and (c) maximum diameter at breast height (DBH) American beech (FG) trees in the dataset. The horizontal dashed line indicates a relative volume of 0.5, the centroid of volume. The dotted vertical line indicates the relative height of the centroid of volume for the dominant stem (DOM.c), the vertical dashed line represents relative crown height, and the dash and dot vertical line indicates the relative height of the centroid of volume for the whole tree (WH.c).	40
Figure 4.1	The mixed-effects of the dominant stem vertical density profile for each species according to models 4.12 - 4.14. For the median sized American beech (FG) tree with $D = 42.9$ cm, and the median sized sugar maple (AS) tree with $D = 42.8$ cm and $H = 34.0$ cm (models 4.13 and 4.14, respectively). American basswood (TA), black cherry (PS), pignut hickory (CG), and slippery elm (UR) were all fit using the all-species model (model 4.12) as there was only one individual of each in the sample. The measured tree densities are shown as triangles. The horizontal dotted line represents the wood density for each species as reported by the Forest Products Laboratory in Madison, WI (U. S. D. A. Forest Service 2010).	59

Figure 4.2	The mixed-effects vertical density profile for the dominant stem of each species according to models 4.12 - 4.14, shown as solid lines, versus relative height. The thicker dashed lines are the mixed-effects density profile for the random branch path of each species according to models 4.15 - 4.17 versus relative path length. For the median sized American beech (FG) tree with $D = 42.9$ cm, and the median sized sugar maple (AS) tree with $D = 42.8$ cm and $H = 34.0$ cm (models 4.13, 4.16 and 4.14, 4.17, respectively). American basswood (TA), black cherry (PS), pignut hickory (CG), and slippery elm (UR) were all fit using the all-species models 4.12 and 4.15 as there was only one individual of each in the sample. The horizontal dotted line represents the wood density for each species as given by the Forest Products Laboratory in Madison, WI (U. S. D. A. Forest Service 2010).	63
Figure 4.3	The mixed effects of the vertical density profile for the dominant stem (solid line) and the random branch path profile (thicker dashed line) for three American beech trees versus relative height or path length. (a) Shows an American beech tree with diameter at breast height (DBH) of 50.1 cm, relative height at which the random path diverges from the dominant stem (RHD) equal to 0.185. (b) Shows an American beech tree with DBH of 47.1 cm and RHD equal to 0.544. (c) Shows an American beech tree with DBH of 42.9 cm and RHD equal to 0.888. The horizontal dotted line represents the wood density for American beech of 560 kg/m^3 as reported by the Forest Products Laboratory in Madison, WI (U. S. D. A. Forest Service 2010).	64
Figure 4.4	The mixed effects of the vertical bark density profile for the combined dominant stem and random branch paths of each species according to models 4.18 - 4.20, shown as solid lines. The thicker dashed line represents the extrapolation of the models beyond the last measured relative height. For the median sized American beech (FG) tree with $D = 50.1$ cm, and the median sized sugar maple (AS) tree with $D = 48.1$ cm (models 4.19 and 4.20, respectively). American basswood (TA), black cherry (PS), pignut hickory (CG), and slippery elm (UR) were all fit using the all-species model 4.18 as there was only one individual of each in the sample. The horizontal dotted line represents the bark density for each species as compiled by the USDA Forest Service (Miles and Smith 2009).	68

Figure 4.5	The mixed effects of the vertical bark density profile for the combined dominant stem and random branch paths of each species according to models 4.18 - 4.20, shown as solid lines, with dashed lines representing the extrapolation of the models beyond the last measured relative height. For the median sized American beech (FG) tree with $D = 50.1$ cm, and the median sized sugar maple (AS) tree with $D = 48.1$ cm (models 4.19 and 4.20, respectively). American basswood (TA), black cherry (PS), pignut hickory (CG), and slippery elm (UR) were all fit using the all-species model 4.18 as there was only one individual of each in the sample. The dotted lines represent the tree density for each species from models 4.12 - 4.14.	69
Figure 4.6	The total mass, in kg, of sampled trees for the dominant stem (DOM) and whole tree (WT) versus diameter at breast height (DBH), in cm, for all trees (ALL), American beech (FG), and sugar maple (AS). . . .	71
Figure 4.7	Cumulative mass, in kg, profiles for the dominant stem modeled by: (1) the non-linear mixed-effects approach (model 4.21, nlme), (2) the density-integral approach (model 4.22, integ), and (3) the constant density approach (model 4.23, const) as a function of relative height along the dominant stem for the (a) minimum, (b) median, and (c) maximum diameter at breast height (DBH) American beech (FG) trees in the dataset. The vertical dashed line represents relative crown height. . .	74
Figure 4.8	Cumulative mass, in kg, profiles for the dominant stem modeled by: (1) the non-linear mixed-effects approach(model 4.21, nlme), (2) the density-integral approach (model 4.22, integ), and (3) the constant density approach (model 4.23, const) as a function of relative height along the dominant stem for the (a) minimum, (b) median, and (c) maximum diameter at breast height (DBH) sugar maple (AS) trees in the dataset. The vertical dashed line represents relative crown height.	75
Figure 4.9	Cumulative mass, in kg, profiles for the dominant stem (model 4.21), represented by a solid line and open triangles above relative crown height, and whole tree (model 4.26, nlme), represented by a solid line with filled-in triangles, as a function of relative height along the dominant stem for the (a) minimum, (b) median, and (c) maximum diameter at breast height (DBH) American beech (FG) trees in the dataset. Above relative crown height the density-integral (model 4.27, integ) and constant density (model 4.28, const) models are shown with dotted and dashed lines, respectively. The vertical dashed line represents relative crown height.	80

Figure 4.10 Cumulative mass, in kg, profiles for the dominant stem (model 4.21), represented by a solid line and open triangles above relative crown height, and whole tree (model 4.26, nlme), represented by a the solid line with filled-in triangles, as a function of relative height along the dominant stem for the (a) minimum, (b) median, and (c) maximum diameter at breast height (DBH) sugar maple (AS) trees in the dataset. Above relative crown height the density-integral (model 4.27, integ) and constant density (model 4.28, const) models are shown with dotted and dashed lines, respectively. The vertical dashed line represents relative crown height. 81

CHAPTER 1

INTRODUCTION

There is significant interest in carbon and the potential role of trees in assimilating CO₂, which could potentially mitigate the amount of greenhouse gases polluting the atmosphere. According to a 2011 report by the United States Environmental Protection Agency (EPA 2011), forested land in the contiguous U.S. sequestered 235.4 million metric tons of C of the 276.8 million metric tons of C sequestered by land-use, land-use change, and forestry. The later estimate is an offset of 15.3% for total U.S. CO₂ emissions. The protocols used in the estimation follow those outlined by the Intergovernmental Panel on Climate Change *2006 Guidelines for National Greenhouse Gas Inventories* (IPCC 2006). Carbon flux estimates for the forested land category are based on data collected by the U.S. Department of Agriculture (USDA) Forest Service Inventory and Analysis program (FIA). Carbon is approximately 50 percent of the oven-dry mass of wood with variation around this simplified estimate being species-dependent (Lamloom and Savidge 2003). However, estimates may be less certain for some forest carbon pools in national scale inventories (Woodbury et al. 2007), such as branches. This research addresses the later by measuring and modeling branches in the framework of whole-tree volume and mass profiles.

Integrated whole-tree mass and volume equations are in great demand due to the simultaneous need to improve estimation of forest carbon *stocks* and to quantify the distribution of wood volume within trees for estimating whole-tree utilization potential. While the volume of the dominant stem of a tree has been extensively studied (Hahn and Hansen 1991, Fonweban et al. 2012), the relative mass and volume of branches has received much less attention (MacFarlane 2011). It is particularly challenging to quantify the branch volume and branch mass in trees with a deliquescent branching architecture (i.e., hardwoods) and it is even difficult to model the dominant stem for such trees because the lack of apical dom-

inance makes definition of the dominant stem more obscure. The focal population of this research is exclusively northern hardwood trees because of their large and complex branching architecture (Oliver and Larson 1996). This research develops models for the dominant stem and whole-tree volume, density, and mass. Whole tree in this research is defined as the aboveground portion of dominant stem and branches outside bark of a tree.

Volume has long been estimated by standard mensuration techniques for the dominant stem of trees (Avery and Burkhardt 2002). The diameter at breast height (DBH, measured at 1.37 m above ground level) and total tree height are the two most common predictor variables for total dominant stem and whole-tree volume estimation (Hahn and Hansen 1991). This research expands total volume estimates into profiles of cumulative volume at different relative heights. Gregoire and Schabenberger (1996a;b), Fonweban et al. (2012) both examined cumulative volume profiles for the dominant stem only and not the whole tree. In Chapter 3, the dominant stem and whole-tree cumulative volume models are developed and discussed.

Mass estimates are generally measured by either direct or indirect methods. The direct method is to physically weigh all or portions of a tree (Montagu et al. 2005), and the indirect method converts volume to mass estimates by measurements of density (Jordan et al. 2006). The indirect method is employed in this research with the development of density profiles in Chapter 4. Also in Chapter 4, three different models are developed for cumulative dominant stem and whole-tree mass profiles. The first model is a new cumulative mass profile that is compared to two common approaches found in the literature: the density-integral (Parresol 1999, Jordan et al. 2006) and the constant density (Chave et al. 2005, Van Deusen and Roesch 2011, Woodall et al. 2011) approaches. The subsequent chapter outlines the methods and study area of the data used for the development of the dominant stem and whole-tree models.

CHAPTER 2

METHODS

2.1 Dominant Stem Volume

The dominant stem in this study was defined by following the largest and most vertical branch at each fork that was in line with the stem prior to branching. For each tree, circumference was measured at stump height, 37 cm above ground level, followed by breast height, 137 cm above ground level. Additional circumference measurements were taken at 2-m length intervals up to the first branch junction, and then continued for all branch junctions until reaching the terminal bud. Upon encountering the first branch, circumference measurements were taken at the before fork (BF) location of the stem and then at the after fork (AF) location of each branch based upon functional branch analysis protocols (van Noordwijk and Mulia 2002). The BF was defined as the location where included bark due to branching was no longer visible as this is most likely the origin of the branches off the dominant stem. The AF was the location immediately after the point at which the fork occurred. The length from the BF to the AF was also recorded to measure the total path length from base to tip along the dominant stem. It is recognized that the dominant stem total path length may be an over-estimate of standing total tree height due to the curvature of the stem. All circumference measurements were divided by the constant π to convert to diameter measurements.

The volume of a section f of the dominant stem was determined by Smalian's formula for volume:

$$v_f = \frac{A_{1f} + A_{2f}}{2} * z, \quad (2.1)$$

where v_f is the volume of section f , in m^3 , A_1 is the cross-sectional area, in m^2 , of the lower end of section f , A_2 is the cross-sectional area, in m^2 , of the upper end of section f , and z ,

in m, is the length of section f (Avery and Burkhart 2002).

The cumulative dominant stem volume profile, $v_{DOM}(h)$, was found by iteratively evaluating

$$v_{DOM}(h) = \sum_{f=0}^{n(h)} v_f, \quad (2.2)$$

where n is the number of segments to a measured height, h , and v_0 is the volume of the stump section. The volume of the stump section was approximated by a cylinder, ignoring the roots near ground level. The total dominant stem volume was determined by summing n segments up to total tree height, H . Figure 2.1 shows a graphical representation of the measurements taken.

2.2 Whole-tree Volume — Random Branch Sampling

An estimate of the total aboveground volume of an entire tree outside bark, V_{WT} , was obtained by the method of random branch sampling (Gregoire et al. 1995). The same measurement methods as for the dominant stem were used, but at each branch junction a segment was selected based on probability proportional to the size of the AF diameter. Based on these probabilities, the selected section either continues to follow the dominant stem or diverges following a different path through the tree until reaching the tip of a branch. The probability, p_q , of selecting a particular AF was determined by

$$p_q = \frac{d_{AFq}^2}{\sum_{q=1}^r d_{AFq}^2} \quad (2.3)$$

where d_{AFq} is the diameter of the q th AF, and r is the number of AF at that particular branch junction. A random number between 0 and 1 was then used to select the path.

For example, the first branch junction shown in Figure 2.1 had three AFs with probabilities of selection of 0.5, 0.3, and 0.2 for AF_1 , AF_2 , and AF_3 , respectively. If the random number generated was less than or equal to 0.5 then AF_1 was selected, between 0.5 and including 0.8 then AF_2 was selected, and greater than 0.8 then AF_3 was selected.

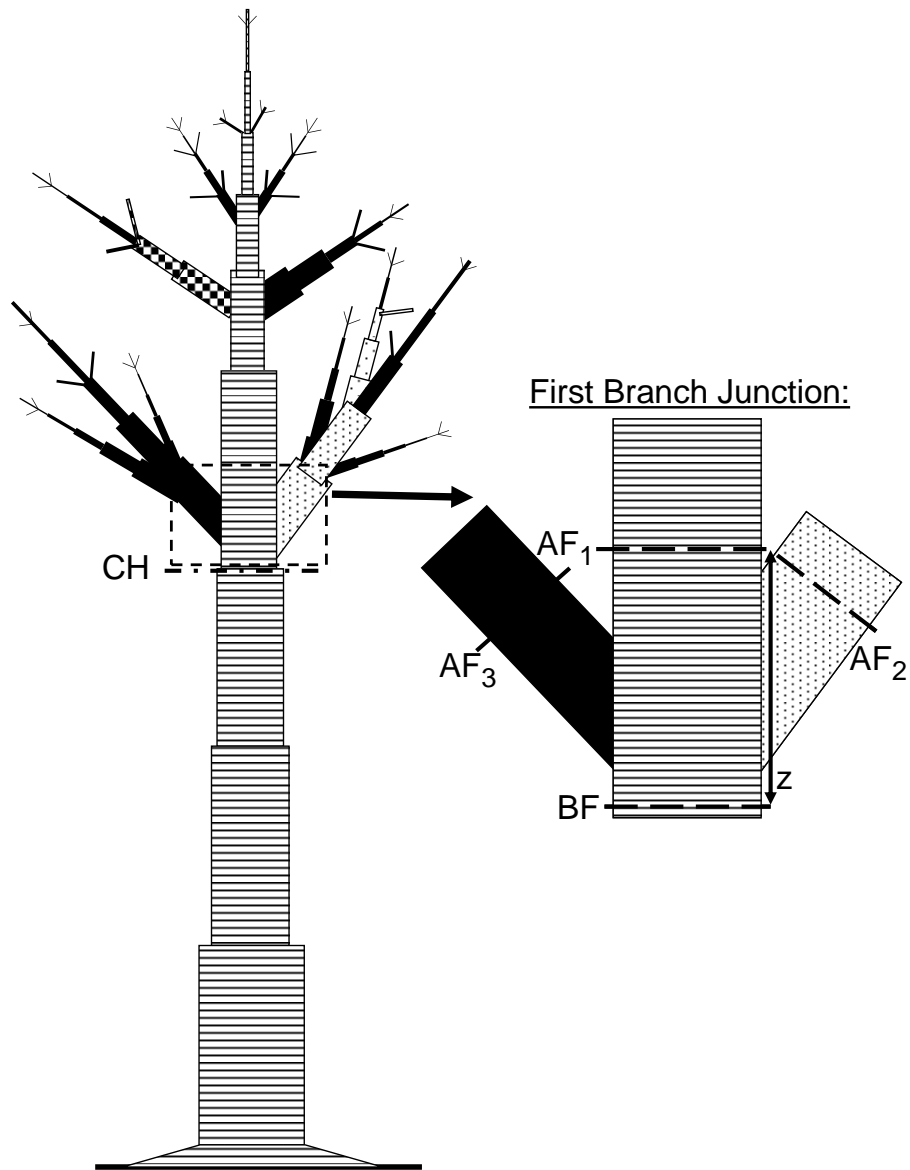


Figure 2.1: A simplified hardwood tree schematic where the dominant stem is indicated by horizontal lines, the first random branch path is indicated by a checkered pattern, the second random branch path is indicated by dots, and non-sampled branches are solid. The first branch junction at crown height (CH) demonstrates the length (z) and circumference measurements taken at each branch junction for the before fork (BF) and the after fork (AF) locations.

The sectional volume for the random path was used to compute the volume of the whole-tree, using the inverse of the cumulative selection probability as expansion factors for a section in the random path (Valentine et al. 1984, Gregoire et al. 1995). As seen in Figure 2.1, possible random branch paths could follow any of the first order branches off of the dominant stem, and then the path continued to be chosen as higher order branches were encountered until terminating at the tip of a branch. The volume of all branches in the tree was then calculated by subtracting the total dominant stem volume from the estimate of whole-tree volume. A second random branch path was sampled on each tree to determine mean whole-tree volume and the variation of whole-tree volume estimates between the two different selected paths.

To describe the distribution of branch volume in the tree, the mean total branch volume, V_B , determined from the two random paths, was then distributed back to each first order branch, v_{Bl} , immediately off the dominant stem by

$$v_{Bl} = V_B * \frac{d_{Bl}^2}{\sum_{l=1}^k d_{Bl}^2} \quad (2.4)$$

where d_{Bl} is the diameter of the l th first order branch, and k is the total number of first order branches in an individual tree. The volume for each first order branch and all attached higher order branches were incorporated into the profile at the relative height of the associated AF of the dominant stem (Fig. 2.2). Large amounts of volume can possibly be added at relative height locations depending on the number of branches and branch sizes at the respective location. The re-distribution of the branch volume ensured that the final observation of the cumulative whole-tree volume profile was equal to the mean total whole-tree volume outside bark from the two random branch paths. From these measurements, models for dominant stem and whole-tree volume were developed in Chapter 3.

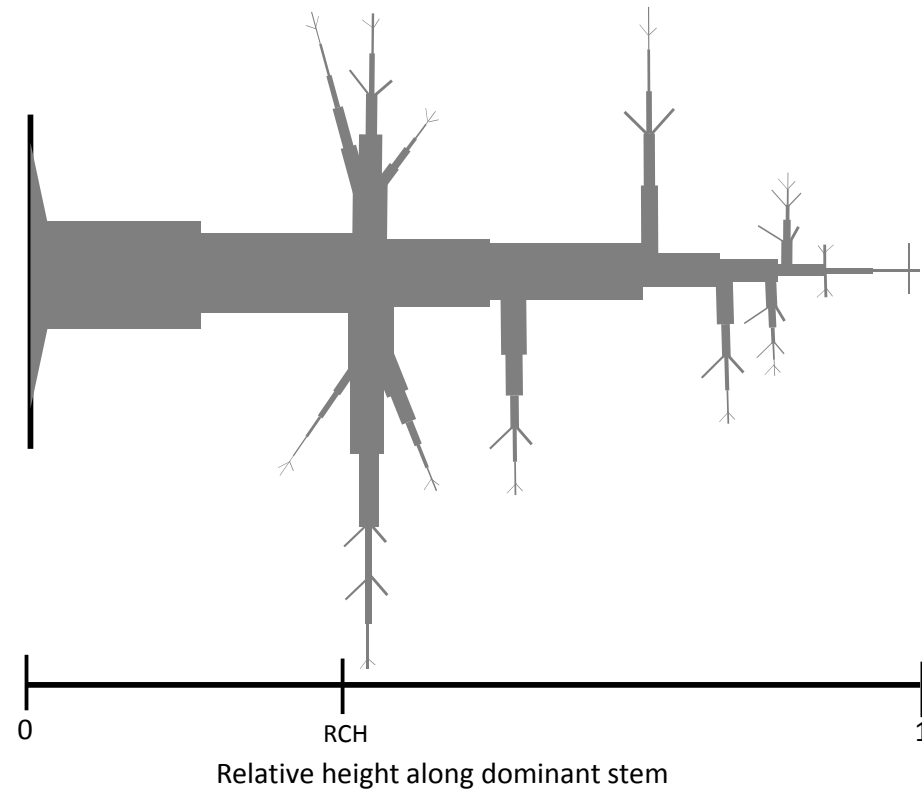


Figure 2.2: A simplified hardwood tree schematic showing the location of branch volume or mass accumulation along the dominant stem as a function of relative height, ranging from zero at base to one at top of the tree. The first branches encountered are at relative crown height (RCH).

2.3 Density Sampling

2.3.1 Tree Density Sampling

For each tree, discs were harvested at every circumference measurement location below crown height. Above crown height, discs were collected at every AF along the dominant stem path. The dominant stem path is typically studied for longitudinal density profiles. Discs were only collected at each AF to reduce the likelihood of sampling discs with more than one pith; however, some sampled discs with an AF in close proximity to the next BF had multiple piths. Approximately 5- and 10-cm-thick discs were harvested for smaller and larger circumferences, respectively. Each disc was measured for green mass and green volume immediately after transportation to the laboratory. Mean disc thickness was calculated by averaging the thickness of eight locations at 45° angles. Green volume was calculated as the product of mean disc thickness and cross-sectional area of the disc. After being oven-dried at 105°C for 5 d, which was determined to be the length of time until constant mass was reached (Fig. 2.3), each disc was re-weighed to calculate moisture content, dry mass, and basic specific gravity (Williamson and Wiemann 2010). The smaller diameter discs were dried for 24 h as these discs reached a constant mass in less time than the larger diameter discs (Fig. 2.3). The basic density, in units of kg/m^3 , of each disc was estimated by multiplying the basic specific gravity of the disc by the basic density of water, $10^3 \text{ kg}/\text{m}^3$. From these disc samples, models were developed for the vertical density of the dominant stem (see Ch. 4).

The second random branch path chosen was used to determine if differences in density exist between the dominant stem path and any other path that could have been chosen. Tree disc samples were harvested at every AF for the random branch path to reduce the cost of sampling. The random branch path discs were processed using the same protocols previously outlined for the dominant stem discs. From these disc samples, models were developed for the density of the random branch path (see Ch. 4).

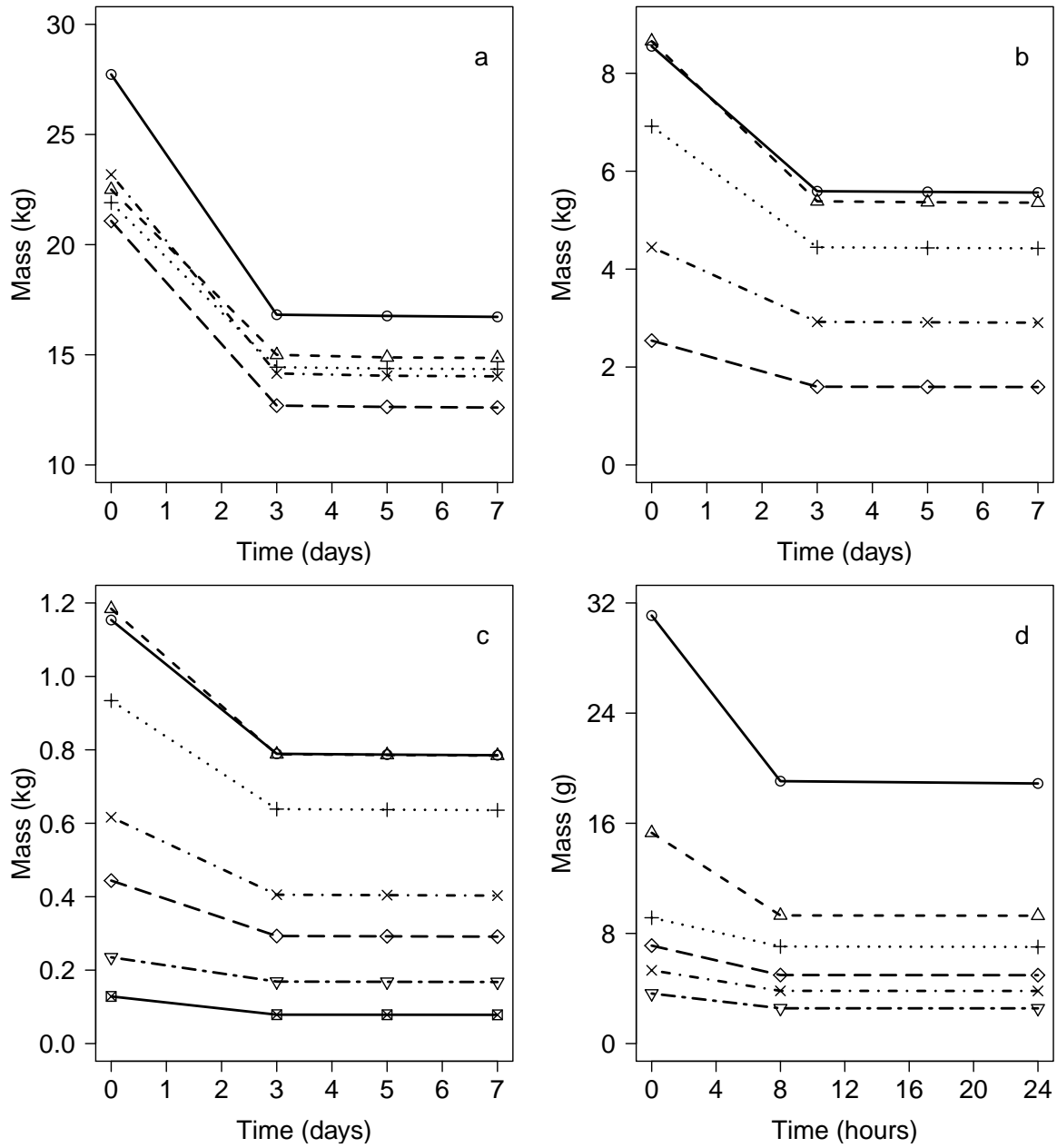


Figure 2.3: The drying time for discs sampled from an American beech tree with a diameter at breast height, DBH, of 75.4 cm. (a) The oven-drying time for large discs with diameter outside bark, dob, greater than 50.0 cm. (b) The oven-drying time for medium discs with dob ranging from 20.1 to 50.0 cm. (c) The oven-drying time for small discs with dob ranging from 5.1 to 20.0 cm. (d) The oven-drying time for very small discs with dob ranging from 0.1 to 5.0 cm. Each line and symbol represents a different sampled disc in the respective dob size class.

2.3.2 Bark Density Sampling

Tree basic density measurements (above) are a combination of wood and bark. Therefore, additional measurements of bark were taken to compare bark density to tree density. For a randomly selected subset of trees that included one tree for each species from each 10-cm DBH class, bark samples approximately 2 x 2 cm were removed from oven-dried discs with a chisel and re-hydrated for 24 h in distilled water. The re-hydrated bark samples were then measured for green volume. For samples that sank during the re-hydration process, the suspension method was used (Hughes 2005). For bark samples that did not sink during the re-hydration process, the water displacement method was applied using a needle instead (Martinez-Cabrera et al. 2009). After green volume was determined, the bark samples were dried for 24 h at 105°C to get oven-dry mass. Basic density for the bark was calculated in the same manner as tree density from previous discs. Due to the difficulty of removing bark from small discs (diameter outside bark < 4.0 cm), bark samples were not taken along the entire path length for both dominant stem and random branch paths of the selected subset of trees.

2.4 Mass Sampling

2.4.1 Dominant Stem Mass Sampling

The dominant stem sectional mass was determined by the product of dominant stem sectional volume (eq. 2.1) and basic densities from sampled discs. The basic density of a section was calculated by a weighted average with cross-sectional area as the weight of basic density for the disc from the top of the section and the previous section's disc. The mass of the stump section was approximated by the product of stump sectional volume and density of the DBH disc. Mass of the top section was approximated by the product of the top sectional volume and density of the last disc sampled. The cumulative dominant stem mass profile was found similarly to volume by substituting mass for volume in equation 2.2.

2.4.2 Whole-tree Mass — Random Branch Sampling

An estimate of the total aboveground mass of an entire tree outside bark, M_{WT} , was obtained similarly to whole-tree volume but using only the second random branch path. For each sectional volume in the random branch path, a weighted average of random branch path basic densities were used to convert the measurements to mass, analogous to the dominant stem mass sampling. Whole-tree mass in this study was defined as the mass of the dominant stem and branches excluding leaves. The total mass of branches was calculated similar to volume by subtracting the total dominant stem mass from the estimate of whole-tree mass. Total branch mass was distributed back to each first order branch immediately off the dominant stem as for volume (eq. 2.4). Figure 2.2 conceptualizes the re-distribution of branch mass to a profile of whole-tree mass (similar to a whole-tree volume profile) as a function of relative height. From these measurements, models for dominant stem and whole-tree mass were developed in Chapter 4.

2.5 Study Site

The study site is 20.8 ha of a 36-ha second-growth maple-beech stand at the Fred Russ Experimental Forest in southwestern Michigan owned by Michigan State University. The Fred Russ Experimental Forest is located in Cass County, in Decatur, Michigan (Fig. 2.4), with a total area of 381 ha that supports a diverse range of species and stand conditions. Kalamazoo, Ormas, and Oshtemo are the three primary soil series found at the site. The Kalamazoo and Oshtemo soil series are fine-loamy and coarse-loamy, mixed, mesic typic hapludalfs, respectively. The Ormas soil series is a coarse-loamy, mixed, mesic arenic hapludalfs on an outwash plain landform with a level topography (Soil Survey Staff 2011). Average annual precipitation over 30 years is 1035 mm (NCDC 2011).

In the spring of 2010, a windstorm uprooted more than 200 trees in the stand. After salvaging the wind-thrown trees, the residual basal area of the stand was $22.13 \frac{m^2}{ha}$. No

inventory data for this stand was available prior to the windstorm, so caution should be taken when generalizing from the models developed from wind-thrown trees to the residual stand. Tables 2.1 and 2.2 summarize the average number of trees per ha and mean basal area in $\frac{m^2}{ha}$ by species and DBH class for the residual stand, respectively.

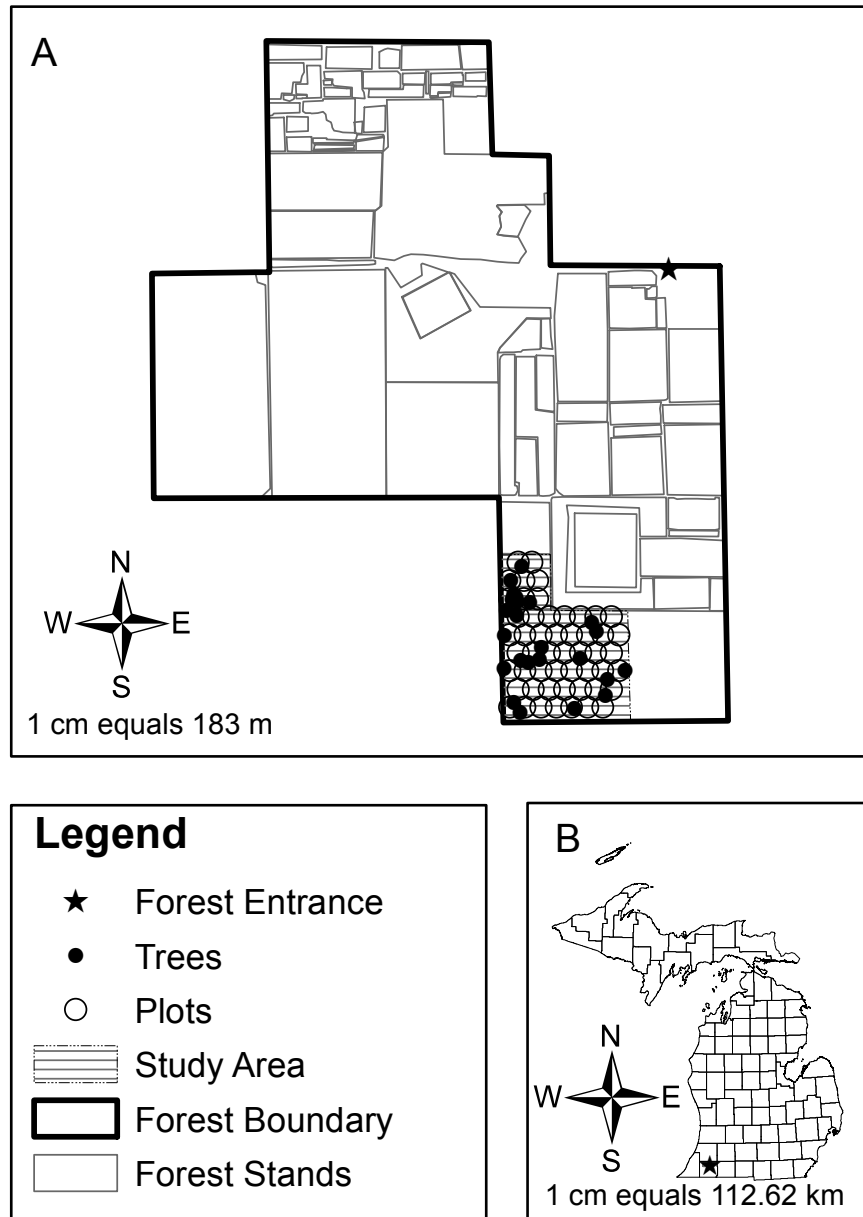


Figure 2.4: (A) Shows the location of the 20.8-hectare research area in the 36-hectare second-growth maple-beech stand, fixed-area plots, and sampled trees within the Fred Russ Experimental Forest. (B) The star represents the location of the entrance to the Fred Russ Experimental Forest in Cass County, Michigan.

Table 2.1: Summary of the mean number of trees per ha by species and 10 cm diameter at breast height (DBH) class for the residual stand.

Species	DBH Class (cm)									
	10	20	30	40	50	60	70	80	90	Total
American beech (<i>Fagus grandifolia</i> Ehrh.)	8.55	4.28	4.75	3.33	5.70	5.70	4.28	3.33	2.38	42.30
Sugar maple (<i>Acer saccharum</i> Marsh.)	21.38	35.17	28.04	22.81	15.21	3.80	1.43	1.90	0.48	130.21
Black cherry (<i>Prunus serotina</i> Ehrh.)	—	0.48	—	—	—	—	—	—	—	0.48
American basswood (<i>Tilia americana</i> L.)	—	—	0.48	0.48	—	—	—	0.48	—	1.44
Slippery elm (<i>Ulmus rubra</i> Muhl.)	1.43	0.95	—	—	—	0.48	0.48	—	—	3.34
American hophornbeam (<i>Ostrya virginiana</i> Mill.)	1.43	—	—	—	—	—	—	—	—	1.43
Tulip-poplar (<i>Liriodendron tulipifera</i> L.)	—	0.48	—	—	—	0.48	—	0.48	0.48	1.92
White ash (<i>Fraxinus americana</i> L.)	—	—	0.48	—	—	—	—	—	—	0.48
All	32.79	41.26	33.75	26.62	20.91	10.46	6.19	6.19	3.34	181.60

Table 2.2: Summary of the average basal area in $\frac{m^2}{ha}$ by species and 10 cm diameter at breast height (DBH) class for the residual stand.

Species	DBH Class (cm)									
	10	20	30	40	50	60	70	80	90	Total
American beech (<i>Fagus grandifolia</i> Ehrh.)	0.09	0.12	0.37	0.43	1.15	1.57	1.59	1.62	1.55	8.47
Sugar maple (<i>Acer saccharum</i> Marsh.)	0.27	1.13	1.96	2.92	2.98	1.04	0.59	0.94	0.33	12.16
Black cherry (<i>Prunus serotina</i> Ehrh.)	—	0.01	—	—	—	—	—	—	—	0.01
American basswood (<i>Tilia americana</i> L.)	—	—	0.04	0.07	—	—	—	0.25	—	0.36
Slippery elm (<i>Ulmus rubra</i> Muhl.)	0.02	0.04	—	—	—	0.14	0.17	—	—	0.37
American hophornbeam (<i>Ostrya virginiana</i> Mill.)	0.02	—	—	—	—	—	—	—	—	0.02
Tulip-poplar (<i>Liriodendron tulipifera</i> L.)	—	0.02	—	—	—	0.15	—	0.25	0.29	0.71
White ash (<i>Fraxinus americana</i> L.)	—	—	0.03	—	—	—	—	—	—	0.03
All	0.40	1.32	2.40	3.42	4.13	2.90	2.35	3.06	2.17	22.13

2.6 Tree Selection

A sample of 32 wind-thrown trees were measured with intact crowns from the population of uprooted trees. Sampling began in late spring of 2010 and included as wide a range of DBH as possible, irrespective of species, with at least one individual in each 10 cm DBH class ranging from 10 - 90 cm classes (Fig. 2.5). Figure 2.5 shows the relative frequency of the DBH distribution for the residual stand in 10 cm classes. Selected trees were relatively isolated from other wind-thrown trees so that the branches were easily measurable. The sample trees had a mean DBH of 50.9 cm and a mean height of 29.4 m with 87.5 percent of the trees being either American beech (*Fagus grandifolia* Ehrh.) or sugar maple (*Acer saccharum* Marsh., Table 2.3). Table 2.3 lists the summary statistics by species of sample size, DBH, and height of the 32 sample trees.

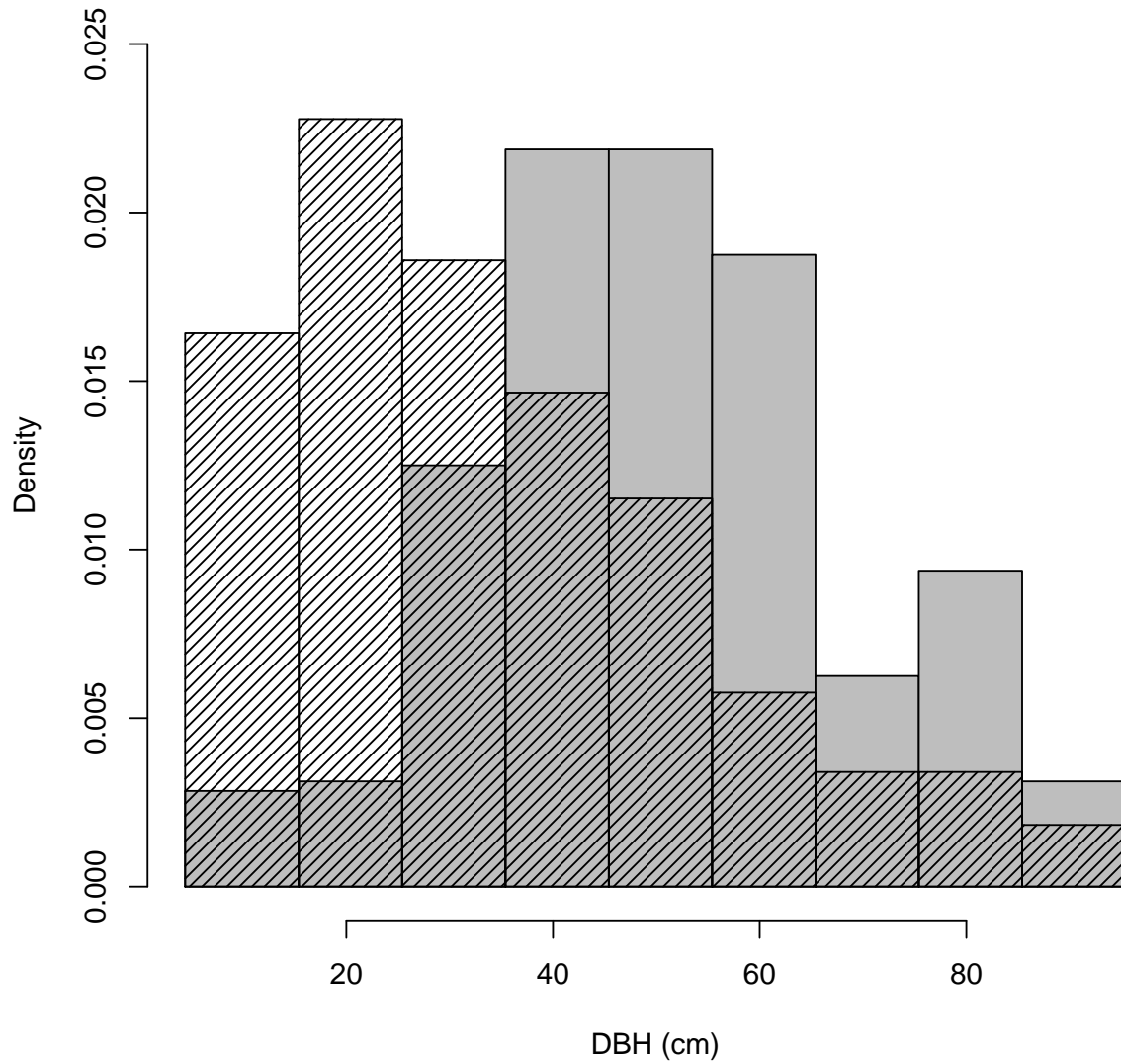


Figure 2.5: Histogram of the relative frequency of the residual stand, represented by diagonal line filled bars, and the sampled trees, represented by gray filled bars, divided into 10 cm diameter at breast height (DBH) classes.

Table 2.3: Species, code, sample size (n), diameter at breast height (DBH), and height (H) summary statistics for the data set.

Species	Code	n	Mean DBH (cm) [SD, min, max]	Mean H (m) [SD, min, max]
American beech (<i>Fagus grandifolia</i> Ehrh.)	FG	15	56.6 [19.5, 15.3, 91.1]	30.8 [4.9, 16.5, 36.1]
Sugar maple (<i>Acer saccharum</i> Marsh.)	AS	13	44.6 [12.4, 27.5, 63.2]	28.4 [3.3, 22.2, 34.0]
Pignut hickory (<i>Carya glabra</i> Mill.)	CG	1	62.6 [NA, NA, NA]	34.5 [NA, NA, NA]
Black cherry (<i>Prunus serotina</i> Ehrh.)	PS	1	23.0 [NA, NA, NA]	19.1 [NA, NA, NA]
American basswood (<i>Tilia americana</i> L.)	TA	1	41.0 [NA, NA, NA]	24.0 [NA, NA, NA]
Slippery elm (<i>Ulmus rubra</i> Muhl.)	UR	1	71.5 [NA, NA, NA]	33.3 [NA, NA, NA]
All	ALL	32	50.9 [17.6, 15.3, 91.1]	29.4 [4.7, 16.5, 36.1]

CHAPTER 3

CUMULATIVE VOLUME PROFILES FOR DOMINANT STEMS AND WHOLE TREES

3.1 Related Dominant Stem Taper and Volume Modeling

3.1.1 Dominant Stem Taper Modeling

Taper modeling is generally defined as the fitting of a mathematical function that graphically represents the form of the observed dominant stem. Foresters widely use taper models because diameter at any point along the dominant stem of a tree can be predicted from a few predictor variables measured on a tree. The most commonly used predictor variables are DBH and total height of a tree. As merchantability standards have changed over time, taper models have been flexible enough to account for the changes in minimum commercially accepted upper stem diameters. Numerous taper models have been developed to describe the dominant stem of specific species, and only a selection of these studies are reviewed here. The taper model examples that follow were chosen based their relevance to this current research.

Many taper models have been formulated for the dominant stem of a tree, as this portion is the simplest to model and has the greatest economic value. Conceptually, the dominant stem is divided into three distinct sections: the lower, the middle, and the upper section. Typically, the geometric shape of the lower section is modeled as a neiloidal shape, the middle section follows a paraboloidal shape, and the top section follows a conical shape (Newnham 1992). Max and Burkhart (1976) applied segmented polynomial functions to each of these different sections and joined them together with indicator variables. On the other hand, Kozak (1988) used a variable-exponent taper model in which a single continuous function was used and only the exponent varied depending on the location along the stem.

In the previous examples and in taper models in general, the effect of branching on the dominant stem has been largely ignored (but see Adu-Bredu et al. 2008). However, it is recognized that crown variables (e.g., crown height, crown length, or crown ratio) effect taper (Larson 1963, Valentine and Gregoire 2001, Leites and Robinson 2004). For example, Valentine and Gregoire (2001) use a combined variable-exponent and variable-form taper model with the height to the base of the live crown as a predictor. Leites and Robinson (2004) found crown length and crown ratio of an individual tree to improve the fit of the dominant stem taper models being tested.

One study directly dealt with the effects of branching on dominant stem taper models; Adu-Bredu et al. (2008) studied the stem profile of teak (*Tectona grandis*, L.f.) in West Africa. Their model explicitly accounted for up to two major forks branching off the dominant stem. Their profiles showed distinct reduction in the dominant stem profile whenever branching occurs. This model accounted for the effect of branching on the dominant stem but did not account for the volume of the branches.

Mixed-effects taper modeling is prevalent in the literature because of the hierarchical structure of the data with measurements taken within an individual tree and between trees (Valentine and Gregoire 2001, Leites and Robinson 2004, Westfall and Scott 2010). Valentine and Gregoire (2001) employed mixed-effects modeling to incorporate the correlation of multiple measurements on the same tree, and found the inclusion of random effects gave better fits to individual trees compared to fixed effects only. As measurements taken closer together within a single tree are more likely to be similar than distant measurements on the same tree. Westfall and Scott (2010) modified the model developed by Valentine and Gregoire (2001) and applied it to commercial tree species of the northeastern U.S. The modified model performed better than the original by re-arranging the random effects parameters and estimating the join points rather than explicitly using the height of the base of the live crown. Leites and Robinson (2004) applied random effects to an existing taper model to improve model fit and determined additional predictor variables explained additional variation that

was not originally considered in the taper model. Due to the hierarchical nature of the data, this research also employs a mixed-effects modeling framework.

A final important principle of continuous taper models is that the volume of the dominant stem can be predicted, or even segments of the stem to a specific limiting diameter or height via integration (Jordan et al. 2006). Conversely, the first derivative of a cumulative volume model is equivalent to a taper model. The current research uses the later principle to develop dominant stem and whole-tree cumulative volume models. The cumulative volume models are then applied to the taper modeling paradigm for the dominant stem and whole-tree so that dominant stem and whole-tree taper can be calculated with respect to relative height.

3.1.2 Volume Modeling

Total volumes have long been estimated by standard mensuration techniques for the dominant stem of trees (Avery and Burkhart 2002). The DBH and total tree height are the two most common predictor variables for total dominant stem volume (Hahn and Hansen 1991). Many different volume models have been developed across different regions of the U.S. (Woodall et al. 2011).

Researchers have not only been interested in total volume, but cumulative volume profiles at differing heights (Gregoire and Schabenberger 1996a;b, Fonweban et al. 2012). In these works, only the dominant stem cumulative volume profile was examined. The current research expands from the dominant stem only to the inclusion of a whole-tree volume profile.

Similar to taper modeling, mixed-effects modeling is prevalent for cumulative volume profiles (Gregoire and Schabenberger 1996a, Fonweban et al. 2012). Gregoire and Schabenberger (1996a) developed a cumulative dominant stem volume model using non-linear mixed effects to account for the spatial correlation of multiple measurements on an individual tree. They found that the mixed-effects model fit the individual trees better than the fixed-effects model, which did not account for within-tree correlation. However, the model fit was poor

for both mixed and fixed effects for the region of the stem below DBH. The follow-up to this study, by Gregoire and Schabenberger (1996b), re-defined parameters in the cumulative volume model to achieve a better fit at lower heights of the dominant stem. Fonweban et al. (2012) also found the mixed-effects modeling approach gave an improved fit over the fixed-effects models. They also modeled the covariance structure of the mixed-effects model and determined an increase in the residual variance of the models was present, so they recommended a simple unstructured covariance structure of the random effects would suffice. Due to the hierarchical nature of the data, this research employs a mixed-effects modeling framework with the assumption of an unstructured covariance structure.

Research on the relative volume of branches has received much less attention than the dominant stem (MacFarlane 2011). The allocation of aboveground volume relationships between tree volume and branch volume have recently been compared among similar trees with and without significant branching by MacFarlane (2010). In this work, the displacement of dominant stem volume to branches has been expanded by including the largest branches in the development of a varying-centroid method to predict volume ratios between the whole-tree and the dominant stem. The best predictor variables of these ratios were the interaction between crown ratio and diameter of largest branch, and then the interaction between crown ratio and DBH. These results indicate that measurements of crown variables are needed to link the estimation of whole-tree volume to dominant stem volume.

Allometric scaling principles have also recently been used to relate large branch volume to dominant stem volume to estimate whole-tree volume. MacFarlane (2011) collected volume data of 11 common hardwood species in Michigan. Volume expansion factors, defined as the ratio of branch-plus-bole to bole volume, were used to estimate the whole-tree volume. It was found that, beyond the usual metrics of DBH and height for inventorying a tree, crown variables were also necessary parameters for accurate calculation of volume expansion factors. Once again, the best predictor variables were found to be the diameter of the largest branch and the crown ratio, indicating that crown variables are important for estimation of

whole-tree volume. However, a minimum upper branch diameter of 9 cm was imposed in the collection of the branch volume data. This research expands upon this previous study by not limiting branch diameter in estimating whole-tree volume.

The primary objective of this chapter is to develop a new vertical profile model to relate whole-tree volume to dominant stem volume, which can estimate component-wise tree attributes of dominant stem and branches. The cumulative volume profiles developed here build upon previous research by expanding dominant stem models to the whole aboveground tree. The first derivative of the cumulative volume profiles is the taper model, and it will be combined with density profiles for mass modeling in Chapter 4.

3.2 Models

The data used for model development were trees sampled from a second-growth maple-beech stand at Fred Russ Experimental Forest (see Ch. 2). A fixed-effects model (shown below, see eqs. 3.1 and 3.2) was selected for each individual tree with parameters estimated using the `nlsList` function from the `nlme` package (Pinheiro et al. 2011). The parameters from the fixed-effects model were used as starting values for the mixed-effects models using the `nlme` function in the `nlme` package. The models were fit to all species, American beech, and sugar maple with the best-fit model being selected based on the lowest Akaike's Information Criterion, AIC, value. American beech and sugar maple were fitted to the model individually as multiple observations of each of these species were present. Models were also selected based on having the smallest mean relative difference in relation to estimated total volumes. All statistical models were developed in the R statistical environment (R Development Core Team 2010).

3.2.1 Dominant Stem Cumulative Volume Models

Non-linear regression modeling was used in developing the cumulative volume profiles for dominant stems in terms of relative height. The base fixed-effects model is modified from

the relative dominant stem volume model of MacFarlane (2010):

$$v_{DOM} = V_{DOM} * (1 - (1 - rh)^{\alpha_1}) + \epsilon, \quad (3.1)$$

where v_{DOM} is the dominant stem cumulative volume in m^3 at a relative height (rh), V_{DOM} is total dominant stem volume in m^3 , α_1 is a parameter to be estimated, and ϵ is an error term.

3.2.2 Whole-tree Cumulative Volume Models

The whole-tree cumulative volume model uses the modified relative dominant stem volume model (eq. 3.1) for the portion below relative crown height with the addition of another model, where the intercept is shifted to relative crown height for the portion above relative crown height:

$$v_{AC} = V_{RCH} + \beta_V * (1 - (1 - (rh - RCH))^{\alpha_2}) + \epsilon, \quad (3.2)$$

where v_{AC} is the dominant stem plus branches cumulative volume in m^3 at a relative height (rh), V_{RCH} is total tree volume at relative crown height (RCH) in m^3 , β_V is either a fixed parameter or an estimated parameter, α_2 is a parameter to be estimated, and ϵ is an error term. In the case where β_V is fixed, the new model has the same form as model 3.2 setting

$$\beta_V = \frac{V_{WT} - V_{RCH}}{1 - RCH^{\alpha_2}}, \quad (3.3)$$

where V_{WT} is the total whole-tree volume in m^3 .

Models 3.1 and 3.2 or models 3.1 and 3.3 are combined to get the whole-tree cumulative volume profile as

$$v_{WT} = I_1 v_{DOM} + I_2 v_{AC}, \quad (3.4)$$

where v_{WT} is the whole-tree cumulative volume in m^3 at a relative height, I_1 is an indicator variable with a value of 1 when relative height is below relative crown height and a value of 0 when relative height is above relative crown height, and I_2 is an indicator variable with values of 0 when relative height is below relative crown height and 1 when relative height is above relative crown height.

3.2.3 Centroid of Dominant Stem and Whole-tree Volume Models

The centroid of volume is defined as the location aboveground in a tree where half of the total volume is above and half of the total volume is below the location (Forslund 1982). This location along the dominant stem has been shown to be an accurate and precise estimate of dominant stem volume requiring a single diameter measurement (Wood et al. 1990, Wiant et al. 1991). MacFarlane (2010) expands the theory of the centroid method to the whole tree. The centroid of dominant stem volume is found by re-arranging the cumulative dominant stem volume (model 3.1) in terms of relative volume, setting relative volume equal to a half, and solving for relative height, similar to equation 4 in MacFarlane (2010):

$$rh_{DOM.c} = 1 - 0.5^{\frac{1}{\alpha_1}}, \quad (3.5)$$

where $rh_{DOM.c}$ is the centroid of dominant stem volume, and α_1 is the estimated parameter from model 3.1.

The centroid of whole-tree volume has two possible solutions due to the segmented model (eq. 3.4). The first solution occurs when the centroid of whole-tree volume occurs in the first segment of the model, below relative crown height:

$$rh_{WT.c} = 1 - \left(1 - \frac{V_{WT}}{2V_{DOM}}\right)^{\frac{1}{\alpha_1}}, \quad (3.6)$$

where $rh_{WT.c}$ is the centroid of whole-tree volume, V_{WT} is the total whole-tree volume, V_{DOM} is the total dominant stem volume, and α_1 is the estimated parameter from model 3.1. Otherwise, the second solution occurs when the centroid of whole-tree volume occurs in the second segment of the model, above relative crown height:

$$rh_{WT.c} = 1 + RCH - \left(1 - \frac{V_{WT}}{2\beta_V} + \frac{V_{RCH}}{\beta_V}\right)^{\frac{1}{\alpha_2}}, \quad (3.7)$$

where RCH is relative crown height, β_V is the fixed parameter from model 3.3, V_{RCH} is the volume at relative crown height, and α_2 is the estimated parameter from model 3.2.

3.3 Results

3.3.1 Total Volume Estimates

Table 3.1 shows the summary statistics for the total volume of dominant stems and whole trees by species and for all trees in the dataset. The total dominant stem volume and mean total whole-tree volume estimates are shown in Table 3.2 for each individual. Table 3.2 also shows the two whole-tree volume estimates for each tree by random branch path, the associated standard deviation, and coefficient of variation around the mean whole-tree total volume. The smallest coefficient of variation of 0.01 was found in the 40 cm DBH class, and the maximum coefficient of variation of 0.49 was found in the largest DBH, 90 cm, class. The average coefficient of variation of whole-tree volume for all trees was 0.11 with 20 of the 32 trees having a coefficient of variation of less than or equal to 0.10. However, a larger coefficient of variation was present in both the small and large DBH classes. The total volume of both dominant stems and whole trees showed an increasing pattern for larger DBH for all species, American beech, and sugar maple (Fig. 3.1).

Table 3.1: Species code (spp), number of trees (n), mean dominant stem volume (V_{DOM}), mean total volume (V_{WT}) with standard deviation (SD), minimum (min), and maximum (max) values by species.

spp	n	Mean V_{DOM} (m ³) [SD, min, max]	Mean V_{WT} (m ³) [SD, min, max]
FG	15	3.70 [2.32, 0.14, 8.06]	8.04 [7.87, 0.23, 33.17]
AS	13	2.27 [1.36, 0.74, 4.86]	3.85 [2.53, 1.06, 8.84]
CG	1	5.16 [NA, NA, NA]	8.60 [NA, NA, NA]
PS	1	0.36 [NA, NA, NA]	0.50 [NA, NA, NA]
TA	1	1.47 [NA, NA, NA]	2.00 [NA, NA, NA]
UR	1	6.39 [NA, NA, NA]	13.85 [NA, NA, NA]
ALL	32	3.07 [2.10, 0.14, 8.06]	6.11 [6.17, 0.23, 33.17]

Table 3.2: Species code (spp), diameter at breast height (DBH), DBH class (Dclass), total dominant stem volume (V_{DOM}), total volume estimate from the first random branch sample (V_{WT_1}), total volume estimate from the second random branch sample (V_{WT_2}), mean total volume (V_{WT}), standard deviation of total volume (SD), and coefficient of variation of total volume (CV) summary statistics for each individual tree.

spp	DBH	Dclass	V_{DOM}	V_{WT_1}	V_{WT_2}	V_{WT}	SD of V_{WT}	CV of V_{WT}
FG	15.3	10	0.14	0.24	0.23	0.23	0.01	0.03
PS	23.0	20	0.36	0.51	0.49	0.50	0.01	0.03
AS	27.5	30	0.74	1.11	1.01	1.06	0.07	0.07
AS	31.7	30	0.82	1.71	1.21	1.46	0.35	0.24
AS	33.1	30	1.13	1.56	1.91	1.73	0.25	0.14
AS	33.9	30	0.95	1.73	2.21	1.97	0.34	0.17
AS	35.6	40	1.29	2.03	2.24	2.13	0.14	0.07
FG	36.7	40	1.25	1.98	2.64	2.31	0.47	0.20
AS	38.8	40	1.54	2.19	2.05	2.12	0.10	0.05
TA	41.0	40	1.47	2.01	1.99	2.00	0.01	0.01
AS	42.8	40	2.39	2.89	2.92	2.90	0.02	0.01
FG	42.9	40	1.86	3.25	3.52	3.38	0.19	0.06
FG	45.1	40	2.73	3.71	5.40	4.55	1.20	0.26
FG	46.0	50	2.51	3.46	4.38	3.92	0.65	0.17
FG	47.1	50	2.42	3.95	4.46	4.21	0.36	0.09
AS	48.1	50	2.26	4.41	3.82	4.11	0.42	0.10
AS	48.5	50	2.79	4.64	4.12	4.38	0.37	0.08
FG	50.1	50	2.10	4.68	6.13	5.41	1.03	0.19
AS	54.6	50	2.85	5.32	4.66	4.99	0.47	0.09
FG	55.1	50	3.32	4.87	5.87	5.37	0.71	0.13
FG	56.3	60	3.77	6.81	7.04	6.92	0.16	0.02
AS	60.4	60	3.49	7.05	6.82	6.94	0.17	0.02
AS	61.9	60	4.86	7.53	7.28	7.40	0.17	0.02
CG	62.6	60	5.16	8.77	8.44	8.60	0.24	0.03
AS	63.2	60	4.35	8.47	9.21	8.84	0.52	0.06
FG	63.6	60	4.34	6.63	7.42	7.03	0.56	0.08
FG	67.5	70	3.91	6.46	8.63	7.55	1.54	0.20
UR	71.5	70	6.39	13.66	14.04	13.85	0.27	0.02
FG	75.4	80	4.47	8.86	11.74	10.30	2.04	0.20
FG	78.2	80	7.04	12.31	16.83	14.57	3.20	0.22
FG	78.5	80	7.61	11.45	11.83	11.64	0.27	0.02
FG	91.1	90	8.06	21.75	44.58	33.17	16.14	0.49

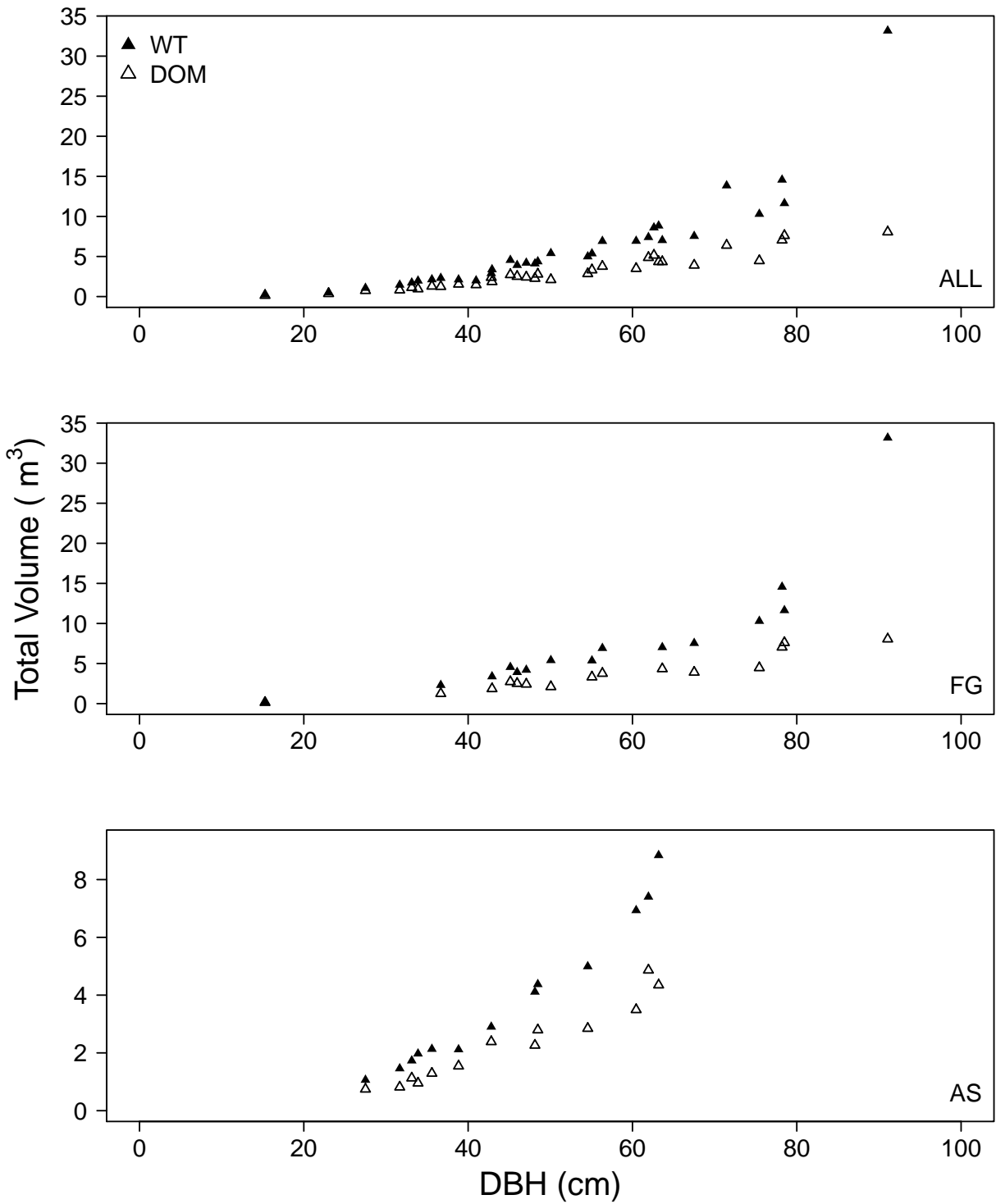


Figure 3.1: The total volume, in m^3 , of sampled trees for the dominant stem (DOM) and whole tree (WT) versus diameter at breast height (DBH), in cm, for all trees (ALL), American beech (FG), and sugar maple (AS).

3.3.2 Cumulative Volume Profiles

The models, below, added random effects to models 3.1 and 3.2 to create mixed-effects models. The model selected for the cumulative volume of the dominant stem applied to all species, American beech, and sugar maple is

$$v_{DOM_{ij}} = V_{DOM_j} * (1 - (1 - rh_{ij})^{\alpha_1 + u_{1j}}) + \epsilon_{ij}, \quad (3.8)$$

where $v_{DOM_{ij}}$ is the cumulative volume of stem position i for tree j in m^3 , V_{DOM_j} is total dominant stem volume in m^3 , rh_{ij} is relative height of position i for tree j , α_1 is a fixed effect parameter to be estimated, u_{1j} is a random effect parameter to be estimated, and ϵ_{ij} is a random error term. Table 3.3 gives the parameter estimates of model 3.8. The all-species model was selected as the best model because it had the lowest AIC of the three models, and the total dominant stem model was compatible with the final observation of total dominant stem volume from Smalian's formula, as the mean relative difference is equal to zero (to three decimal places).

Table 3.3: Parameter estimates of model 3.8 for the cumulative volume of the dominant stem for the all-species (ALL), American beech (FG), and sugar maple (AS) mixed-effects models. For the fixed parameters, the standard error of estimates is given in parantheses.

Parameter	ALL Estimate	FG Estimate	AS Estimate
α_1	2.783 (0.048)	2.833 (0.068)	2.782 (0.076)
$\text{var}(u_{1j})$	0.067	0.062	0.072
ϵ_{ij}	0.045	0.049	0.030
AIC	-6479.677	-3199.169	-2955.086
Mean Relative Difference	0.000	0.000	0.000

Two potential mixed-effects models for the portion of the whole-tree model above relative crown height are given below:

$$v_{AC_{ij}} = V_{RCH_j} + (\beta_V + u_{3j}) * (1 - (1 - (rh_{ij} - RCH_j))^{\alpha_2 + u_{2j}}) + \epsilon_{ij}, \quad (3.9)$$

where $v_{AC_{ij}}$ is the whole-tree cumulative volume of stem position i in tree j in m^3 , V_{RCH_j} is total tree volume at relative crown height (RCH) in m^3 , β_V and α_2 are fixed effect

parameters to be estimated, u_{2j} and u_{3j} are random effect parameters to be estimated, and ϵ_{ij} is a random error term. In the case where β_V is fixed for tree j , the new model has the same form as model 3.9, except only one random effect parameter (u_{2j}), with

$$\beta_{Vj} = \frac{V_{WTj} - V_{RCHj}}{1 - RCH_j^{\alpha_2 + u_{2j}}}, \quad (3.10)$$

where V_{WTj} is the total whole-tree volume for tree j in m^3 .

The final whole-tree cumulative volume profile (similar to eq. 3.4) now uses models 3.8 and 3.9 or models 3.8 and 3.10 for the segmented model:

$$v_{WTij} = I_1 v_{DOMij} + I_2 v_{ACij}, \quad (3.11)$$

where v_{WTij} is the whole-tree cumulative volume of stem position i in tree j in m^3 , I_1 is an indicator variable with a value of 1 when relative height is below relative crown height and a value of 0 when relative height is above relative crown height, and I_2 is an indicator variable with values of 0 when relative height is below relative crown height and 1 when relative height is above relative crown height. Tables 3.4 and 3.5 give the parameter estimates for models 3.9 and 3.10.

Model 3.10 was chosen as the best-fit final model of the two for the portion of the segmented whole-tree cumulative volume model above relative crown height as it had a lower AIC of -644.505 for the all-species model compared to an AIC of -375.868 for the all-species model 3.9. The total whole-tree volume for model 3.10 is also compatible with the total whole-tree volume estimate given by random branch sampling. The all-species model 3.10 was selected over the American beech model based on AIC; however, the sugar maple model would be selected over the all-species model using AIC. The all-species model was selected as the final model for whole-tree volume of all trees rather than applying a separate sugar maple model to maple trees to be compatible with the first segment of the segmented model, as the first segment of the model below relative crown height was fit using an all-species model.

Table 3.4: Parameter estimates of model 3.9 for the cumulative whole-tree volume above relative crown height for the all-species (ALL), American beech (FG), and sugar maple (AS) mixed-effects models. For the fixed parameters, the standard error of estimates is given in parantheses.

Parameter	ALL Estimate	FG Estimate	AS Estimate
α_2	4.328 (0.289)	4.345 (0.407)	4.339 (0.418)
β	4.054 (0.879)	5.596 (1.670)	2.326 (0.498)
$\text{var}(u_{2j})$	2.233	2.177	2.104
$\text{var}(u_{3j})$	24.683	41.736	3.216
$\text{cov}(u_{2j}, u_{3j})$	0.512	0.448	-0.156
ϵ_{ij}	0.191	0.242	0.091
AIC	-375.868	220.736	-1059.232
Mean Relative Difference	0.499	0.496	0.664

Table 3.5: Parameter estimates of model 3.10 for the cumulative whole-tree volume above relative crown height for the all-species (ALL), American beech (FG), and sugar maple (AS) mixed-effects models. For the fixed parameters, the standard error of estimates is given in parantheses.

Parameter	ALL Estimate	FG Estimate	AS Estimate
α_2	4.461 (0.274)	4.487 (0.405)	4.445 (0.383)
$\text{var}(u_{2j})$	2.077	2.184	1.789
ϵ_{ij}	0.195	0.245	0.096
AIC	-644.505	80.574	-1115.357
Mean Relative Difference	0.000	0.000	0.000

Figures 3.2 and 3.3 show the dominant stem and whole-tree cumulative volume profile for the (a) minimum, (b) median, and (c) maximum DBH trees of American beech and sugar maple, respectively. The all-species parameter estimates were used for both the dominant stem (eq. 3.8) and whole-tree (eq. 3.11) profiles for both American beech and sugar maple. For American beech, the total whole-tree volume increases by a factor of ten in each successive profile, and the relative crown height also decreases with increasing DBH. A noticeable increase in branch volume, which is the region between the whole-tree and dominant stem cumulative volume profiles, is also present in each successive profile. The sugar maple profiles show similar patterns to the American beech with total whole-tree volume increasing by a factor of three in each successive profile. However, the relative crown height appears to

increase before decreasing with increasing DBH, and the branch volume also decreases before increasing with increasing DBH.

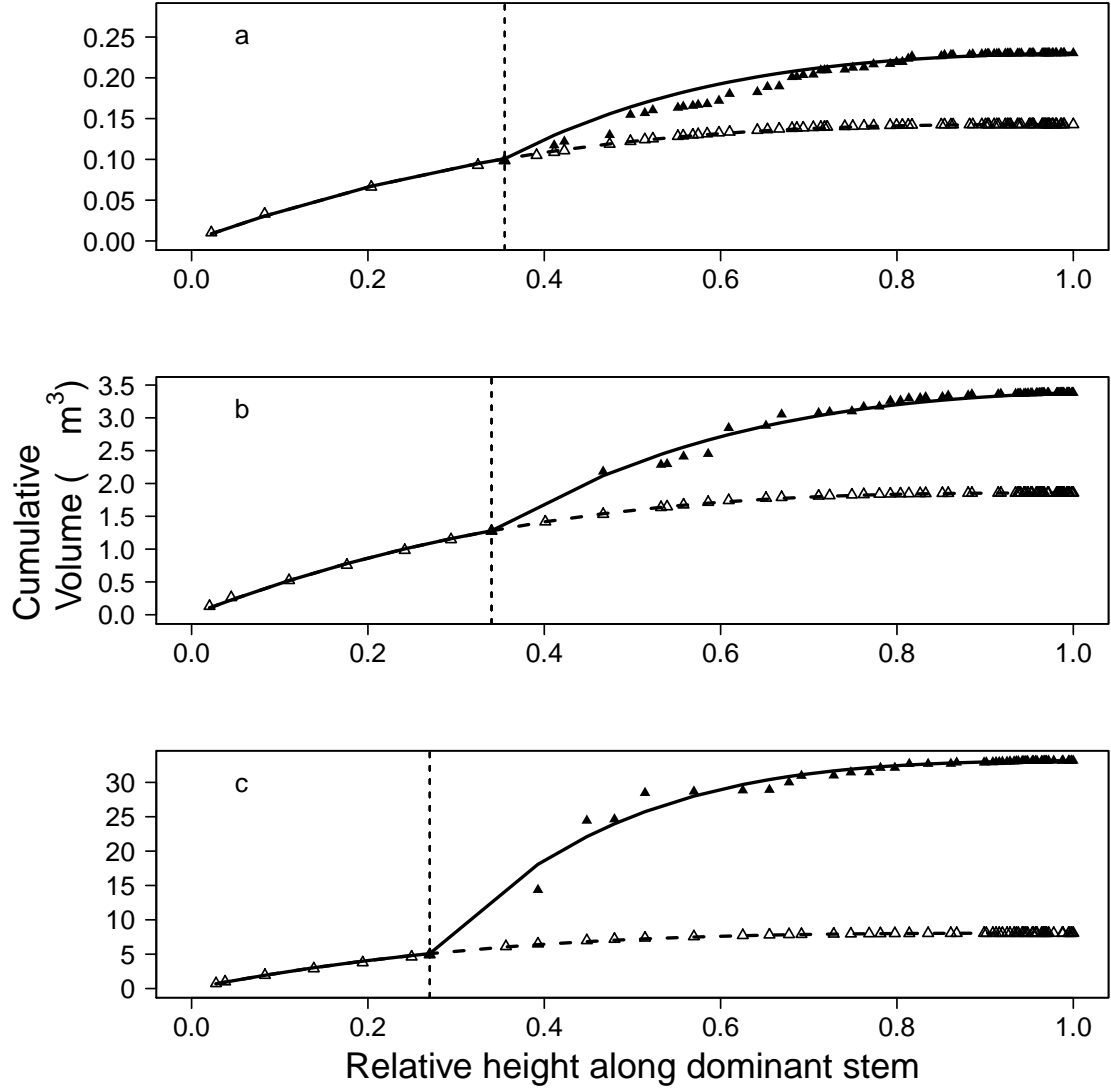


Figure 3.2: Cumulative volume, m^3 , profiles for the dominant stem (model 3.8), represented by a dashed line above relative crown height, and whole tree (model 3.11), represented as the solid line, as a function of relative height along the dominant stem for the (a) minimum, (b) median, and (c) maximum diameter at breast height (DBH) American beech (FG) trees. The vertical dashed line represents relative crown height.

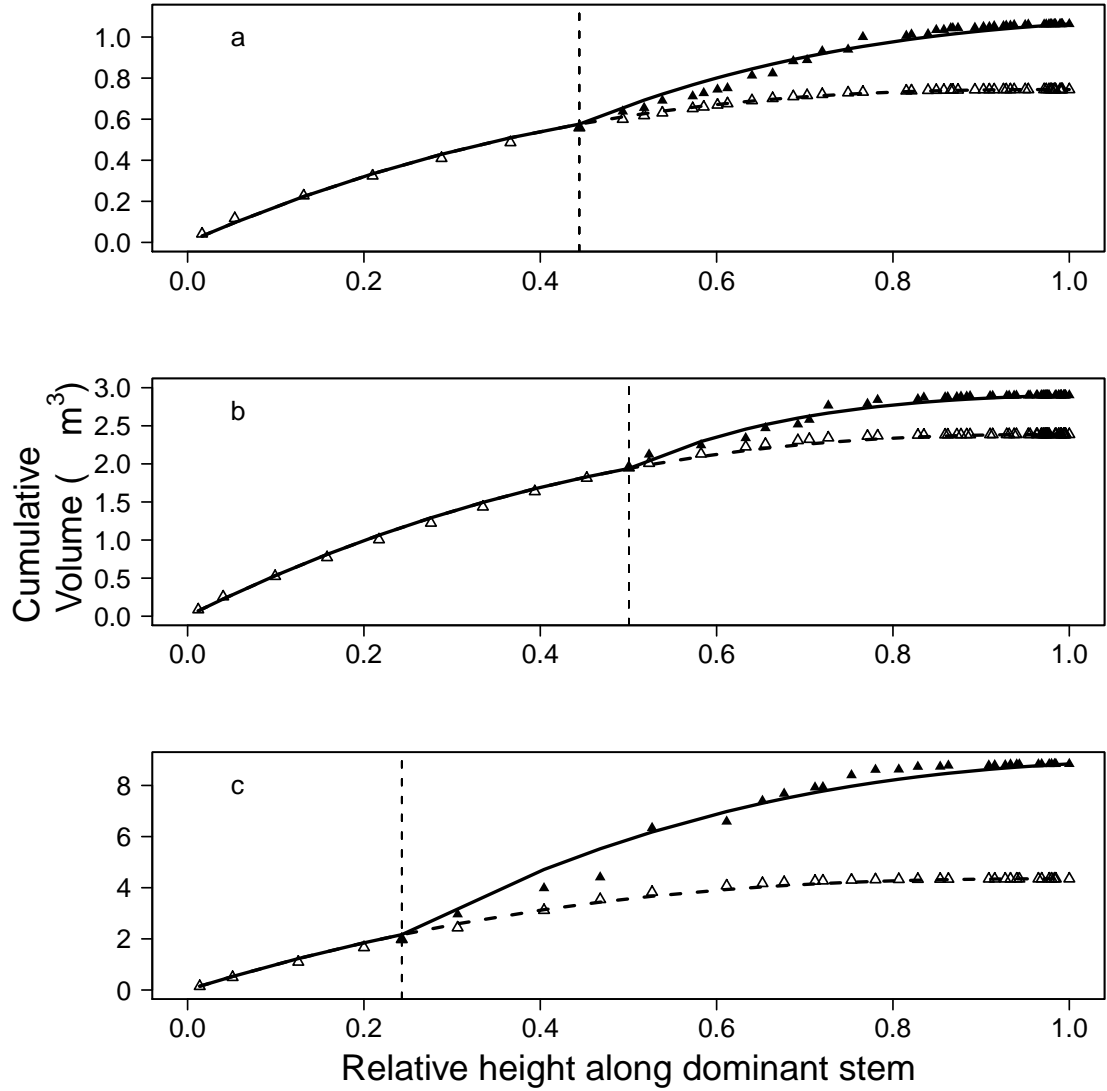


Figure 3.3: Cumulative volume, m^3 , profiles for the dominant stem (model 3.8), represented by a dashed line above relative crown height, and whole tree (model 3.11), represented as the solid line, as a function of relative height along the dominant stem for the (a) minimum, (b) median, and (c) maximum diameter at breast height (DBH) sugar maple (AS) trees. The vertical dashed line represents relative crown height.

3.3.3 Centroid of Dominant Stem and Whole-tree Volume Profiles

The centroid of dominant stem volume profile for tree j is similar to model 3.5 with the addition of a random effect, u_{1j} :

$$rh_{DOM.c_j} = 1 - 0.5^{\frac{1}{\alpha_1 + u_{1j}}}. \quad (3.12)$$

The mean centroid of dominant stem volume for all species was 0.222 (Table 3.6). Across species, the mean centroid of dominant stem volume ranged between 0.218 for American beech to 0.251 for pignut hickory. No definitive pattern for the centroid of dominant stem volume was seen across 10 cm DBH classes. Crown ratio ($CR = 1 - RCH$) was also examined for a potential pattern in the centroid of dominant stem volume (Table 3.7). Crown ratio classes (CRC) were divided to the nearest tenth with classes ranging from 0.5 to 0.9 indicating all of the trees had fairly long crowns. Unlike the DBH classes, the centroid of dominant stem volume showed a decreasing pattern across crown ratio classes.

Table 3.6: The mean centroid of dominant stem volume by species and 10 cm diameter at breast height (DBH) classes. Standard deviation is given in parentheses.

Species	DBH Class (cm)									
	10	20	30	40	50	60	70	80	90	All
FG	0.220 (NA)			0.227 (0.014)	0.222 (0.017)	0.220 (0.006)	0.206 (NA)	0.215 (0.028)	0.197 (NA)	0.218 (0.016)
AS			0.223 (0.017)	0.235 (0.016)	0.214 (0.014)	0.217 (0.027)				0.222 (0.018)
CG						0.251 (NA)				0.251 (NA)
PS		0.222 (NA)								0.222 (NA)
TA				0.241 (NA)						0.241 (NA)
UR							0.219 (NA)			0.219 (NA)
ALL	0.220 (NA)	0.222 (NA)	0.223 (0.017)	0.232 (0.014)	0.218 (0.015)	0.223 (0.022)	0.213 (0.009)	0.215 (0.028)	0.197 (NA)	0.222 (0.017)

Table 3.7: The mean centroid of dominant stem volume by species and crown ratio class (CRC). Standard deviation is given in parentheses.

Species	CRC					
	0.5	0.6	0.7	0.8	0.9	All
FG	0.229 (0.011)	0.236 (0.010)	0.208 (0.016)	0.213 (0.006)	0.201 (NA)	0.218 (0.016)
AS	0.240 (0.013)	0.225 (0.012)	0.208 (0.018)	0.232 (0.018)		0.222 (0.018)
CG		0.251 (NA)				0.251 (NA)
PS				0.222 (NA)		0.222 (NA)
TA		0.241 (NA)				0.241 (NA)
UR	0.219 (NA)					0.219 (NA)
ALL	0.231 (0.012)	0.233 (0.013)	0.208 (0.016)	0.221 (0.013)	0.201 (NA)	0.222 (0.017)

The centroid of whole-tree volume for tree j has two possible solutions due to the segmented model (eq. 3.11). Similar to the centroid of dominant stem volume profile, the final two solutions for the centroid of whole-tree volume have random effects added, u_{1j} and u_{2j} , to models 3.6 and 3.7, respectively:

$$rh_{WT.cj} = 1 - \left(1 - \frac{V_{WTj}}{2V_{DOMj}}\right)^{\frac{1}{\alpha_1 + u_{1j}}}, \quad (3.13)$$

$$rh_{WT.cj} = 1 + RCH_j - \left(1 - \frac{V_{WTj}}{2\beta} + \frac{V_{RCHj}}{\beta}\right)^{\frac{1}{\alpha_2 + u_{2j}}}. \quad (3.14)$$

Twenty-four trees had a centroid of whole-tree volume occur above relative crown height (eq. 3.14) with the remainder of the trees having centroids below relative crown height (eq. 3.13). The mean whole-tree centroid of volume for all species is 0.390 (Table 3.8). Across species, centroids of whole-tree volume ranged from 0.302 for black cherry to 0.499 for slippery elm, which was considerably larger than the centroid of dominant stem. No distinct pattern was observed for the centroid of whole-tree volume along DBH classes;

however, centroids of whole-tree volume clearly decreased with increasing crown ratio class (Table 3.9).

Figure 3.4 shows the relative cumulative volume profiles for the dominant stem and whole tree for the (a) minimum, (b) median, and (c) maximum DBH American beech trees. In terms of relative height, the dominant stem relative volume profile will always be greater than the whole-tree relative volume profile because the denominator of relative volume of total whole-tree volume will always be larger than dominant stem volume. For the three beech trees, the mean centroid shift from dominant stem to whole tree was 0.173. This was similar to the mean centroid shift from dominant stem to whole tree for all trees of 0.178.

Table 3.8: The mean centroid of whole-tree volume classified by species and 10 cm diameter at breast height (DBH) classes with the standard deviation given in parentheses.

Species	DBH Class (cm)									
	10	20	30	40	50	60	70	80	90	All
FG	0.382 (NA)			0.408 (0.042)	0.403 (0.101)	0.396 (0.108)	0.316 (NA)	0.414 (0.058)	0.375 (NA)	0.396 (0.066)
AS			0.383 (0.032)	0.362 (0.051)	0.393 (0.037)	0.380 (0.015)				0.380 (0.033)
CG						0.419 (NA)				0.419 (NA)
PS		0.302 (NA)								0.302 (NA)
TA				0.364 (NA)						0.364 (NA)
UR							0.499 (NA)			0.499 (NA)
ALL	0.382 (NA)	0.302 (NA)	0.383 (0.032)	0.382 (0.045)	0.399 (0.075)	0.392 (0.052)	0.407 (0.130)	0.414 (0.058)	0.375 (NA)	0.390 (0.056)

Table 3.9: The mean centroid of whole-tree volume by species and crown ratio class (CRC). Standard deviation is given in parentheses.

Species	CRC					
	0.5	0.6	0.7	0.8	0.9	All
FG	0.460 (0.052)	0.468 (0.012)	0.378 (0.012)	0.322 (0.008)	0.303 (NA)	0.396 (0.066)
AS	0.373 (0.073)	0.410 (0.022)	0.362 (0.011)	0.372 (0.016)		0.380 (0.033)
CG		0.419 (NA)				0.419 (NA)
PS				0.302 (NA)		0.302 (NA)
TA		0.364 (NA)				0.364 (NA)
UR	0.499 (NA)					0.499 (NA)
ALL	0.438 (0.070)	0.425 (0.039)	0.370 (0.014)	0.335 (0.031)	0.303 (NA)	0.390 (0.056)

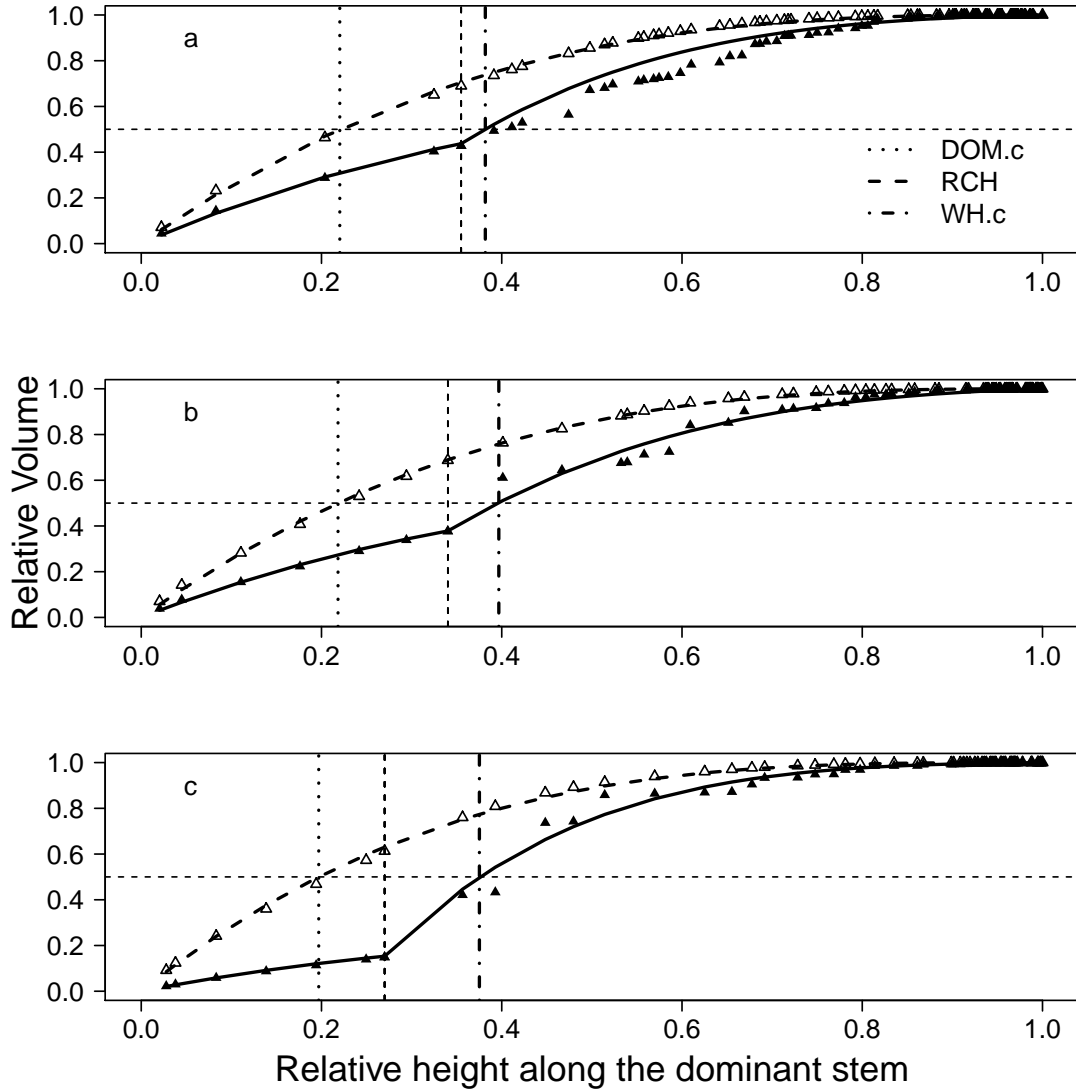


Figure 3.4: Dominant stem (model 3.8), represented by a dashed line, and whole-tree (model 3.11), represented as the solid line, relative volume profiles as a function of relative height along the dominant stem for the (a) minimum, (b) median, and (c) maximum diameter at breast height (DBH) American beech (FG) trees in the dataset. The horizontal dashed line indicates a relative volume of 0.5, the centroid of volume. The dotted vertical line indicates the relative height of the centroid of volume for the dominant stem (DOM.c), the vertical dashed line represents relative crown height, and the dash and dot vertical line indicates the relative height of the centroid of volume for the whole tree (WH.c).

3.4 Discussion

The majority of trees in the dataset had whole-tree volume estimates with a coefficient of variation less than 10 percent. However, a few trees had a much larger coefficient of variation. Trees with a high coefficient of variation appeared independent of DBH. For those trees with a large coefficient of variation, more than two paths may be necessary to decrease the variation in the mean total whole-tree volume estimate due to a more complex branching structure.

Dominant stem cumulative volume profiles required total dominant stem volume and total height as predictor variables into the model. Total height is a measurable attribute for a standing tree using common mensuration techniques. An estimate of total dominant stem volume can be calculated, as in this study, using Smalian's formula by sampling either standing trees with a dendrometer or felling trees. Many other models in the literature have been developed for estimation of total dominant stem volume using allometric scaling principles (e.g., Avery and Burkhart 2002) that could be applied prior to using the cumulative dominant stem profile.

The segmented whole-tree cumulative volume profiles require the same predictor variables as the model for dominant stem with additional measures of relative crown height, cumulative volume at relative crown height, and total whole-tree volume. Relative crown height and cumulative volume at relative crown height can be estimated on either a standing tree with a dendrometer or felling trees. The estimate for total whole-tree volume is not as straightforward. Unlike total dominant stem volume, models using allometric scaling principles for whole-tree volume are not as prevalent (MacFarlane 2011). MacFarlane (2011) identified the diameter of the largest branch and crown ratio as the two best metrics for the ratio of whole-tree to dominant stem volume. Van Deusen and Roesch (2011) offer another non-destructive sampling method of difference sampling to estimate total whole-tree volume without dividing the estimates into profiles. Otherwise, destructive sampling is currently

necessary to estimate the total whole-tree volume either by measuring the entire tree or by random branch sampling (Gregoire et al. 1995). Any of these methods would be necessary prior to using the segmented whole-tree cumulative volume profile.

A species-composite model was shown to be sufficient for the cumulative dominant stem volume profile for the hardwood trees in the dataset. However, the segment of the whole-tree model above relative crown height showed a sugar maple species-specific model resulted in a lower AIC than the all-species model. A possible explanation could be the narrower size range covered by the sampled maple trees having a similar branching structure compared to the species-composite model fitted to all trees across a wider size range. The confidence intervals of the fixed-effect parameter for the species-composite and species-specific models do overlap. A species-composite model is also recommended for the segmented whole-tree cumulative volume profile. Zakrzewski (2011) showed different cumulative whole-tree models are needed for sugar maple trees with merchantable branch volume (defined as branches with diameter greater than 9 cm) compared to those without merchantable branches. All of the trees except for three in the three smallest DBH classes had by definition merchantable branches.

The mean centroid of dominant stem volume for all trees in the dataset was 0.222. MacFarlane (2010) found a very similar mean centroid of dominant stem volume, 0.217, for 11 common hardwood tree species in Michigan with merchantable sized branches. However, MacFarlane (2010) found the mean centroid of dominant stem volume, 0.256, for trees without merchantable branches to be significantly different from trees with merchantable branches. As the majority of the sampled trees had merchantable branches, it is expected the mean centroid of dominant stem volume would be similar to the mean value of other trees with merchantable branches. Both of these values for trees with merchantable branches are lower than the 0.3 value for the centroid identified by Forslund (1982) for aspen (*Populus tremuloides* Michx.) trees indicating a reduction in dominant stem volume due to branching. Another possible difference among the datasets is the smaller trees and exclusion of forked

trees used by Forslund (1982).

The mean centroid of whole-tree volume for all trees in the dataset was 0.390, and significantly larger than the centroid of dominant stem volume. The only evident pattern seen for both the centroid of dominant stem volume and the centroid of whole-tree volume was between the centroid of volume and crown ratio class. The pattern of a decreasing centroid of volume with increasing crown ratio class is indicative of branch volume dispersed throughout the height of a tree resulting in a lower centroid.

The final mixed-effects cumulative volume models developed here may only be relevant for hardwood trees with significant proportions of branch volume to whole-tree volume compared to conifers. The selected mixed-effects models were all compatible with the total estimates from Smalian's formula for dominant stems and with random branch sampling for whole trees.

CHAPTER 4

CUMULATIVE MASS AND DENSITY PROFILES FOR DOMINANT STEMS AND WHOLE TREES

4.1 Related Biomass Modeling

4.1.1 Diameter at Breast Height Based Biomass Modeling

Whole-tree biomass equations are in great demand due to the simultaneous need to improve estimation of forest carbon *stocks* and to quantify the distribution of wood mass within trees for estimating whole-tree utilization potential (Avery and Burkhart 2002). Generalized biomass equations have recently become more important with the desire to have consistency at the national scale. For the U.S., Jenkins et al. (2003) compiled published biomass equations to create a nationally consistent diameter at breast height (DBH, measured at 1.37 m above ground level) based biomass equation. Several problems with this method were summarized by the Canadian national biomass study (Lambert et al. 2005): (1) pseudodata were used as if it was real data for parameter estimation, which generated highly correlated observations, (2) the variances of the estimates and tests of significance are not valid, (3) bias in the sample selection because a study conducted in a single area was equally weighted to a study conducted in multiple areas, and (4) selecting publications could also have a bias in those chosen. Lambert et al. (2005) improved upon some of these drawbacks by compiling actual data from a previous study that was designed for sampling biomass at the provincial and regional level. However, they too had large regions of Canada with missing data from an entire province (e.g., British Columbia) and the sampling methods were not consistent across all provinces.

Hansen (2002) compared regional differences between total biomass models in the Eastern U.S. used by Forest Inventory and Analysis (FIA) program of the USDA Forest Service. For

example, the Northeast region used a DBH only model to predict total biomass, and the Central States and Lake States both used DBH and gross cubic foot volume to predict total biomass. The use of different models by region for a specific species and DBH gave varying results to the amount of total biomass in a particular tree. These studies show the need for consistent sampling methodology across regions in the development of national biomass equations.

4.1.2 Component Ratio Method

In 2009, the FIA addressed the regional inconsistencies in tree biomass estimation by adopting the component ratio method (Heath et al. 2009), and Woodall et al. (2011) outlined the methods with examples. The current FIA methods use regional volume equations for dominant stems which are converted to mass by species-specific constant densities compiled by Miles and Smith (2009). A component ratio adjustment factor is calculated between the biomass derived from the regional volume equations and the dominant stem biomass estimates from Jenkins et al. (2004). The same component ratio is used to derive the estimates of whole tree and tree components (e.g., branches and foliage).

4.1.3 Weight-ratio and Density-integral Biomass Modeling

Parresol (1999) reviewed several different methods of biomass modeling, including the weight-ratio and density-integral approaches, beyond DBH-based biomass modeling with examples for individual trees and stands of trees. The weight-ratio approach estimates the ratio of the merchantable dominant stem mass to whole-tree mass. Many different model forms exist for modeling the ratio, as demonstrated by Parresol et al. (1987).

The density-integral approach to biomass modeling was first proposed by Parresol and Thomas (1989), which integrates a density model with a taper model over the entire height of a tree. The specific model was applied to slash pine with predictor variables of relative height and tree age for the density function integrated with a simple taper function requiring

measurements of diameter inside bark at different relative heights and DBH. They found the density-integral approach gave more precise estimates of biomass compared to the weight-ratio approach. Parresol and Thomas (1996) further examined the density-integral approach for slash pine and willow oak for correlations among taper, volume, and mass equations. They found the use of seemingly unrelated regression was more efficient than ordinary least squares regression. The density function employed also had predictor variables of relative height and tree age integrated with a simple geometric taper function requiring measurements of diameter inside bark at different relative heights and DBH. Jordan et al. (2006) also used seemingly unrelated regression with the density-integral approach and found a non-linear model for density to fit the best in relation to relative height for slash pine. They also used a self-referencing density function with density at DBH as the reference observation to improve estimation of biomass. Here, a variation of the density-integral approach is employed in this study to take the first derivative of a vertical volume (dominant or whole-tree) profile to get a taper model before integrating with a density profile. Prior to the mass profile modeling, the necessary density profiles must be developed to generate the mass models.

4.2 Related Tree Density Modeling

Tree density is of interest to scientists for a number of reasons, and primarily because it is a determinant of wood quality (Zobel and Buijtenen 1989, Shmulsky and Jones 2011). The density of a tree is dependent upon many factors such as species, geographical location, age, crown class, and environmental factors (U. S. D. A. Forest Service 2010). Wood density is a key variable in tree biomass and forest carbon estimates, especially in the tropics where large variability of wood density within an individual site exists (Muller-Landau 2004, Chave et al. 2009). The variation in wood density is an important factor in examining the regional variability of aboveground biomass in the Amazon (Baker et al. 2004, Chave et al. 2006).

Wood density is generally examined in one of two ways: either the radial direction or the longitudinal direction of a tree. The change in radial density has been studied by sampling

tree cores or whole-discs at DBH. Wiemann and Williamson (1989) examined the specific gravity (sg, a unitless measurement similar to density) for some tropical and temperate tree species. The specific gravity of the tropical trees associated as pioneer species increased from the pith to the bark; however, the temperate species did not show a clear pattern. Woodcock and Shier (2002; 2003) studied six temperate species in which the three species classified as early-successional had a radial increasing specific gravity pattern, and the three late-successional species had a radial decreasing specific gravity pattern. They also determined a species average specific gravity of 0.55 to be the cutoff between an increasing ($sg < 0.55$) and decreasing ($sg > 0.55$) pattern in the radial direction. Barbour et al. (1994) examined the effects of different thinning intensities on wood density in the radial direction for jack pine. Thinning was shown to decrease the wood density of the residual trees.

Fewer studies have examined changes in density in the longitudinal direction than the radial direction. Tasissa and Burkhart (1998) modeled both radial and longitudinal gradients for wood specific gravities across a large region of loblolly pine's range. They found thinning to have a limited effect on the ring specific gravity of loblolly pine. Specific gravity was also shown to vary by region, to decrease along the longitudinal gradient of tree height, and to increase in the radial direction before reaching a constant level. Antony et al. (2010) also found the same specific gravity patterns for loblolly pine as Tasissa and Burkhart (1998) when modeling specific gravity in loblolly pine for longitudinal variation in an individual tree across the natural range of loblolly pine. For red pine, Baker and Shottafer (1968) found specific gravity to increase along a longitudinal gradient, but the pattern was also dependent upon the spacing of the plantation trees. However, Wahlgren et al. (1966) studied six conifers in Maine and found specific gravity of red pine to decrease along a longitudinal gradient. Repola (2006) examined the vertical densities of Scots pine, Norway spruce, and birch in Finland using a linear mixed-effects model form. The density of each species was found to be dependent upon vertical location to varying degrees. The general consensus from these studies is that density decreases with increasing height along the dominant stem, and the

majority of studies examine the density of conifers.

A greater understanding of branch density is necessary for quantifying the density of the whole tree, which presently has not been studied, for indirect estimation of whole-tree mass and the mass of individual components of trees. A major issue in tree mass estimation is how to determine a density value for the whole tree when different parts of the tree have different densities. One indirect method of biomass estimation that is prevalent in the literature is the density-integral approach (Parresol 1999), discussed in the previous section. Jordan et al. (2006) examined many density profiles of both linear and non-linear form and found a non-linear model for density to fit the best in relation to relative height for slash pine incorporated into the density-integral approach. A second method that will be compared in this research will be referred to as the constant density approach. The USDA Forest Service's Forest Inventory and Analysis (FIA) program for example, which is responsible for collecting and maintaining national level inventory data for forest variables, uses constant values for wood density (or specific gravity) in their methods and models for estimating tree biomass (Woodall et al. 2011). The method outlined uses constant values of wood density by species from the Forest Products Laboratory (FPL) and both wood density and bark density by species are compiled from the literature by Miles and Smith (2009).

Tree density is comprised of both wood and bark components. The separation of wood and bark is necessary in combining an inside bark taper model with a wood density profile for biomass estimation (e.g., Jordan et al. 2006). A greater amount of research has examined wood density compared to bark density because of differences in economic value. Martin and Crist (1968) found the density of the bark of eastern hardwoods to be much greater than softwoods and also quite variable within an individual species. Lamb and Marden (1968) took bark samples at DBH and divided bark into components of inner and outer bark to compare different specific gravities of selected pulpwood species from Minnesota. They found varying relationships between the two bark components by species. The specific gravity of bark also is dependent upon the height at which the sample is taken (Koch 1970, Manwiller

1979). Koch (1970) found bark specific gravity to increase with height before decreasing as heights approached the top of the tree for selected hardwood species. Manwiller (1979) also compared dominant stem bark specific gravity with dominant stem wood, branch wood, and branch bark. The relationships gave different results among the species examined.

The primary objective of this chapter is to develop a new vertical profile mass model to relate whole-tree mass to dominant stem mass, which can estimate component-wise tree attributes of dominant stem and branches. The new model is then compared to models using the density-integral approach and a constant species-specific density throughout an entire tree approach. Additional objectives for the density portion of this chapter are: (i) to determine if significant differences exist between the density profile of the dominant stem of trees and random paths profiling other parts of trees, (ii) to determine if different hardwood tree species growing in the same forest show similar patterns in their vertical density profiles, both dominant and random path profiles, and (iii) to examine the contribution of bark to the vertical density profiles for trees.

4.3 Models

The data used for density and mass model development were trees sampled from a second-growth maple-beech stand at Fred Russ Experimental Forest (see Ch. 2).

4.3.1 Dominant Stem Vertical Density Models

General linear regression modeling was used in developing vertical density profiles for dominant stems, including terms to describe the size of the tree (i.e., DBH and tree height) and the location of measurements along the dominant stem (i.e., relative crown height and relative height) as a third-degree polynomial function of relative height:

$$\rho_{ij} = \beta_0 + \beta_1 D_j + \beta_2 H_j + \beta_3 RCH_j + \beta_4 rh_{ij} + \beta_5 rh_{ij}^2 + \beta_6 rh_{ij}^3 + \epsilon_{ij}, \quad (4.1)$$

where ρ_{ij} , is basic density of stem position i for tree j in $\frac{kg}{m^3}$, D_j is tree diameter at breast height in cm, H_j is total tree height in m, RCH_j is tree relative crown height, rh_{ij} is relative height of position i for tree j (ranging from 0 at ground level to 1 at the tip of the dominant stem), β_0, \dots, β_6 are parameters to be estimated, and ϵ_{ij} is a random error term. Total height and relative height of the tree are computed from the total and relative length of the dominant path through the tree.

Statistical analyses were performed in the R statistical environment (R Development Core Team 2010). A step function with both forward and backward selection, including all interaction terms, was used to determine the best model with the lowest Aikake's Information Criterion (AIC). After the final step, the selected model was checked for statistical significance by an F-test followed by checking the individual parameters for statistical significance from zero at an α of 0.05 level by a t-test, until only statistically significant terms remained. For some final models, the inclusion of all interaction terms resulted in higher order terms than a third-degree polynomial function of relative height. A multinomial categorical variable for species was added to eq. 4.1 to test for species differences as follows:

$$\begin{aligned} \rho_{ij} = & \beta_0 + \beta_1 TA + \beta_2 PS + \beta_3 CG + \beta_4 UR + \beta_5 AS \\ & + \beta_6 D_j + \beta_7 H_j + \beta_8 RCH_j + \beta_9 rh_{ij} + \beta_{10} rh_{ij}^2 + \beta_{11} rh_{ij}^3 + \epsilon_{ij}, \end{aligned} \quad (4.2)$$

where TA , PS , CG , UR , and AS are indicator variables with values of 0 or 1 depending upon the species. A t-test determined the species effect was statistically significant from zero, so that species-specific mixed-effects models were developed for beech and maple trees; species-specific models were not developed for the others because only one individual was sampled.

Mixed-effects modeling was chosen because of the hierarchical structure of the dataset with measurements taken at the tree-level and within-tree level; density measurements taken closer together within a single tree are more likely to be similar than distant measurements on the same tree. The nlme package was used to fit the mixed-effects models (Pinheiro et al. 2011). A combination of different random effects were added to each model, and the model

with the lowest AIC was selected. The assumption of an unstructured covariance structure was used for the random effects.

Relative crown height (RCH) was included as a possible significant independent variable for the dominant stem models of all species, American beech, and sugar maple because of the possible influence branching beginning at different relative heights has on the density of the dominant stem. Table 4.1 shows the summary statistics of the RCH for the three species groups. However, the model forms for all species and American beech changed completely with the inclusion of RCH and gave larger AIC and random error values compared to excluding RCH from models 4.1 and 4.2. For sugar maple, RCH was found to be a non-significant independent variable in the model development. Thus, RCH was omitted from all of the final models.

Table 4.1: Relative crown height of the dominant stem (RCH) summary statistics for all species (ALL), American beech (FG), and sugar maple (AS).

Species	Mean RCH	SD	Min	Max
ALL	0.356	0.105	0.107	0.508
FG	0.340	0.122	0.107	0.508
AS	0.367	0.091	0.228	0.500

4.3.2 Random Branch Path Density Models

Random branch path density profiles were developed to examine how different any other path in a tree is compared to the dominant stem density profile. The destructively sampled random branch path data for each tree was fit to a density profile model following the same procedures described for the dominant stem. The base model for the random branch path with a species categorical variable included:

$$\begin{aligned}
 \rho_{ij} = & \beta_0 + \beta_1 TA + \beta_2 PS + \beta_3 CG + \beta_4 UR + \beta_5 AS \\
 & + \beta_6 D_j + \beta_7 L_j + \beta_8 RHD_j + \beta_9 rh_{ij} + \beta_{10} rh_{ij}^2 + \beta_{11} rh_{ij}^3 + \epsilon_{ij},
 \end{aligned}
 \tag{4.3}$$

is similar to model 4.2 with the exception of total random path length in m, L_j , replacing total tree height, H_j , and the tree relative height at which the random path diverges from the dominant stem, RHD_j , replacing tree relative crown height (RCH_j).

Relative height at which the random path diverged from the dominant stem (RHD) was included as a possible significant independent variable for the random branch path models of all species, American beech, and sugar maple because of the possible different densities of the sampled branches at different heights off of the dominant stem. Table 4.2 shows the summary statistics of the RHD for the three species groups. However, as was the case for the dominant path all three groups had a RHD that was found to be a non-significant independent variable in the model development, so that it was not included in the final models.

Table 4.2: Relative height at which the random path diverges from the dominant stem (RHD) summary statistics for all species (ALL), American beech (FG), and sugar maple (AS).

Species	Mean RHD	SD	Min	Max
ALL	0.702	0.178	0.185	0.961
FG	0.655	0.197	0.185	0.934
AS	0.719	0.161	0.400	0.961

4.3.3 Bark Density Models

A subset of one tree per species per 10-cm DBH class was used to develop bark density models. The bark density models followed the same procedures described for the multinomial categorical species model for the dominant stem (eq. 4.2). The separation of wood and bark into components is important because of their structural differences. Due to a small number of bark samples per tree for the dominant stem (DOM) and the random branch path (RBP), the observations by path were combined when developing the bark density models for the subset of trees (Table 4.3).

Table 4.3: The bark sample size by species, dominant (DOM), and random branch paths (RBP).

Path	ALL	FG	AS	CG	PS	TA	UR
DOM	279	109	97	25	17	15	16
RBP	86	55	18	2	2	0	9

4.3.4 Dominant Stem Cumulative Mass Models

Statistical analyses were performed in the R statistical environment (R Development Core Team 2010). A fixed-effects model, shown below (see eqs. 4.4 and 4.7), was first selected for each individual tree with parameters estimated using the `nlsList` function from the `nlme` package (Pinheiro et al. 2011). Mixed-effects modeling was then chosen because of the hierarchical structure of the dataset with measurements taken at the tree-level and within-tree level. As measurements taken closer together within a single tree are more likely to be similar than distant measurements on the same tree. The assumption of an unstructured covariance structure was used for the random effects. The parameters from the fixed-effects model were used as starting values for the mixed-effects models using the `nlme` function in the `nlme` package. The models were fit to all of the species, American beech, and sugar maple with the best-fit model being selected based on the lowest Akaike’s Information Criterion, AIC, value. American beech and sugar maple were fitted to the model individually as multiple observations of each of these species were present. Models were also selected based on having the smallest mean relative difference in relation to estimated total mass.

Two additional approaches for modeling the cumulative mass profile were the density-integral approach and a constant basic density approach applied to cumulative volume profiles. The density-integral approach combines a basic density function and taper function in terms of relative height using integral calculus (Parresol and Thomas 1989, Parresol 1999, Jordan et al. 2006). The `integrate` function in the R statistical environment was used for solving the integrals; however, the integrals could also be solved using integration by parts. The `integrate` function was chosen over integration by parts due to need of integrating the

fifth order polynomial function of the basic density profile. For the constant density approach, published species-specific densities compiled by Miles and Smith (2009) for the U.S. were applied to cumulative volume profiles of each tree.

Non-linear regression modeling was used in developing the cumulative mass profiles for dominant stems in terms of relative height. The base fixed-effects model is analogous to modifying the relative dominant stem volume model of MacFarlane (2010), but for mass:

$$m_{DOM} = M_{DOM} * (1 - (1 - rh)^{\alpha_1}) + \epsilon, \quad (4.4)$$

where m_{DOM} is the dominant stem cumulative mass in kg at a relative height (rh), M_{DOM} is total dominant stem mass in kg, α_1 is a parameter to be estimated, and ϵ is an error term.

The second approach for modeling the dominant stem mass was to use the density-integral approach. The basic density function, $\rho(rh)$, and the first derivative of a cumulative dominant stem volume model, $v'_{DOM}(rh)$, were used to predict mass at any relative height:

$$m_{DOM} = \int_{rh_l}^{rh_u} \rho(rh) v'_{DOM}(rh) drh, \quad (4.5)$$

where rh_l is the lower limit of relative height and rh_u is the upper limit of relative height.

The final approach to modeling the dominant stem mass was to apply a species-specific constant basic density, ρ_c , throughout the entire dominant stem to a cumulative dominant stem model, $v_{DOM}(rh)$:

$$m_{DOM} = \rho_c * v_{DOM}(rh), \quad (4.6)$$

where ρ_c is the species-specific densities compiled by Miles and Smith (2009).

4.3.5 Whole-tree Cumulative Mass Models

The whole-tree cumulative mass model uses the modified relative dominant stem mass model (eq. 4.4) for the portion below relative crown height with the addition of a modified mass model where the intercept is shifted to relative crown height for the portion above relative crown height:

$$m_{AC} = M_{RCH} + \beta_M * (1 - (1 - (rh - RCH))^{\alpha_2}) + \epsilon, \quad (4.7)$$

where m_{AC} is the whole-tree cumulative mass, in kg, above relative crown height at a relative height (rh), M_{RCH} is total tree mass at relative crown height (RCH) in kg, β_M is either a fixed parameter or an estimated parameter, α_2 is a parameter to be estimated, and ϵ is an error term. In the case where β_M is fixed, the new model has the same form as model 4.7 setting

$$\beta_M = \frac{M_{WT} - M_{RCH}}{1 - RCH^{\alpha_2}}, \quad (4.8)$$

where M_{WT} is the total whole-tree mass in kg.

Models 4.4 and 4.7 or models 4.4 and 4.8 are combined to get the whole-tree cumulative mass profile as

$$m_{WT} = I_1 m_{DOM} + I_2 m_{AC}, \quad (4.9)$$

where m_{WT} is the whole-tree cumulative mass in kg at a relative height, I_1 is an indicator variable with a value of 1 when relative height is below relative crown height and a value of 0 when relative height is above relative crown height, and I_2 is an indicator variable with values of 0 when relative height is below relative crown height and 1 when relative height is above relative crown height.

Similar to the dominant stem, the second approach to modeling whole-tree mass was to use the density-integral approach. Due to the segmented model of whole-tree mass profile (eq. 4.9), two integrals are needed to estimate whole-tree mass for relative heights above relative crown height:

$$m_{WT} = \int_{rh_l}^{RCH} \rho(rh) v'_{DOM}(rh) drh + \int_{RCH}^{rh_u} \rho(rh) v'_{AC}(rh) drh, \quad (4.10)$$

where rh_l is the lower limit of relative height and rh_u is the upper limit of relative height. The dominant stem basic density profile was used for both integrals for whole-tree mass estimation as it is a more conservative estimate, and the whole tree above relative crown height is a mixture of dominant stem and branches.

The final approach to modeling whole-tree mass was to apply a species-specific constant basic density, ρ_c , throughout the entire tree to a cumulative whole-tree volume model,

$v_{WT}(rh)$:

$$m_{WT} = \rho_c * v_{WT}(rh). \quad (4.11)$$

4.4 Results

4.4.1 Dominant Stem Vertical Density Profiles

The final best-fit all-species and species-specific dominant stem models were as follows:

All:

$$\begin{aligned} \rho_{ij} = & \beta_0 + u_{0j} + \beta_1 TA + \beta_2 PS + \beta_3 CG + \beta_4 UR + \beta_5 AS \\ & + \beta_6 rh_{ij}^2 + (\beta_7 + u_{1j}) rh_{ij}^3 + \beta_8 rh_{ij}^4 + \beta_9 rh_{ij}^5 \\ & + \beta_{10} D_j rh_{ij}^2 + \epsilon_{ij}, \end{aligned} \quad (4.12)$$

American beech:

$$\begin{aligned} \rho_{ij} = & \beta_0 + u_{0j} + (\beta_1 + u_{1j}) rh_{ij}^2 + \beta_2 rh_{ij}^3 + \beta_3 rh_{ij}^4 + \beta_4 rh_{ij}^5 \\ & + \beta_5 D_j rh_{ij}^3 + \epsilon_{ij}, \end{aligned} \quad (4.13)$$

Sugar maple:

$$\begin{aligned} \rho_{ij} = & u_{0j} + \beta_1 D_j + \beta_2 H_j + (\beta_3 + u_{1j}) rh_{ij} + (\beta_4 + u_{2j}) rh_{ij}^2 \\ & + \beta_5 rh_{ij}^3 + \beta_6 D_j H_j + \epsilon_{ij}, \end{aligned} \quad (4.14)$$

where $\beta_0, \dots, \beta_{10}$ are the fixed effects parameters to be estimated, and u_{0j}, \dots, u_{2j} are the random effects parameters to be estimated for tree j . American beech and sugar maple had multiple sample trees so a species-specific model was fit to each of them. For the other four species, the all-species model was applied as only one individual was sampled for each species.

Dominant stem vertical density profiles for all six species varied with relative height along the stem. Table 4.4 summarizes the best-fit models for the dominant stem of each species. Each species examined had a complex vertical density profile (Fig. 4.1). American beech, pignut hickory, and black cherry had a decreasing density from the base of the tree until

an approximate relative height of 0.3, density then increased back to its previous density at the base of the tree, and then decreased once again before increasing one final time prior to reaching the tip of the stem. Sugar maple, basswood, and slippery elm also had a decreasing density from the base of the tree until an approximate relative height of 0.3, and density then began to increase once more before decreasing again towards the tip of the stem. In comparison to the reported species average given by the Forest Products Laboratory (FPL) in Madison, WI (U. S. D. A. Forest Service 2010), these American beech trees were nearly 50 kg/m³ denser at its maximum than the FPL average and denser for the entire vertical profile. These sugar maple, basswood, black cherry, and slippery elm had densities at the base of the tree that began near the reported FPL species average, and showed fluctuating patterns with increasing height. However, the one hickory tree examined had a density fluctuating nearly 100 kg/m³ below the reported FPL species average.

Table 4.4: Parameter estimates of models 4.12 - 4.14 for the vertical profile of the basic density of the dominant stem for the all-species (ALL), American beech (FG), and sugar maple (AS) mixed-effects models. For the fixed parameters, the standard error of estimates is given in parantheses.

Parameter	ALL Estimate (4.12)	FG Estimate (4.13)	AS Estimate (4.14)
β_0	583.179 (8.025)	602.280 (11.215)	
β_1	-273.345 (24.221)	-1885.849 (424.101)	12.053 (1.422)
β_2	-105.364 (24.508)	7931.054 (1621.901)	19.296 (1.059)
β_3	-37.450 (23.733)	-10968.578 (2127.776)	-350.696 (88.638)
β_4	-108.073 (24.227)	4988.697 (928.895)	1153.375 (149.937)
β_5	-36.164 (8.960)	-1.543 (0.772)	-849.595 (85.583)
β_6	-1293.481 (270.449)		-0.424 (0.043)
β_7	5739.937 (1035.995)		
β_8	-7837.064 (1370.802)		
β_9	3425.819 (603.524)		
β_{10}	-1.015 (0.515)		
$\text{var}(u_{0j})$	668.328	961.666	2975.325
$\text{var}(u_{1j})$	4346.393	5413.880	51888.220
$\text{var}(u_{2j})$			53832.660
$\text{cov}(u_{0j}, u_{1j})$	-927.167	-1613.191	-9505.240
$\text{cov}(u_{0j}, u_{2j})$			7922.540
$\text{cov}(u_{1j}, u_{2j})$			-51583.07
ϵ_{ij}	34.672	38.925	24.278
AIC	9022.73	4749.19	3142.52

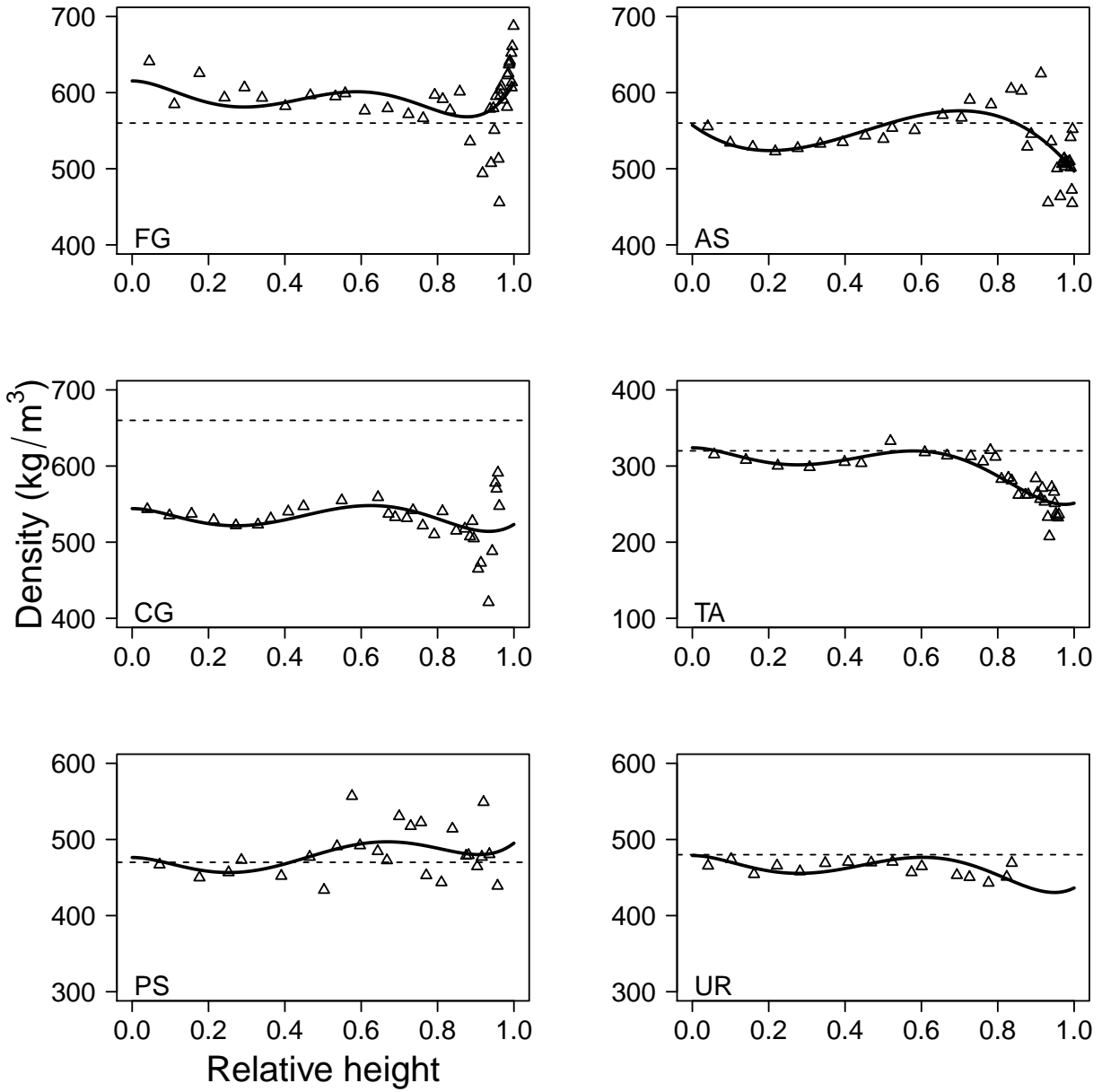


Figure 4.1: The mixed-effects of the dominant stem vertical density profile for each species according to models 4.12 - 4.14. For the median sized American beech (FG) tree with $D = 42.9$ cm, and the median sized sugar maple (AS) tree with $D = 42.8$ cm and $H = 34.0$ cm (models 4.13 and 4.14, respectively). American basswood (TA), black cherry (PS), pignut hickory (CG), and slippery elm (UR) were all fit using the all-species model (model 4.12) as there was only one individual of each in the sample. The measured tree densities are shown as triangles. The horizontal dotted line represents the wood density for each species as reported by the Forest Products Laboratory in Madison, WI (U. S. D. A. Forest Service 2010).

4.4.2 Random Branch Path Density Profiles

The final best-fit all-species and species-specific models for the random branch profiles are as follows:

All:

$$\begin{aligned}\rho_{ij} = & \beta_0 + u_{0j} + \beta_1 TA + \beta_2 PS + \beta_3 CG + \beta_4 UR + \beta_5 AS \\ & + (\beta_6 + u_{1j})rh_{ij} + \beta_7 rh_{ij}^2 + (\beta_8 + u_{2j})rh_{ij}^3 + \beta_9 rh_{ij}^4 \\ & + \beta_{10} rh_{ij}^5 + \beta_{11} L_j rh_{ij}^3 + \epsilon_{ij},\end{aligned}\tag{4.15}$$

American beech:

$$\begin{aligned}\rho_{ij} = & \beta_0 + u_{0j} + \beta_1 rh_{ij}^2 + \beta_2 rh_{ij}^3 + \beta_3 rh_{ij}^4 + \beta_4 rh_{ij}^5 \\ & + \beta_5 L_j rh_{ij}^3 + \beta_6 L_j rh_{ij}^2 + \epsilon_{ij},\end{aligned}\tag{4.16}$$

Sugar maple:

$$\begin{aligned}\rho_{ij} = & u_{0j} + \beta_1 D_j + \beta_2 L_j + (\beta_3 + u_{1j})rh_{ij} \\ & + (\beta_4 + u_{2j})rh_{ij}^2 + \beta_5 rh_{ij}^3 + \beta_6 D_j L_j + \beta_7 L_j rh_{ij}^3 \\ & + \beta_8 L_j rh_{ij}^2 + \beta_9 L_j rh_{ij} + \epsilon_{ij},\end{aligned}\tag{4.17}$$

where L_j is the total random branch path length, $\beta_0, \dots, \beta_{11}$ are the fixed effects parameters to be estimated, and u_{0j}, \dots, u_{2j} are the random effects parameters to be estimated for tree j . Table 4.5 summarizes the best-fit models for the random branch path density of each species. The density profiles for all six species derived from random branch sampling also varied with relative height, indicating a non-constant and non-linear density profile for the tree.

Table 4.5: Parameter estimates of models 4.15 - 4.17 for the basic density profile of the random branch path for the all-species (ALL), American beech (FG), and sugar maple (AS) mixed-effects models. For the fixed parameters, the standard error of estimates is given in parantheses.

Parameter	ALL Estimate (4.15)	FG Estimate (4.16)	AS Estimate (4.17)
β_0	558.853 (16.698)	609.963 (8.974)	
β_1	-281.124 (20.990)	-3064.950 (464.381)	8.552 (2.641)
β_2	-125.705 (22.370)	12028.253 (1639.495)	20.658 (1.099)
β_3	-47.121 (20.819)	-16523.545 (2113.572)	1308.307 (550.599)
β_4	-98.433 (20.768)	7773.176 (911.859)	-2723.536 (1093.127)
β_5	-43.537 (7.704)	-19.917 (5.895)	1689.574 (648.788)
β_6	628.361 (252.462)	13.817 (5.866)	-0.332 (0.101)
β_7	-5307.591 (1371.455)		-79.676 (25.019)
β_8	15948.619 (3146.769)		126.844 (42.108)
β_9	-19142.133 (3195.509)		-56.874 (21.199)
β_{10}	8055.966 (1186.348)		
β_{11}	-4.020 (0.995)		
$\text{var}(u_{0j})$	1860.944	221.624	2595.301
$\text{var}(u_{1j})$	18270.89		15939.370
$\text{var}(u_{2j})$	13815.23		13449.170
$\text{cov}(u_{0j}, u_{1j})$	-5049.686		-5544.173
$\text{cov}(u_{0j}, u_{2j})$	4010.719		3940.647
$\text{cov}(u_{1j}, u_{2j})$	-15490.43		-13821.51
ϵ_{ij}	34.687	37.911	27.861
AIC	8503.868	4288.547	3116.386

4.4.3 Comparative Dominant and Random Branch Path Density Profiles

Separate density models for the dominant stem and random branch path were fit to examine if statistical differences exist between the dominant stem and random branch path. The density profiles were developed and compared based upon relative height or relative path length. Dominant stem and random branch path models were considered statistically different if either model forms were different or at least one parameter's 95 percent confidence interval did not overlap (Rubin and MacFarlane 2008). Comparing the best-fit model forms of models 4.12 - 4.14 to models 4.15 - 4.17 by respective species, the dominant and random branch path densities are statistically different from one another due to different model forms.

Figure 4.2 shows the comparison between the vertical density of the dominant stem and

the random branch path for each species. Each species shows similar varying patterns for the random branch path as the dominant stem because a majority of each random branch path follows the dominant stem until branching is encountered, as the mean RHD for all sampled species was 0.702. Greater densities occur for the random branch path near the top than for the dominant stems for all species except sugar maple. This shows that the vertical density profile of the dominant path is not representative of the whole tree because of significant differences in the density of branches. All of the species random branch path density profiles are complex and non-constant, as was the case for dominant stems, compared to the reported species average of the FPL.

One possible explanation for the difference of vertical densities near the top of the profiles was the relative height at which the dominant path and the random branch path diverged from one another (RHD); however, RHD was not a significant variable in the final best-fit random branch path density models. Figure 4.3 shows three American beech trees that represent (a) the minimum RHD, (b) a RHD near the middle of a tree, and (c) a RHD near the top of a tree. All three trees show the divergence between the dominant stem and random branch path models to precede the RHD. The difference between the densities continues to the location of the RHD, but the greatest difference between densities of the two paths occurs closer to the top of each relative path length. The significance of the higher order relative height terms in each model accounts for the differences between the dominant stem and the random branch path.

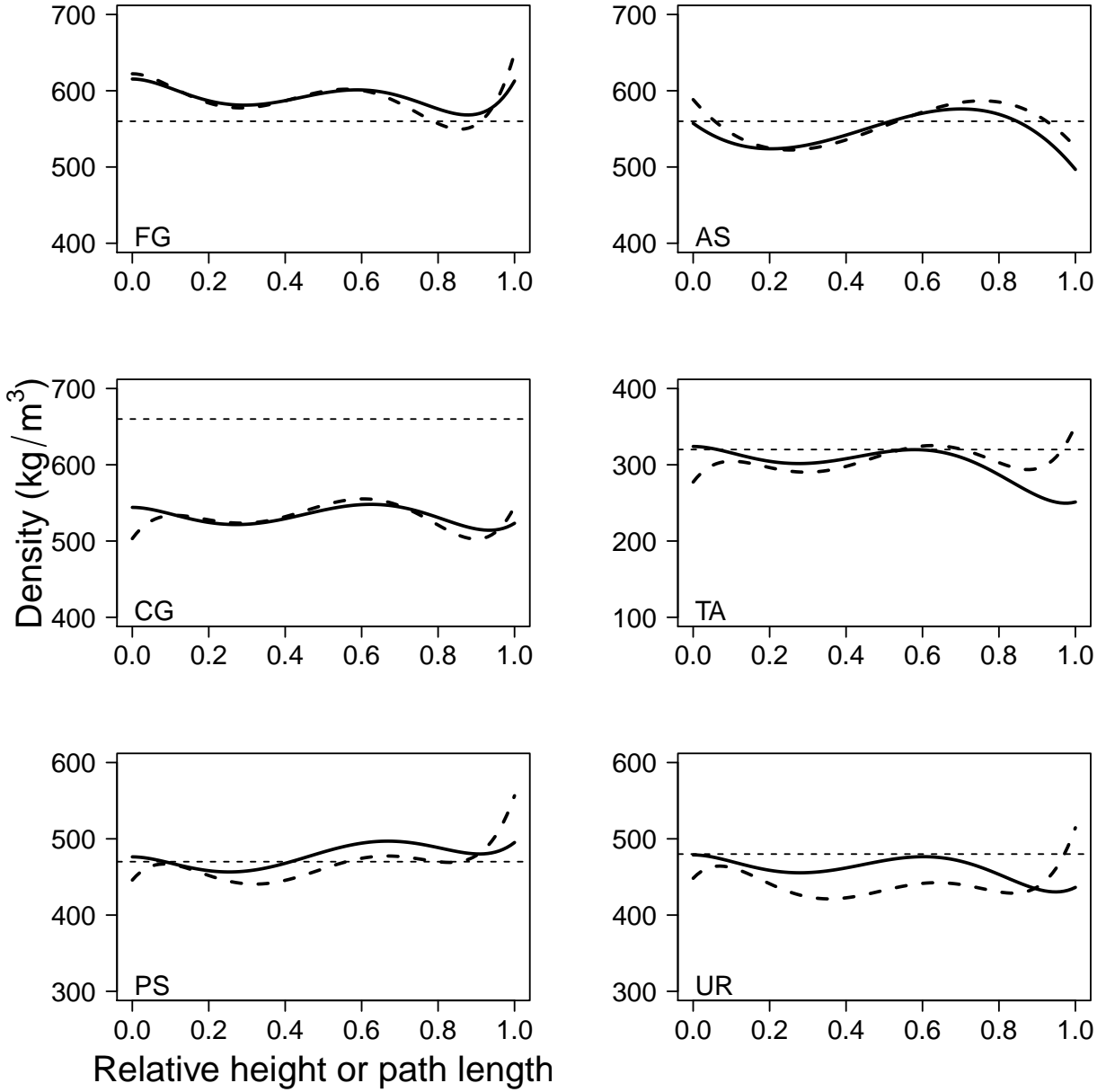


Figure 4.2: The mixed-effects vertical density profile for the dominant stem of each species according to models 4.12 - 4.14, shown as solid lines, versus relative height. The thicker dashed lines are the mixed-effects density profile for the random branch path of each species according to models 4.15 - 4.17 versus relative path length. For the median sized American beech (FG) tree with $D = 42.9$ cm, and the median sized sugar maple (AS) tree with $D = 42.8$ cm and $H = 34.0$ cm (models 4.13, 4.16 and 4.14, 4.17, respectively). American basswood (TA), black cherry (PS), pignut hickory (CG), and slippery elm (UR) were all fit using the all-species models 4.12 and 4.15 as there was only one individual of each in the sample. The horizontal dotted line represents the wood density for each species as given by the Forest Products Laboratory in Madison, WI (U. S. D. A. Forest Service 2010).

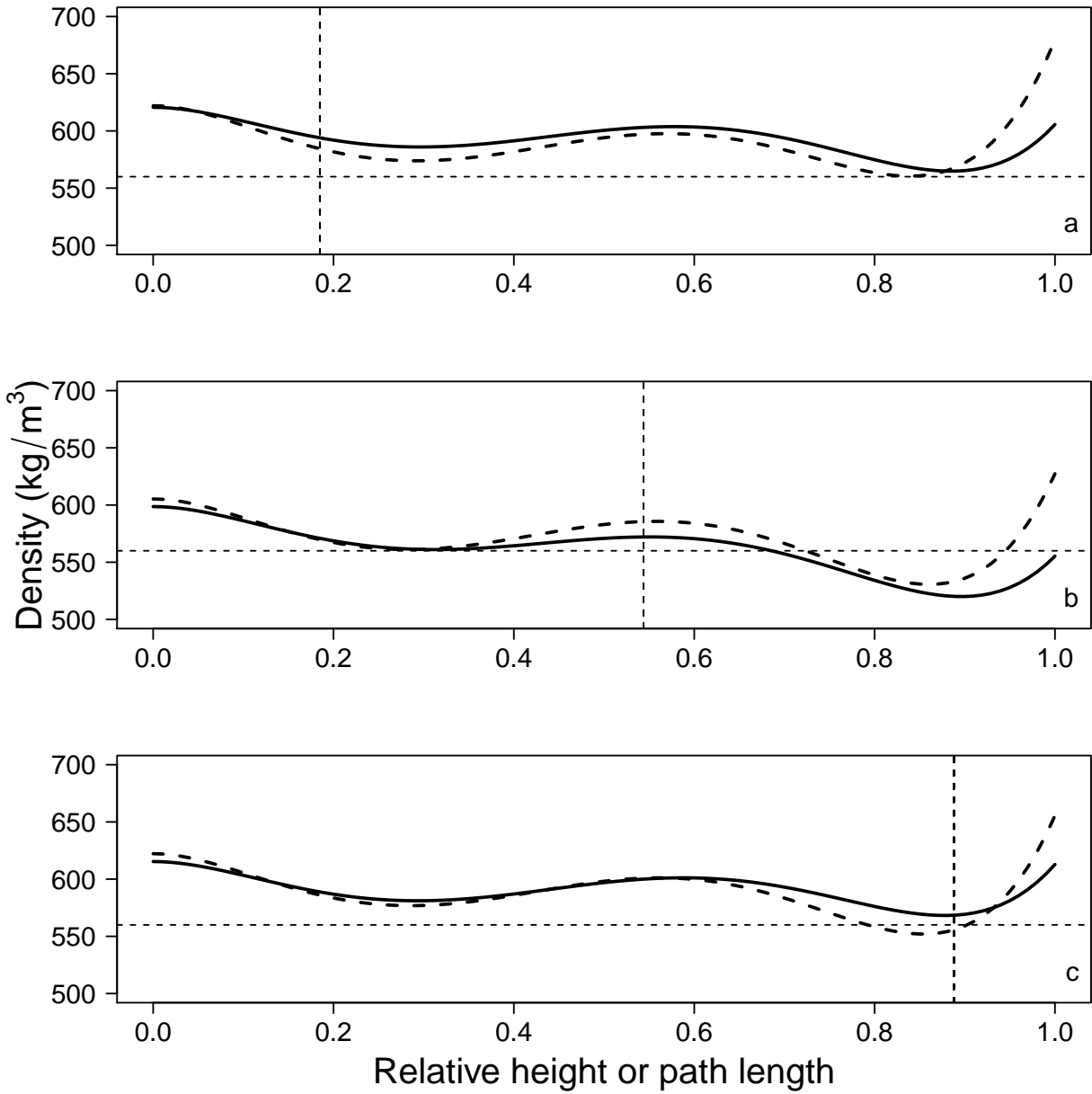


Figure 4.3: The mixed effects of the vertical density profile for the dominant stem (solid line) and the random branch path profile (thicker dashed line) for three American beech trees versus relative height or path length. (a) Shows an American beech tree with diameter at breast height (DBH) of 50.1 cm, relative height at which the random path diverges from the dominant stem (RHD) equal to 0.185. (b) Shows an American beech tree with DBH of 47.1 cm and RHD equal to 0.544. (c) Shows an American beech tree with DBH of 42.9 cm and RHD equal to 0.888. The horizontal dotted line represents the wood density for American beech of 560 kg/m³ as reported by the Forest Products Laboratory in Madison, WI (U. S. D. A. Forest Service 2010).

4.4.4 Bark Vertical Density Profiles

The final best-fit all-species and species-specific models for bark density are as follows:

All:

$$\begin{aligned}\rho_{ij} = & \beta_0 + \beta_1 TA + \beta_2 PS + \beta_3 CG + \beta_4 UR + \beta_5 AS \\ & + \beta_6 rh_{ij}^3 + \beta_7 H_j rh_{ij} + u_{0j} + u_{1j} rh_{ij}^3 + \epsilon_{ij},\end{aligned}\tag{4.18}$$

American beech:

$$\begin{aligned}\rho_{ij} = & \beta_0 + \beta_1 rh_{ij}^3 + \beta_2 rh_{ij}^5 + \beta_3 D_j rh_{ij}^2 + \beta_4 D_j rh_{ij}^3 \\ & + u_{0j} + u_{1j} rh_{ij}^3 + \epsilon_{ij},\end{aligned}\tag{4.19}$$

Sugar maple:

$$\rho_{ij} = \beta_0 + \beta_1 rh_{ij}^2 + \beta_2 rh_{ij}^3 + u_{0j} + u_{1j} rh_{ij}^3 + \epsilon_{ij},\tag{4.20}$$

where β_0, \dots, β_7 are the fixed effects parameters to be estimated, and u_{0j}, u_{1j} are the random effects parameters to be estimated for tree j . Table 4.6 summarizes the best-fit models for bark vertical density of each species.

Table 4.6: Parameter estimates of models 4.18 - 4.20 for the vertical profile of the bark basic density of the combined dominant and random branch path for the all-species (ALL), American beech (FG) and sugar maple (AS) mixed-effects models. For the fixed parameters, the standard error of estimates is given in parantheses.

Parameter	ALL Estimate (4.18)	FG Estimate (4.19)	AS Estimate (4.20)
β_0	689.653 (16.283)	695.107 (20.006)	679.016 (13.375)
β_1	-247.682 (41.389)	-446.841 (110.959)	401.756 (68.538)
β_2	-115.497 (41.254)	403.666 (122.688)	-510.651 (76.923)
β_3	-129.827 (40.949)	8.245 (1.744)	
β_4	-268.368 (41.005)	-7.085 (2.136)	
β_5	-6.058 (22.996)		
β_6	-160.196 (24.654)		
β_7	3.371 (0.562)		
$\text{var}(u_{0j})$	1371.970	2242.472	649.081
$\text{var}(u_{1j})$	4551.853	2152.330	2238.560
$\text{cov}(u_{0j}, u_{1j})$	-162.435	1195.135	-206.125
ϵ_{ij}	29.431	24.206	28.973
AIC	3547.357	1531.046	1108.966

For the subset of trees in which bark was separated from wood, the bark vertical density profiles for all six species varied with location along relative height. The bark vertical densities for American beech, sugar maple, black cherry, and slippery elm were greater along the entire vertical profile than those compiled by Miles and Smith (2009) and used by the FIA (Fig. 4.4). Pignut hickory and basswood were less than the species average compiled by Miles and Smith (2009) for nearly the entire vertical profile. However, Harkin and Rowe (1971) reports average values of bark specific gravity (using oven-dry mass and oven-dry volume) for American beech and sugar maple that are very similar to the values of the bark density profiles. Five of the six species showed a gradual increase in bark density with increasing relative height followed by a drastic decline in bark density approaching the top of the path, with the exception of American beech. The beech bark density actually increased approaching the top of the path. The top of the bark profiles have been extrapolated beyond the last measured relative height, represented as dashed lines in Fig. 4.4, which can be problematic when fitted with a polynomial function. Extrapolation does not appear to be an issue for American beech, sugar maple, pignut hickory, and slippery elm as the last

measured relative height locations are greater than 0.9. However, some caution is necessary for black cherry and basswood with the last measured density at a relative height near 0.8.

The vertical bark density profile is greater than the vertical tree density profile for the dominant stem for the majority of the species examined (Fig. 4.5). American beech, sugar maple, and black cherry have bark densities nearly 100 kg/m^3 greater than tree densities along the entire profile, except near the tip of the stem for sugar maple. The same is true for pignut hickory and basswood for most of the profile except near the tip the bark density is less than tree density. Slippery elm is the only one with bark less dense than the tree density for nearly the entire profile, which was also seen in the reported species average densities for elm.

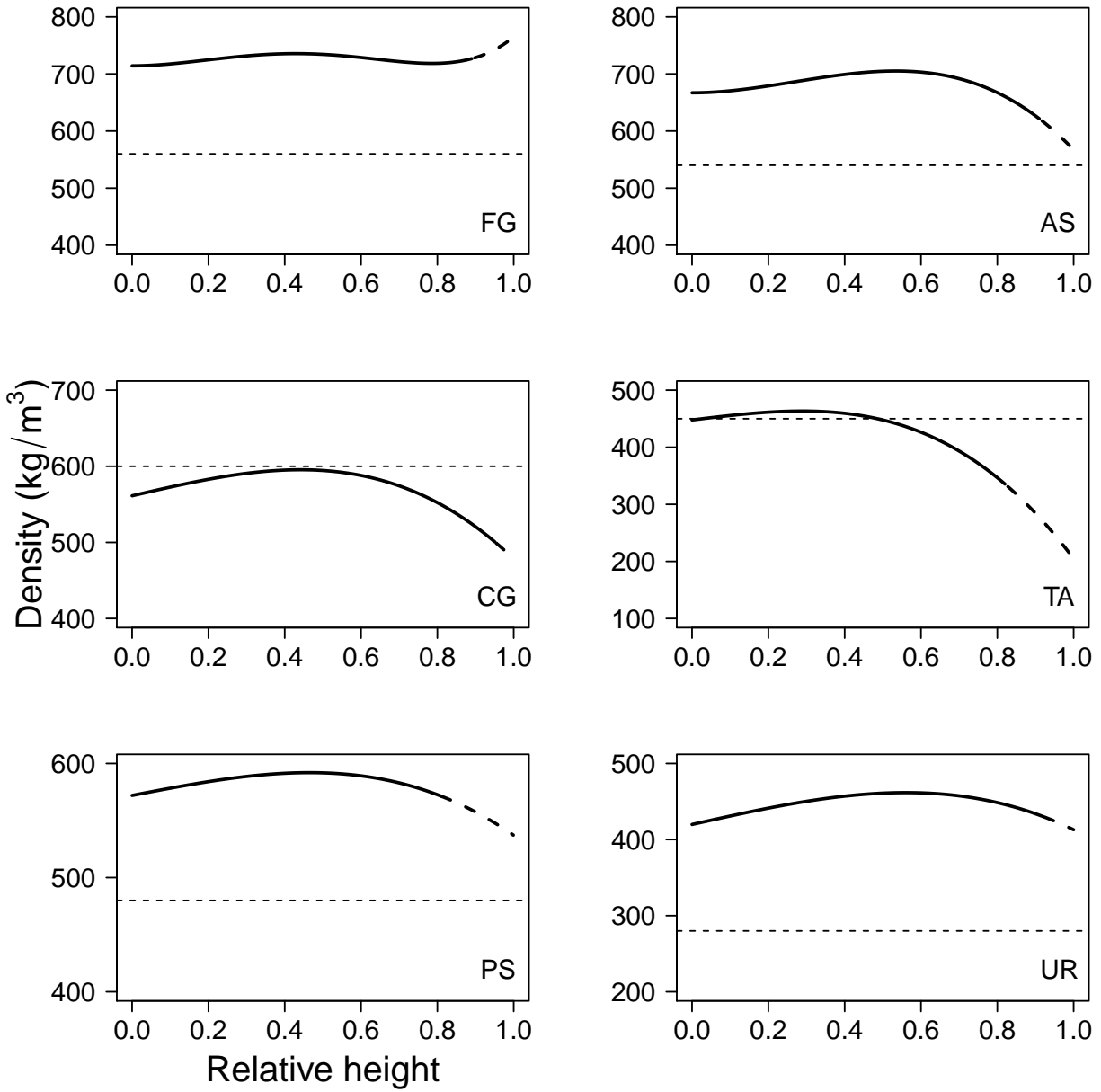


Figure 4.4: The mixed effects of the vertical bark density profile for the combined dominant stem and random branch paths of each species according to models 4.18 - 4.20, shown as solid lines. The thicker dashed line represents the extrapolation of the models beyond the last measured relative height. For the median sized American beech (FG) tree with $D = 50.1$ cm, and the median sized sugar maple (AS) tree with $D = 48.1$ cm (models 4.19 and 4.20, respectively). American basswood (TA), black cherry (PS), pignut hickory (CG), and slippery elm (UR) were all fit using the all-species model 4.18 as there was only one individual of each in the sample. The horizontal dotted line represents the bark density for each species as compiled by the USDA Forest Service (Miles and Smith 2009).

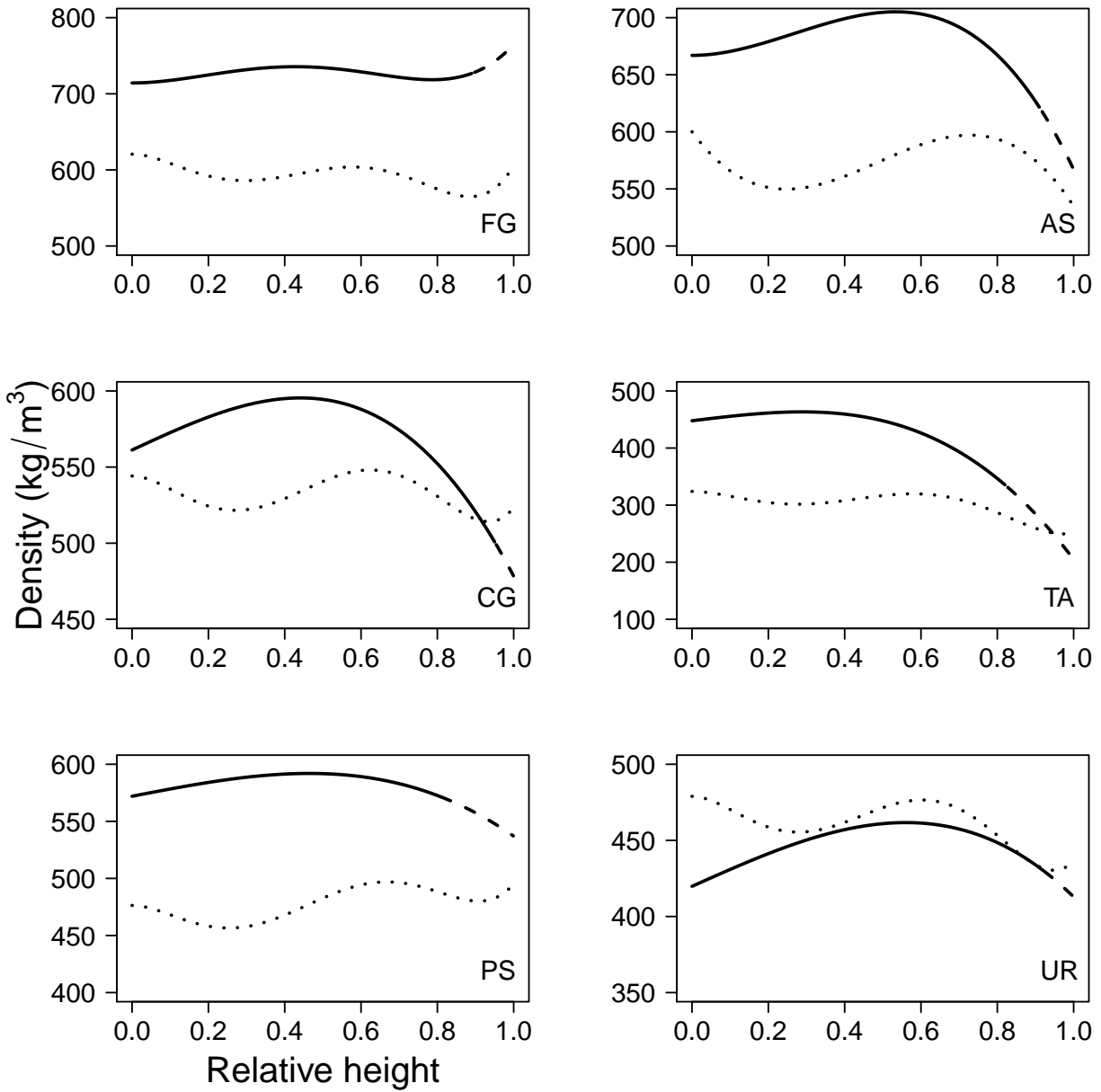


Figure 4.5: The mixed effects of the vertical bark density profile for the combined dominant stem and random branch paths of each species according to models 4.18 - 4.20, shown as solid lines, with dashed lines representing the extrapolation of the models beyond the last measured relative height. For the median sized American beech (FG) tree with $D = 50.1$ cm, and the median sized sugar maple (AS) tree with $D = 48.1$ cm (models 4.19 and 4.20, respectively). American basswood (TA), black cherry (PS), pignut hickory (CG), and slippery elm (UR) were all fit using the all-species model 4.18 as there was only one individual of each in the sample. The dotted lines represent the tree density for each species from models 4.12 - 4.14.

4.4.5 Total Mass Estimates

Table 4.7 shows the summary statistics for the total mass of dominant stems and whole trees by species and for all trees in the dataset. The total mass of both dominant stems and whole trees show an increasing pattern for larger DBH for all species, American beech, and sugar maple (Fig. 4.6).

Table 4.7: Species code (spp), number of trees (n), mean dominant stem mass (M_{DOM}), mean total mass (M_{WT}) with standard deviation (SD), minimum (min), and maximum (max) values by species.

spp	n	Mean M_{DOM} (kg) [SD, min, max]	Mean M_{WT} (kg) [SD, min, max]
FG	15	2140 [1327, 81, 4552]	5349 [5801, 131, 24354]
AS	13	1196 [728, 410, 2536]	2047 [1395, 557, 5043]
CG	1	2772 [NA, NA, NA]	4492 [NA, NA, NA]
PS	1	170 [NA, NA, NA]	229 [NA, NA, NA]
TA	1	455 [NA, NA, NA]	620 [NA, NA, NA]
UR	1	2973 [NA, NA, NA]	6541 [NA, NA, NA]
ALL	32	1688 [1189, 81, 4552]	3711 [4403, 131, 24354]

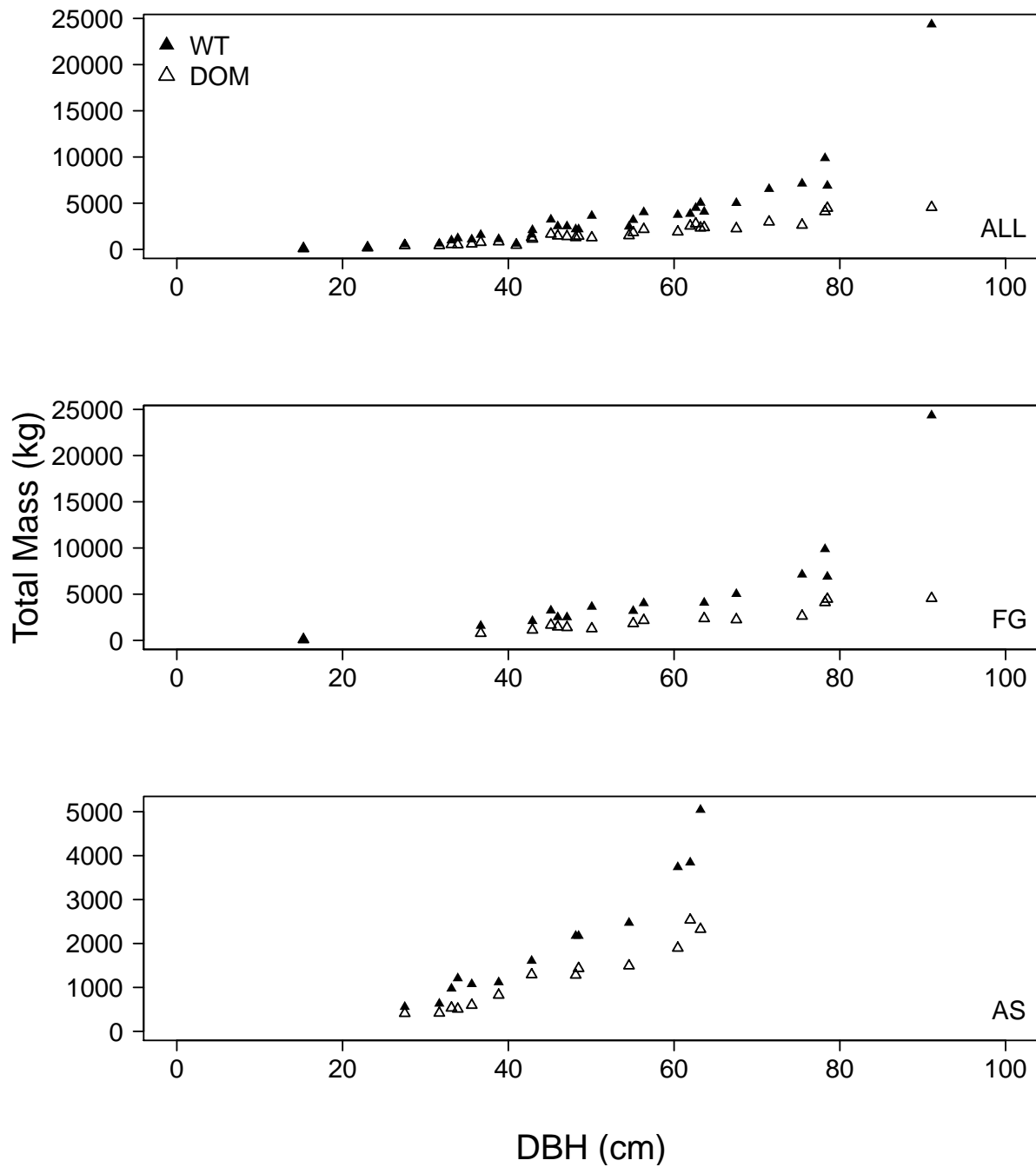


Figure 4.6: The total mass, in kg, of sampled trees for the dominant stem (DOM) and whole tree (WT) versus diameter at breast height (DBH), in cm, for all trees (ALL), American beech (FG), and sugar maple (AS).

4.4.6 Cumulative Mass Profiles

Dominant Stem Mass Profiles

The final model, below, for the dominant stem mass added a random effect to model 4.4 to create a mixed-effects model. The final cumulative mass of the dominant stem model applied to all species, American beech, and sugar maple is

$$m_{DOM_{ij}} = M_{DOM_j} * (1 - (1 - rh_{ij})^{\alpha_1 + u_{1j}}) + \epsilon_{ij}, \quad (4.21)$$

where $m_{DOM_{ij}}$ is the cumulative mass of stem position i for tree j in kg, M_{DOM_j} is total dominant stem mass in kg, rh_{ij} is relative height of position i for tree j , α_1 is a fixed effect parameter to be estimated, u_{1j} is a random effect parameter to be estimated, and ϵ_{ij} is a random error term. Table 4.8 gives the parameter estimates for model 4.21. The species-specific models are selected over the all-species model as the best models because they have lower AIC values. The total dominant stem mass given by the model is also compatible with the final observation of total dominant stem mass, as the mean relative difference is equal to zero.

Table 4.8: Parameter estimates of model 4.21 for the cumulative mass of the dominant stem for the all-species (ALL), American beech (FG), and sugar maple (AS) mixed-effects models. For the fixed parameters, the standard error of estimates is given in parantheses.

Parameter	ALL Estimate	FG Estimate	AS Estimate
α_1	2.775 (0.049)	2.865 (0.068)	2.722 (0.072)
$\text{var}(u_{1j})$	0.069	0.064	0.066
ϵ_{ij}	25.605	29.532	15.694
AIC	18359.7	9821.4	6088.0
Mean Relative Difference	0	0	0

The final model for the density-integral approach to modeling the dominant stem mass is similar to model 4.5 with the addition of subscripts for measurements taken at stem position i for tree j :

$$m_{DOM_{ij}} = \int_{rh_l}^{rh_u} \rho_{ij} v'_{DOM_{ij}} drh, \quad (4.22)$$

where rh_l is the lower limit of relative height and rh_u is the upper limit of relative height. The density function for the dominant stem is a species-specific function, and the taper function is a species-composite function.

The final constant density approach model also applies a species-specific constant density and a species-composite cumulative volume function similar to model 4.6 with the addition of subscripts for measurements taken at stem position i for tree j :

$$m_{DOM_{ij}} = \rho_c * v_{DOM_{ij}}. \quad (4.23)$$

Figures 4.7 and 4.8 show the dominant stem cumulative mass for the (a) minimum, (b) median, and (c) maximum DBH of American beech and sugar maple trees, respectively. For each tree, the profiles are shown based upon the three modeling approaches of (1) non-linear mixed-effects (nlme), (2) density-integral (integ), and (3) constant density (const). For both species the non-linear mixed-effects and density-integral approaches gave similar results throughout the profile; however, the non-linear mixed-effects approach assured that the total dominant stem mass observed was equal to the total dominant stem mass predicted. For the American beech trees, the constant density approach underestimated the observed dominant stem mass throughout the profiles. The opposite was true for the sugar maple trees with the constant density approach overestimating the observed dominant stem mass throughout the profiles.

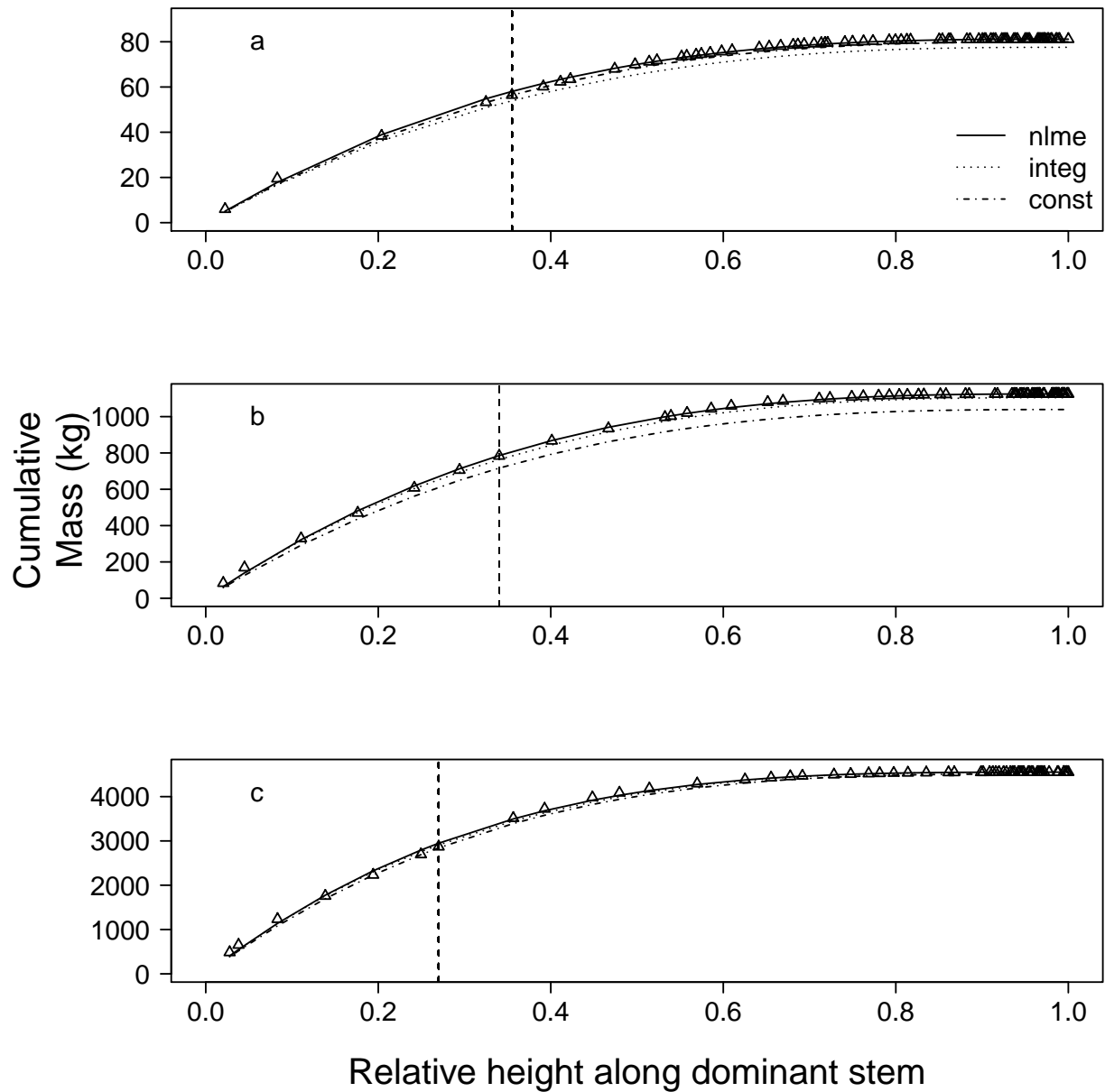


Figure 4.7: Cumulative mass, in kg, profiles for the dominant stem modeled by: (1) the non-linear mixed-effects approach (model 4.21, nlme), (2) the density-integral approach (model 4.22, integ), and (3) the constant density approach (model 4.23, const) as a function of relative height along the dominant stem for the (a) minimum, (b) median, and (c) maximum diameter at breast height (DBH) American beech (FG) trees in the dataset. The vertical dashed line represents relative crown height.

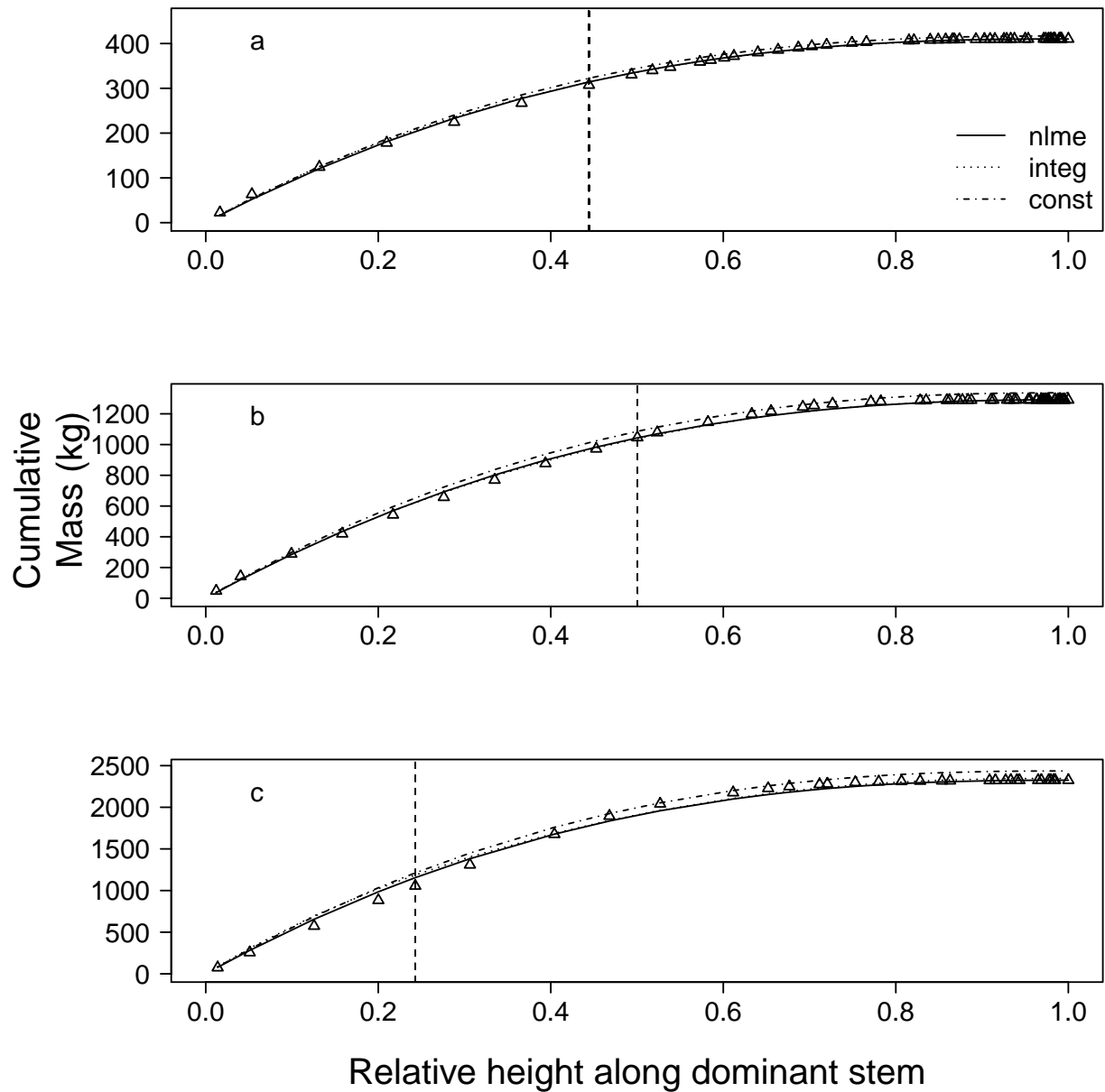


Figure 4.8: Cumulative mass, in kg, profiles for the dominant stem modeled by: (1) the non-linear mixed-effects approach(model 4.21, nlme), (2) the density-integral approach (model 4.22, integ), and (3) the constant density approach (model 4.23, const) as a function of relative height along the dominant stem for the (a) minimum, (b) median, and (c) maximum diameter at breast height (DBH) sugar maple (AS) trees in the dataset. The vertical dashed line represents relative crown height.

Table 4.9 shows the summary statistics for residuals of the three methods of modeling dominant stem mass profiles for all trees, American beech, and sugar maple. The magnitude of the mean residual was lowest for the density-integral approach for all trees, sugar maple only, and nearly equal to the non-linear mixed-effects approach for American beech only. The constant density approach had a much larger magnitude for the mean residual for all trees, American beech, and sugar maple compared to the other two methods.

Table 4.9: Model comparison of the residuals among the cumulative dominant stem mass profiles: (1) non-linear mixed-effects (nlme) model 4.21, (2) density-integral (integ) model 4.22, and (3) the constant density (const) model 4.23 for all (ALL), American beech (FG), and sugar maple (AS) trees.

Statistic	nlme	integ	const
ALL Trees			
N	1957	1957	1957
Mean Residual	3.89	3.38	-7.19
SD	25.12	32.10	138.71
Min Residual	-139.50	-155.87	-630.07
Max Residual	419.72	432.57	461.81
FG Trees			
N	1016	1016	1016
Mean Residual	4.49	4.51	70.16
SD	29.00	38.95	72.50
Min Residual	-139.50	-155.87	-65.52
Max Residual	419.72	432.57	461.81
AS Trees			
N	723	723	723
Mean Residual	2.46	-1.17	-60.11
SD	15.37	16.80	53.10
Min Residual	-101.70	-138.84	-188.17
Max Residual	127.52	113.01	105.10

Whole-tree Mass Profiles

The final model, below, for whole-tree mass added random effects to model 4.7 to create a mixed-effects model. Two potential final mixed-effects models for the portion of the whole-

tree model above relative crown height are given below:

$$m_{AC_{ij}} = M_{RCH_j} + (\beta_M + u_{3j}) * (1 - (1 - (rh_{ij} - RCH_j))^{\alpha_2 + u_{2j}}) + \epsilon_{ij}, \quad (4.24)$$

where $m_{AC_{ij}}$ is the whole-tree cumulative mass above relative crown height of stem position i in tree j in kg, M_{RCH_j} is total tree mass at relative crown height (RCH) in kg, β_M and α_2 are fixed effect parameters to be estimated, u_{2j} and u_{3j} are random effect parameters to be estimated, and ϵ_{ij} is a random error term. In the case where β_M is fixed for tree j , the new model has the same form as model 4.24, except only one random effect parameter (u_{2j}), with

$$\beta_{Mj} = \frac{M_{WT_j} - M_{RCH_j}}{1 - RCH_j^{\alpha_2 + u_{2j}}}, \quad (4.25)$$

where M_{WT_j} is the total whole-tree mass for tree j in kg.

The final whole-tree cumulative mass profile (similar to eq. 4.9) now uses models 4.21 and 4.24 or models 4.21 and 4.25 for the segmented model:

$$m_{WT_{ij}} = I_1 m_{DOM_{ij}} + I_2 m_{AC_{ij}}, \quad (4.26)$$

where $m_{WT_{ij}}$ is the whole-tree cumulative mass of stem position i in tree j in kg, I_1 is an indicator variable with a value of 1 when relative height is below relative crown height and a value of 0 when relative height is above relative crown height, and I_2 is an indicator variable with values of 0 when relative height is below relative crown height and 1 when relative height is above relative crown height. Tables 4.10 and 4.11 give the parameter estimates for models 4.24 and 4.25.

Model 4.25 is chosen as the best-fit final model of the two for the whole-tree above relative crown height portion of the segmented mass model as it has a lower AIC of 22219.50 for the all-species model compared to an AIC of 22505.42 for the all-species model 4.24. The total whole-tree mass for model 4.25 is also compatible with the total whole-tree mass estimate given by random branch sampling as the mean relative difference is zero. The species-specific models for American beech and sugar maple for model 4.25 are selected as the best models over the all-species model based on having lower AIC values.

Table 4.10: Parameter estimates of model 4.24 for cumulative whole-tree mass above relative crown height for the all-species (ALL), American beech (FG), and sugar maple (AS) mixed-effects models. For the fixed parameters, the standard error of estimates is given in parantheses.

Parameter	ALL Estimate	FG Estimate	AS Estimate
α_2	4.285 (0.298)	4.253 (0.399)	4.306 (0.410)
β	2590.80 (663.23)	3943.47 (1286.95)	1255.66 (284.75)
$\text{var}(u_{2j})$	2.209	2.044	2.011
$\text{var}(u_{3j})$	14058457	24787417	1050508
$\text{cov}(u_{2j}, u_{3j})$	256.340	476.850	-168.604
ϵ_{ij}	140.281	185.157	51.497
AIC	22505.42	12313.63	6966.18
Mean Relative Difference	0.520	0.579	0.703

Table 4.11: Parameter estimates of model 4.25 for cumulative whole-tree mass above relative crown height for the all-species (ALL), American beech (FG), and sugar maple (AS) mixed-effects models. For the fixed parameters, the standard error of estimates is given in parantheses.

Parameter	ALL Estimate	FG Estimate	AS Estimate
α_2	4.430 (0.283)	4.410 (0.399)	4.415 (0.377)
$\text{var}(u_{2j})$	2.065	2.086	1.718
ϵ_{ij}	142.080	186.862	54.809
AIC	22219.50	12170.65	6916.13
Mean Relative Difference	0	0	0

The final density-integral approach model to the whole-tree mass profile is similar to model 4.10 with the addition of subscripts for measurements taken at stem position i for tree j :

$$m_{WTij} = \int_{rh_l}^{RCH_j} \rho_{ij} v'_{DOMij} drh + \int_{RCH_j}^{rh_u} \rho_{ij} v'_{ACij} drh, \quad (4.27)$$

where rh_l is the lower limit of relative height and rh_u is the upper limit of relative height. The species-specific dominant stem density function is used for both integrals, and the taper function for both integrals is a species-composite function.

The final model for the constant density approach also applies a species-specific constant basic density and a species-composite cumulative volume function similar to model 4.11 with

the addition of subscripts for measurements taken at stem position i for tree j :

$$m_{WT_{ij}} = \rho_c * v_{WT_{ij}}. \quad (4.28)$$

Figures 4.9 and 4.10 show the dominant stem and whole-tree cumulative mass profile for the (a) minimum, (b) median, and (c) maximum DBH trees of American beech and sugar maple, respectively. For American beech, the total whole-tree mass increases by a factor of ten in each successive profile, and the relative crown height also decreases with increasing DBH. A noticeable increase in branch mass, which is the region between the whole-tree and dominant stem cumulative mass profiles, is also present in each successive profile. Comparing the three methods for whole-tree mass estimation above relative crown height, the non-linear mixed-effects model fits all three trees well. Both the density-integral and constant density approaches show worse fits to the observed data with each successive profile. The sugar maple profiles show similar patterns to the American beech with total whole-tree mass increasing by a factor of three in each successive profile. However, the relative crown height appears to increase before decreasing with increasing DBH, and the branch mass also decreases before increasing with increasing DBH. The three methods for whole-tree estimation above relative crown height appear to fit the three profiles well for sugar maple with slight over-prediction and under-prediction for the density-integral and constant density approaches.

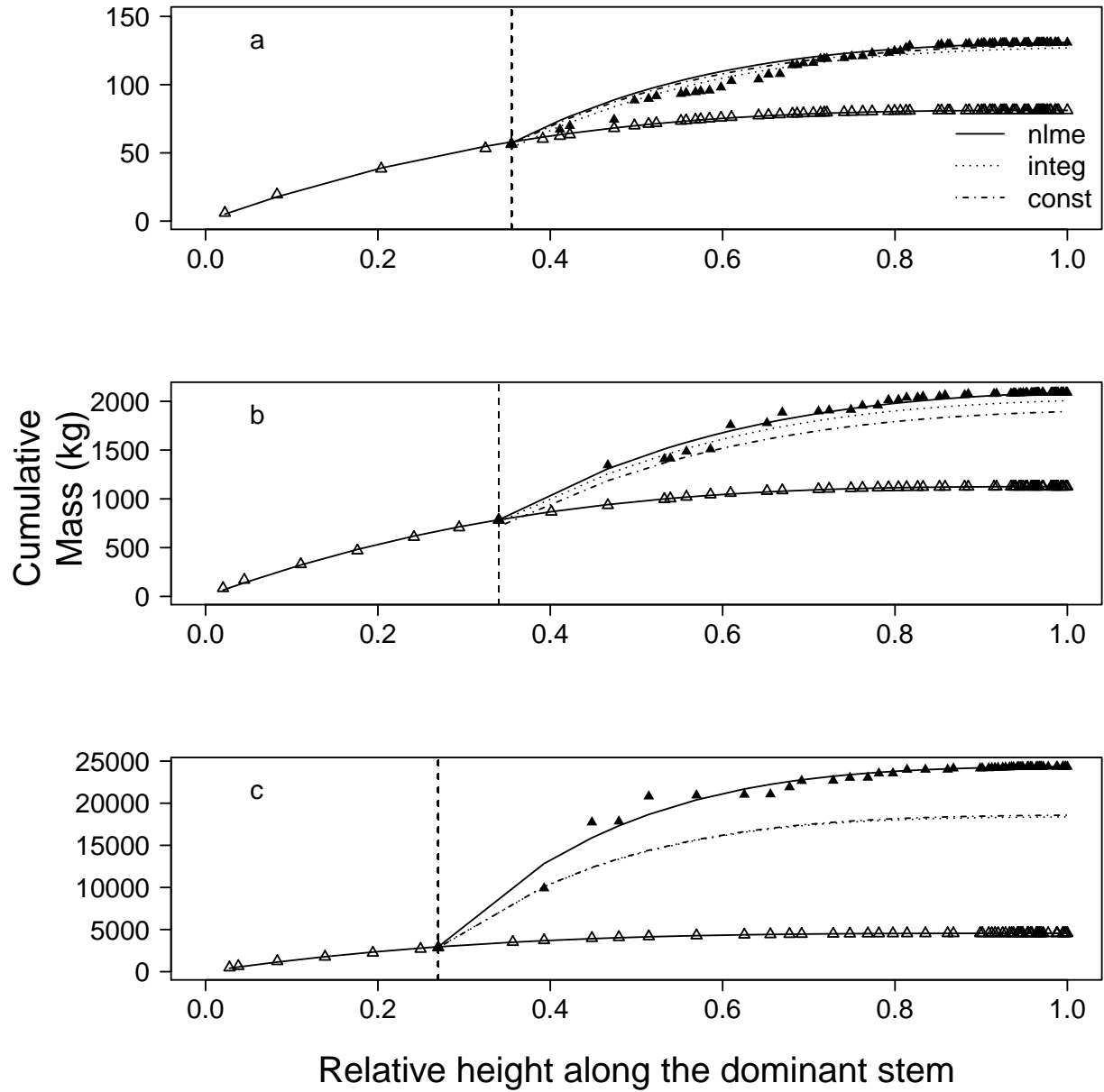


Figure 4.9: Cumulative mass, in kg, profiles for the dominant stem (model 4.21), represented by a solid line and open triangles above relative crown height, and whole tree (model 4.26, nlme), represented by a solid line with filled-in triangles, as a function of relative height along the dominant stem for the (a) minimum, (b) median, and (c) maximum diameter at breast height (DBH) American beech (FG) trees in the dataset. Above relative crown height the density-integral (model 4.27, integ) and constant density (model 4.28, const) models are shown with dotted and dashed lines, respectively. The vertical dashed line represents relative crown height.

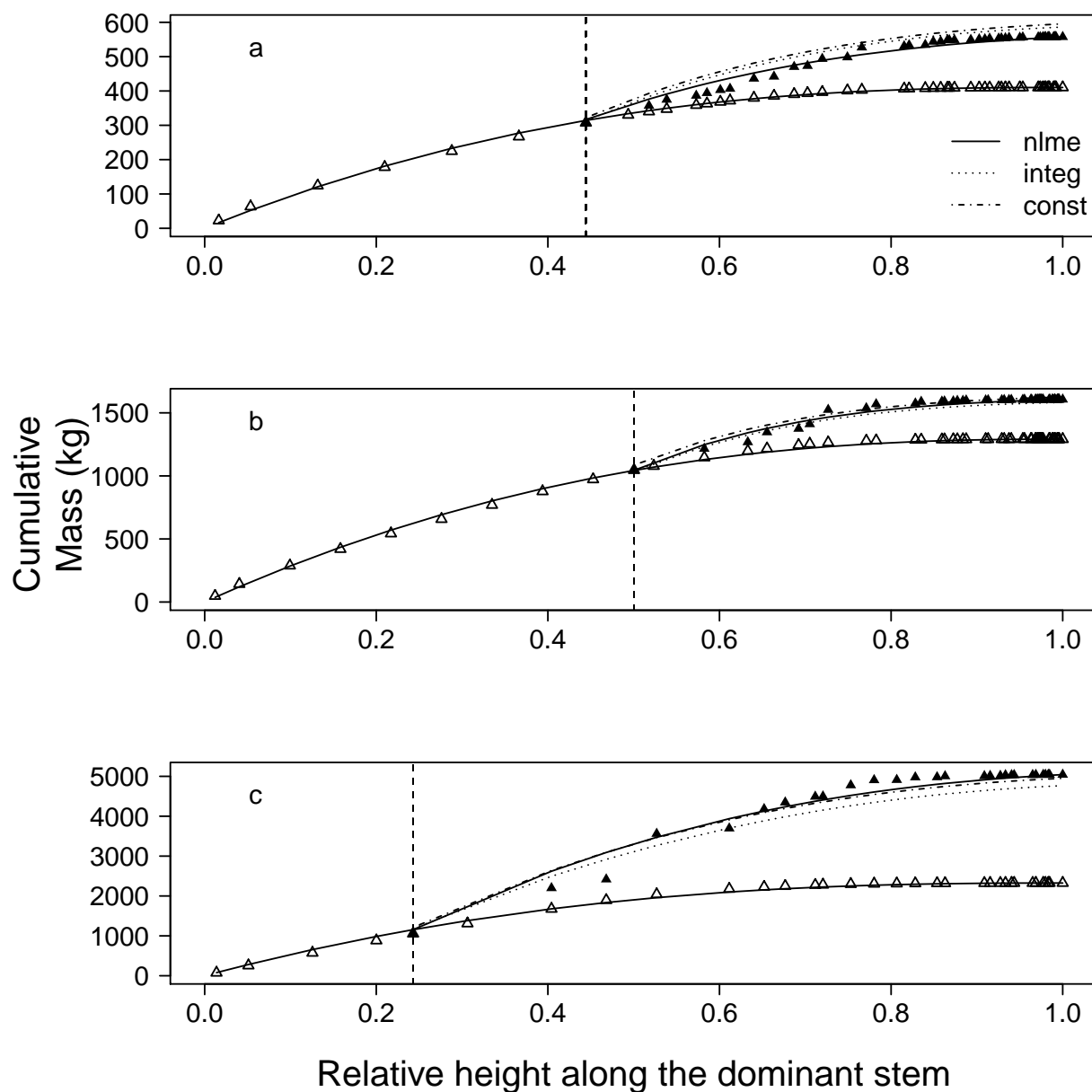


Figure 4.10: Cumulative mass, in kg, profiles for the dominant stem (model 4.21), represented by a solid line and open triangles above relative crown height, and whole tree (model 4.26, nlme), represented by a the solid line with filled-in triangles, as a function of relative height along the dominant stem for the (a) minimum, (b) median, and (c) maximum diameter at breast height (DBH) sugar maple (AS) trees in the dataset. Above relative crown height the density-integral (model 4.27, integ) and constant density (model 4.28, const) models are shown with dotted and dashed lines, respectively. The vertical dashed line represents relative crown height.

Table 4.12 shows the summary statistics for residuals of the three methods of modeling whole-tree mass profiles for all trees, American beech, and sugar maple. The magnitude of the mean residual was lowest for the non-linear mixed-effects approach for all trees, American beech, and sugar maple. The density-integral and constant density approaches had much larger magnitudes for the mean residual for all trees, American beech, and sugar maple.

Table 4.12: Model comparison of the residuals among the cumulative whole-tree mass profiles above relative crown height: (1) non-linear mixed-effects (nlme) model 4.25, (2) density-integral (integ) model 4.27, and (3) the constant density (const) model 4.28 for all (ALL), American beech (FG), and sugar maple (AS) trees.

Statistic	nlme	integ	const
ALL Trees			
N	1735	1735	1735
Mean Residual	8.21	322.66	311.67
SD	140.85	996.12	1038.47
Min Residual	-2924.47	-795.95	-1255.90
Max Residual	2150.16	6471.32	6406.94
FG Trees			
N	911	911	911
Mean Residual	11.64	635.94	743.02
SD	185.25	1292.55	1261.23
Min Residual	-2924.47	-795.95	-570.60
Max Residual	2150.16	6471.32	6406.94
AS Trees			
N	633	633	633
Mean Residual	3.82	-28.17	-106.50
SD	54.19	127.68	132.23
Min Residual	-673.24	-500.68	-676.86
Max Residual	318.14	560.18	361.19

4.5 Discussion

4.5.1 Density

The dominant stem density model forms were different from the random branch path model forms for all six species sampled in the dataset. Random branch path densities were fairly

similar in magnitude compared to dominant stem densities because most of the profile was shared between the random branch and dominant paths (average RHD was 0.702 for all trees), except near the top of the relative path length. For four of the six species, the random branch path density was considerably greater than the dominant stem path near the top of the relative path length indicating that the branches were denser than the dominant stem. Okai and Yeboah (2003) also found the density of branch wood to be greater than stem wood for two tropical hardwood species. However, Swenson and Enquist (2008) found a high correlation between the dominant stem and branch wood density indicating that branch wood densities could be used as a proxy for dominant stem wood density.

Wood density has been identified as an important predictor variable in aboveground biomass estimation (Chave et al. 2005, Woodall et al. 2011). Chave et al. (2005) used a species-specific constant wood density or recommended a stand-level average if species-specific values were unavailable for aboveground biomass estimation across the tropics. Woodall et al. (2011) also used published species-specific constant wood density values for the FIA's estimation of aboveground biomass. Given the complex pattern of wood density seen here, the aboveground biomass estimates would be overestimated for the lower half of a sugar maple tree and underestimated for the upper half. In the case of American beech, aboveground biomass is underestimated using the species constant value for the entire vertical profile. Branches comprised on average 42 percent of the total volume of study trees, so that the random branch profile indicated branches to be denser than the dominant stem would also contribute to greater aboveground biomass estimates. However, the denser random branch profile was near the end of the profile where the volume of branches contributes small additional amounts to the total volume of a tree.

American beech and sugar maple are both late-successional species in a northern hardwood forest (Dickmann and Leefer 2003). Each of the sampled species came from within the same stand and experienced the same site conditions, so it was hypothesized that both species would have a similar vertical density profile shape. However, the vertical density

profiles for American beech and sugar maple were quite different in shape from one another indicating a species dependence. Repola (2006) also found the density of Scots pine, Norway spruce, and birch from the same forest type to be species dependent upon vertical location to varying degrees. The vertical density profiles seen here were more complex than a general increasing or decreasing density pattern in the longitudinal direction.

The magnitude of the dominant stem and random branch path tree density models could be slightly greater than a wood density model due to the inclusion of bark with the wood. The bark vertical density models for five of the six species, except for slippery elm, had much greater densities than the dominant stem models along the entire vertical profile. However, bark on average only contributed 6.5 percent to the total green volume of a given sample disc, without accounting for bark voids. Miles and Smith (2009) report a similar percentage for bark volume of total volume of 5.7 percent for beech, and a slightly greater percentage of 13.0 percent for general hardwoods. Although the contribution of bark by volume is very small to the tree density models, the separation of bark from wood is recommended at the onset of measurements to remove this possible difference. Both Koch (1970) and Manwiller (1979) used water saturation of bark samples to determine the green volume before estimating bark specific gravity. Koch (1970) found hardwood trees with DBH from 10 to 40 cm, which is below the mean of the sample trees, to have bark specific gravity dependent upon the species, and the pattern with height is also species dependent. The variation in bark specific gravity with height within DBH classes was generally greater than the variation at a specific height between DBH classes. The specific gravity increased with height before leveling off to the maximum height investigated, unlike the sharp declines that were seen in five of the six species in this study. Manwiller (1979) examined smaller diameter (15 cm) hardwoods on pine sites and found the specific gravity to be denser than values reported by U. S. D. A. Forest Service (2010). Significant differences were found among the species for specific gravity of bark and among the different types of bark (i.e., stem, branch, and tree) for each species. In this study, the bark densities used to develop the bark profile were a combination

of stem bark and branch bark depending upon the selected random path that was followed for the random branch path profile, so there could be more or less branch bark included in the bark profile.

An area for further examination would be to extend this study for each species with larger sample sizes across a broader geographic region. As studies have shown species, geographic variation, age, and size to be significant variables along with the longitudinal gradient of a tree (Tasissa and Burkhart 1998, Antony et al. 2010). Bayesian statistics and linear model theory can then be applied to calibrate a broad geographic region's generalized linear mixed-effects model to a specific forest stand (Lappi 1991). Repola (2006) predicted the random effects of models by measuring two densities of an individual tree to calibrate models for pine, spruce, and birch stems in Finland.

4.5.2 Mass

The non-linear mixed-effects models for dominant stem and whole-tree cumulative mass profiles resulted in the smallest or nearly equally small residuals compared to the density-integral and constant density methods. The non-linear mixed-effects models were compatible with the total estimates of dominant stem and whole-tree mass by constraining the model, and the density-integral and constant density models were incompatible with the total mass estimates. The non-linear mixed-effects profiles for dominant stem cumulative mass require total dominant stem mass and total height as predictor variables into the final model, which total dominant stem mass would require an allometric equation as input into the model with measurable attributes. The same predictor variables are needed for the whole-tree cumulative mass profile with the additions of total whole-tree mass, relative crown height, and the mass at relative crown height. The need for the additional value for mass at relative crown height as a predictor variable for the whole-tree profile would require measurements of volume with a dendrometer on a standing tree and the use of a density profile to convert volume to a mass estimate. Total whole-tree mass would also require the need for an allometric scaling

relationship. The use of both the dominant stem and whole-tree profiles allows for the mass of branches to be estimated by simple subtraction rather than a separate model for branches.

Several studies offer solutions to the need for an estimate of total whole-tree mass as an input into the profile model. Cannell (1984) offers a possible solution for measurable attributes of diameter, height, form factor, and density as predictor variables for total mass. Chave et al. (2005) applied a similar model for total aboveground biomass in the tropics with the same predictor variables except making form factor a constant. MacFarlane and Ver Planck (2012) also examined the possibility of measuring form factor as an additional measurement to improve whole-tree mass estimation.

A species-specific model was shown to give better individual fits for the cumulative dominant stem and whole-tree profiles for the American beech and sugar maple trees. The inherent differences in density among species can be attributed to the need for species-specific models for mass estimation. Often single species are the focus of biomass studies in order to get a large and representative sample size (e.g., Parresol and Thomas 1989, Jordan et al. 2006). A suggestion for future biomass studies would be to focus on a single species of interest.

The density-integral method performed well based on the summary statistics of the residuals for the dominant stem. Of the three methods, the density-integral is most likely to be implemented with the large availability of taper functions to be combined with needed density profiles (Jordan et al. 2006). However, the density-integral performed far worse for the whole-tree cumulative mass profile above relative crown height. Perhaps this is because the first derivative of the cumulative volume in this dataset was not a true representation of a whole-tree taper function. As when branches were encountered all of the volume was assumed to be located at that relative height. Van Deusen and Roesch (2011) offer another method of conceptualizing a whole-tree taper profile by compressing all the branches into a cylinder and measuring diameters of branches at the same heights along the dominant stem. Another possibility for the whole-tree density-integral not fitting well above relative crown

height was the use of the dominant stem density profile. As the crown portion of the tree is comprised of both branches and dominant stem, some composite density profile may be needed to better model the observed data.

The method of applying a constant species-specific density to a cumulative volume profile performed the worst of the three methods. The mean residuals for both the dominant stem and whole-tree mass profiles were some of the largest. Total whole-tree mass estimates using the constant density method also resulted in large under- and over-prediction of the observed total mass of individual trees. The FIA currently uses constant densities to convert volume estimates to mass estimates showing the need for the adoption of another method for biomass estimation (Woodall et al. 2011).

CHAPTER 5

CONCLUSION

The non-linear mixed-effects models for volume and mass of dominant stems were compatible to the total volume and mass estimates from Smalian's formula and random branch sampling. This is a very important principle for estimates that are generated from models, especially when the estimates are of economic importance such as whole-tree utilization for energy or estimating carbon *stocks* for potential carbon markets. The current study also added to the limited amount of research focusing on tree branches in relation to a whole tree framework.

A species-composite model was shown to be sufficient for a cumulative volume profile. The composite model was acceptable for volume based on all the trees being sampled from windfall coming from the same stand and with similar tree architecture, which may have resulted in these trees mortality. Examination of the sampled trees relative to the residual stand makes it difficult to apply these models to the residual trees in the stand as it appears more larger trees were destructively sampled compared to the residual trees in the stand. It would be interesting to relate the centroid of volume of these wind-thrown trees to the residual trees, and perhaps because of a higher centroid these trees were more susceptible to the wind. Newer technologies are making parameters easier to measure on the residual trees or other standing trees that once were impractical, such as volume at relative crown height.

Species-specific density models gave the best fit, which makes sense based upon the large differences in density between species, e.g., the light wood of American basswood and denser wood of American beech. Densities of a given tree or stand were shown to be much more variable than assuming a constant value based on species. For future studies, it is highly recommended to separate bark from wood at the onset due to major differences in structure and density.

The cumulative mass models also had better fits with a species-specific model. The

current research offers a good starting point for whole-tree mass profile modeling with needed improvements in capturing the various densities of branches. The density-integral approach is more practical for implementation than the non-linear mixed-effects models, but the density-integral approach for whole-tree mass was only slightly better than assuming a constant density approach. A more representative density profile could drastically improve the whole-tree mass estimates. An area for further examination would be to sample multiple branch paths per tree to see how different each branch path is from one another and the dominant stem path. It would aid in determining if a composite density model is needed for the whole-tree portion of mass modeling above relative crown height.

BIBLIOGRAPHY

BIBLIOGRAPHY

- S. Adu-Bredu, A. Bi, J. Bouillet, M. Mé, S. Kyei, and L. Saint-André. An explicit stem profile model for forked and un-forked teak (*Tectona grandis*) trees in West Africa. *Forest ecology and management*, 255(7):2189–2203, 2008.
- F. Antony, L. R. Schimleck, R. F. Daniels, A. Clark, and D. B. Hall. Modeling the longitudinal variation in wood specific gravity of planted loblolly pine (*Pinus taeda*) in the United States. *Canadian Journal of Forest Research*, 40:2439 – 2451, 2010.
- T. E. Avery and H. E. Burkhart. *Forest measurements, 5th ed.* McGraw-Hill Book Company, 2002.
- G. Baker and J. E. Shottafer. Specific gravity relationships in plantation-grown red pine. 1968.
- T. R. Baker, O. L. Phillips, Y. Malhi, S. Almeida, L. Arroyo, A. D. Fiore, T. Erwin, T. L. Killeen, S. G. Laurance, W. F. Laurance, S. L. Lewis, J. Lloyd, A. Monteagudo, D. A. Neill, S. Patino, N. C. A. Pitman, J. N. M. Silva, and R. V. Martinez. Variation in wood density determines spatial patterns in amazonian forest biomass. *Global Change Biology*, 10(5):545–562, 2004.
- R. J. Barbour, D. C. Fayle, G. Chauret, J. Cook, M. B. Karsh, and S. Ran. Breast-height relative density and radial growth in mature jack pine (*Pinus banksiana*) for 38 years after thinning. *Canadian Journal of Forest Research*, 24(12):2439–2447, 1994. doi: 10.1139/x94-315.
- M. G. Cannell. Woody biomass of forest stands. *Forest Ecology and Management*, 8(3): 299–312, 1984.
- J. Chave, C. Andalo, S. Brown, M. Cairns, J. Chambers, D. Easmus, H. Fölster, F. Fromard, N. Higuchi, T. Kira, J.-P. Lescure, B. Nelson, H. Ogawa, H. Puig, B. Riera, and T. Yamakura. Tree allometry and improved estimation of carbon stocks and balance in tropical forests. *Oecologia*, 145:87–99, 2005.
- J. Chave, H. C. Muller-Landau, T. R. Baker, T. A. Easdale, H. ter Steege, and C. O. Webb. Regional and phylogenetic variation of wood density across 2456 neotropical tree species. *Ecological Applications*, 16(6):2356–2367, 2006.
- J. Chave, D. Coomes, S. Jansen, S. L. Lewis, N. G. Swenson, and A. E. Zanne. Towards a worldwide wood economics spectrum. *Ecology Letters*, 12(4):351–366, 2009.
- D. I. Dickmann and L. A. Leefers. *The Forests of Michigan*. University of Michigan Press/Regional, 2003.
- EPA. *Inventory of U.S. greenhouse gas emissions and sinks: 1990-2009*. U.S. Environmental Protection Agency, Washington, DC, 2011.

- J. Fonweban, B. Gardiner, and D. Auty. Variable-top merchantable volume equations for Scots pine (*Pinus sylvestris*) and Sitka spruce (*Picea sitchensis* (Bong.) Carr.) in Northern Britain. *Forestry*, 85(2):237–253, 2012.
- R. R. Forslund. A geometrical tree volume model based on the location of the centre of gravity of the bole. *Canadian Journal of Forest Research*, 12(2):215–221, 1982.
- T. G. Gregoire and O. Schabenberger. Nonlinear mixed-effects modeling of cumulative bole volume with spatially correlated within-tree data. *Journal of Agricultural, Biological, and Environmental Statistics*, pages 107–119, 1996a.
- T. G. Gregoire and O. Schabenberger. A non-linear mixed-effects model to predict cumulative bole volume of standing trees. *Journal of Applied Statistics*, 23(2-3):257–272, 1996b.
- T. G. Gregoire, H. T. Valentine, and G. M. Furnival. Sampling methods to estimate foliage and other characteristics of individual trees. 76(4):1181–1194, 1995.
- J. T. Hahn and M. H. Hansen. Cubic and board foot volume models for the central states. *Northern Journal of Applied Forestry*, 8:47–57, 1991.
- M. Hansen. Volume and biomass estimation in FIA: national consistency vs. regional accuracy. In *Proceedings of the third annual forest inventory and analysis symposium*, pages 109–120, 2002.
- J. Harkin and J. Rowe. *Bark and its possible uses*, volume 91. Forest Products Laboratory, US Forest Service, 1971.
- L. S. Heath, M. Hansen, J. E. Smith, P. D. Miles, and B. W. Smith. Investigation into calculating tree biomass and carbon in the FIADB using a biomass expansion factor approach. In: *McWilliams, Will; Moisen, Gretchen; Czaplewski, Ray, comps. 2008 Forest Inventory and Analysis (FIA) Symposium; 2008 October 21-23; Park City, UT. Proc. RMRS-P-56CD. Fort Collins, CO: U.S. Department of Agriculture, Forest Service, Rocky Mountain Research Station. 26 p.*, 2009.
- S. W. Hughes. Archimedes revisited: a faster, better, cheaper method of accurately measuring the volume of small objects. *Physics Education*, 40(5):468, 2005.
- IPCC. *2006 IPCC Guidelines for National greenhouse gas inventories*. Institute for Global Environmental Strategies, Hayama, Japan, 2006.
- J. C. Jenkins, D. C. Chojnacky, L. S. Heath, and R. A. Birdsey. National-scale biomass estimators for united states tree species. *Forest Science*, 49(1):12–35, 2003.
- J. C. Jenkins, D. C. Chojnacky, L. S. Heath, and R. A. Birdsey. *Comprehensive database of diameter-based biomass regressions for North American tree species*. US Department of Agriculture, Forest Service, Northeastern Research Station Newtown Square, PA, 2004.
- L. Jordan, R. Souter, B. Parresol, and R. F. Daniels. Application of the algebraic difference approach for developing self-referencing specific gravity and biomass equations. *Forest Science*, 52(1):81–92, 2006.

- B. Koch. Variation in bark specific gravity of selected appalachian hardwoods. *Wood Science*, 3:41 – 47, 1970.
- A. Kozak. A variable-exponent taper equation. *Canadian Journal of Forest Research*, 18(11):1363–1368, 1988.
- F. Lamb and R. Marden. Bark specific gravities of selected Minnesota tree species. *Forest Products Journal*, 18:76 – 83, 1968.
- M.-C. Lambert, C.-H. Ung, and F. Raulier. Canadian national tree aboveground biomass equations. *Canadian Journal of Forest Research*, 35(8):1996–2018, 2005.
- S. Lamtom and R. Savidge. A reassessment of carbon content in wood: variation within and between 41 North American species. *Biomass and Bioenergy*, 25(4):381–388, 2003.
- J. Lappi. Calibration of height and volume equation with random parameter. *Forest Science*, 37(3):781 – 801, 1991.
- P. R. Larson. Stem form development of forest trees. *Forest Science*, 9(Supplement 5):1–42, 1963.
- L. P. Leites and A. P. Robinson. Improving taper equations of loblolly pine with crown dimensions in a mixed-effects modeling framework. *Forest Science*, 50(2):204–212, 2004.
- D. W. MacFarlane. Predicting branch to bole volume scaling relationships from varying centroids of tree bole volume. *Canadian Journal of Forest Research*, 40(12):2278–2289, 2010.
- D. W. MacFarlane. Allometric scaling of large branch volume in hardwood trees in Michigan, USA: Implications for aboveground forest carbon stock inventories. *Forest Science*, 57(6):451–459, 2011.
- D. W. MacFarlane and N. R. Ver Planck. Improved prediction of hardwood tree biomass derived from wood density estimates and form factors for whole trees. In *Moving from Status to Trends: Forest Inventory and Analysis Symposium 2012*, pages 353–356, 2012.
- F. Manwiller. Wood and bark specific gravity of small-diameter, pine-site hardwood in the south. *Wood Science*, 11:234 – 240, 1979.
- R. Martin and J. Crist. Selected physical-mechanical properties of eastern tree barks. *Forest Products Journal*, 18, 1968.
- H. I. Martinez-Cabrera, C. S. Jones, S. Espino, and H. J. Schenk. Wood anatomy and wood density in shrubs: response to varying aridity along transcontinental transects. *American Journal of Botany*, 96(8):1388–1398, 2009.
- T. A. Max and H. E. Burkhart. Segmented polynomial regression applied to taper equations. *Forest Science*, 22(3):283–289, 1976.

- P. D. Miles and B. W. Smith. Specific gravity and other properties of wood and bark for 156 tree species found in North America. *Res. Note NRS-38. Newtown Square, PA: U.S. Department of Agriculture, Forest Service, Northern Research Station.*, page 35, 2009.
- K. D. Montagu, K. Duttmer, C. V. M. Barton, and A. L. Cowie. Developing general allometric relationships for regional estimates of carbon sequestration—an example using *Eucalyptus pilularis* from seven contrasting sites. *Forest Ecology and Management*, 204: 113–127, 2005.
- H. C. Muller-Landau. Interspecific and inter-site variation in wood specific gravity of tropical trees. *Biotropica*, 36(1):20–32, 2004.
- U. S. D. o. C. NCDC, National Climatic Data Center, 2011. URL <http://ncdc.noaa.gov/>. Accessed: (June 5, 2012).
- R. M. Newnham. Variable-form taper functions for four Alberta tree species. *Canadian Journal of Forest Research*, 22(2):210–223, 1992.
- C. D. Oliver and B. C. Larson. *Forest stand dynamics: update edition*. John Wiley & Sons, Inc., New York, 1996.
- B. R. Parresol. Assessing tree and stand biomass: A review with examples and critical comparisons. *Forest Science*, 45(4):573–593, 1999.
- B. R. Parresol and C. E. Thomas. A density-integral approach to estimating stem biomass. *Forest Ecology and Management*, 26(4):285 – 297, 1989. ISSN 0378-1127. doi: 10.1016/0378-1127(89)90089-3.
- B. R. Parresol and C. E. Thomas. A simultaneous density-integral system for estimating stem profile and biomass: slash pine and willow oak. *Canadian Journal of Forest Research*, 26(5):773 – 781, 1996.
- B. R. Parresol, J. E. Hotvedt, and Q. V. Cao. A volume and taper prediction system for bald cypress. *Canadian Journal of Forest Research*, 17(3):250–259, 1987.
- J. Pinheiro, D. Bates, S. DebRoy, D. Sarkar, and R. D. C. Team. *nlme: Linear and Nonlinear Mixed Effects Models*, 2011. R package version 3.1-98.
- R Development Core Team. *R: A Language and Environment for Statistical Computing*. R Foundation for Statistical Computing, Vienna, Austria, 2010. URL <http://www.R-project.org>. ISBN 3-900051-07-0.
- J. Repola. Models for vertical wood density of scots pine, norway spruce and birch stems, and their application to determine average wood density. *Silva Fennica*, 40(4):673 – 685, 2006.
- B. Rubin and D. W. MacFarlane. Using the space-time permutation scan statistic to map anomalous diameter distributions drawn from landscape-scale forest inventories. *Forest Science*, 54(5):523–533, 2008.

- R. Shmulsky and P. D. Jones. *Forest products and wood science: An introduction, 6th ed.* Wiley-Blackwell, 2011. ISBN 9780470960035.
- U. S. D. o. A. Soil Survey Staff, Natural Resources Conservation Service. Web soil survey, 2011. URL <http://websoilsurvey.nrcs.usda.gov/>. Accessed: (June 4, 2012).
- N. G. Swenson and B. J. Enquist. The relationship between stem and branch wood specific gravity and the ability of each measure to predict leaf area. *American Journal of Botany*, 95:516 – 519, 2008.
- G. Tasissa and H. E. Burkhart. Modeling thinning effects on ring specific gravity of loblolly pine (*Pinus taeda* L.). *Forest Science*, 44:212 – 223, 1998.
- U. S. D. A. Forest Service. Wood handbook - wood as an engineering material. Technical Report FPL-190, Madison WI: U.S. Department of Agriculture, Forest Service, Forest Products Laboratory, 2010.
- H. T. Valentine and T. G. Gregoire. A switching model of bole taper. *Canadian Journal of Forest Research*, 31(8):1400–1409, 2001.
- H. T. Valentine, L. M. Tritton, and G. M. Furnival. Subsampling trees for biomass, volume, or mineral content. *Forest Science*, 30(3):673–681, 1984.
- P. Van Deusen and F. A. Roesch. Sampling a tree for total volume, biomass, and carbon. *Journal of Forestry*, 109(3):131–135, 2011.
- M. van Noordwijk and R. Mulia. Functional branch analysis as tool for fractal scaling above- and belowground trees for their additive and non-additive properties. *Ecological Modelling*, 149(1 - 2):41 – 51, 2002. ISSN 0304-3800. doi: 10.1016/S0304-3800(01)00513-0.
- H. E. Wahlgren, A. C. Hart, and R. R. Maeglin. Estimating tree specific gravity of Maine conifers. *U.S.D.A. Forest Service Research Paper FPL-61. Forest Products Laboratory, Madison, WI*, 1966.
- J. A. Westfall and C. T. Scott. Taper models for commercial tree species in the Northeastern United States. *Forest Science*, 56(6):515–528, 2010.
- H. V. Wiant, Jr., G. B. Wood, and R. R. Forslund. Comparison of centroid and paracone estimates of tree volume. *Canadian Journal of Forest Research*, 21(5):714–717, 1991.
- M. C. Wiemann and G. B. Williamson. Radial gradients in the specific gravity of wood in some tropical and temperate trees. *Forest Science*, 35(1):197–210, 1989.
- G. B. Williamson and M. C. Wiemann. Measuring wood specific gravity...correctly. *American Journal of Botany*, 97(3):519–524, 2010.
- G. B. Wood, H. V. W. Jr., R. J. Loy, and J. A. Miles. Centroid sampling: a variant of importance sampling for estimating the volume of sample trees of radiata pine. *Forest Ecology and Management*, 36(2):233–243, 1990.

- C. W. Woodall, L. S. Heath, G. M. Domke, and M. C. Nichols. Methods and equations for estimating aboveground volume, biomass, and carbon for trees in the u.s. forest inventory, 2010. *Gen. Tech. Rep. NRS-88. Newtown Square, PA: U.S. Department of Agriculture, Forest Service, Northern Research Station.* 30 p., 2011.
- P. B. Woodbury, J. E. Smith, and L. S. Heath. Carbon sequestration in the u.s. forest sector from 1990 to 2010. *Forest Ecology and Management*, 241:14–27, 2007.
- D. W. Woodcock and A. D. Shier. Wood specific gravity and its radial variations: the many ways to make a tree. *Trees - Structure and Function*, 16(6):437–443, 2002.
- D. W. Woodcock and A. D. Shier. Does canopy position affect wood specific gravity in temperate forests? *Annals of Botany*, 91(5):529–537, 2003.
- W. T. Zakrzewski. Estimating wood volume of the stem and branches of sugar maple (*Acer saccharum* marsh.) using a stem profile model with implicit height. *Forest Science*, 57(2): 117–133, 2011.
- B. Zobel and J. P. V. Buijtenen. *Wood variation: its causes and control*. Springer-Verlag, Berlin, 1989.